

Department of Pure and Applied Chemistry

**The Application of Density Functional Theory for Understanding
Organic Reactivity: Nitration; Super Electrophiles; Iridium Catalysts;
Methanol Formation.**

By

Christopher Idziak

A thesis is presented to the Department of Pure and Applied Chemistry, University of Strathclyde, in fulfilment of the requirements for the degree of Doctor of Philosophy

2013

DECLARATION OF COPYRIGHT

This thesis is the result of the author's original research. It has been composed by the author and has not been previously submitted for examination which has lead to the award of a degree.

The copyright of this thesis belongs to the author under the terms of the United Kingdom Copyright Acts as qualified by University of Strathclyde Regulation 3.50. Due acknowledgement must always be made of the use of any material contained in, or derived from, this thesis.

Signed:

Date:

Acknowledgements

The following individuals are noted for contributions to the work undertaken in this thesis:

Dr Tell Tuttle for overall supervision of the projects as primary supervisor, as well as input into the other sections of the project which complemented, but are not included, in this thesis.

Professor John Murphy, as secondary supervisor, and for discussions concerning the experimental details of the work undertaken on the superelectrophilic activation studies of amidine dications.

Professor Colin Suckling and Dr. Craig McInnes for helpful discussions on the electrophilic aromatic substitution section of the thesis and for performance of the experimental work which formed the basis of the work presented in the NO₂ component of the thesis.

Professor William Kerr and Dr. Alison Cochrane who performed the experimental component of the work performed on the iridium project.

Members of the Tuttle group, past and present are acknowledged for a number of helpful discussions and pointers regarding the mechanistic and computational details of the reactions studied. In particular, Dr Bhaskar Mondal for guidance provided on all aspects

of the projects undertaken, and especially for assistance in the iridium work; Dr Jörg Sassmanshaussen for guidance in the early stages of the work performed on the NO₂ project; and Dr Qinghua Ren, Dr. Pim Frederix, Joseph Cameron, Daniel Cannon, Ivan Ramos Sasselli, Marc Reid and Nicola Caldwell for numerous discussions and support.

Acknowledgement is also given to Dr. Hans Martin Senn and Dr. Grant Hill and members of their research groups at the University of Glasgow for helpful pointers concerning mechanistic details during WestChem meetings of the Computational and Theoretical Chemistry research group.

The following lecturers at the University of Stirling, past and present, are also acknowledged, Professor Nicholas C. Price, Dr. Ted Porter, Dr. Ian Alberts, Dr. Lewis Stevens, Dr. Mick North, Dr. Timothy Whalley, Dr. Maureen Cooper, Dr. Jacqueline Nairn, Dr. Michael Wyman, Dr. Robin Phillips, and Professor Grant Reid, each for contributions made in the lucid presentation of lecturers focusing of mechanism and its regulation in enzyme systems, secondary metabolism and biochemical control systems respectively; the themes of which underpin the commentary in this presentation.

In addition the Department of Management Science, University of Strathclyde, particularly Professor John Quigley, Dr. Victor Dörfler, Dr. Farhad Shafti, Dr. Robert van der Meer, Dr. Jason Whalley, Dr. Tibor Illés, Professor Susan Howick, Professor Lesley Walls, Mr Mik Wisniewski and Professor Tim Bedford are acknowledged for constructive feedback and clearly presented lectures regarding the modeling of systems,

with particular emphasis on stochastic and optimization modeling; the content of which were very helpful in understanding the algorithms which were employed in the transition state geometry elucidations, equilibrium structure calculations, and statistical/mathematical aspects of the theory which are referred to in the introduction to the thesis, and also presented in seminars and posters during the course of this study.

Abstract

In this thesis, the ability of modern density functional theory to model organic reaction mechanisms is examined. The insights that can be obtained from computational chemistry range from the very nature of the mechanisms – the fundamental forces that drive the reaction forward – through to the role of the environment and the properties of the resulting molecules. However, the importance of these insights is most readily displayed through their application to challenging experimental problems. Therefore, the projects that are described in this work are all associated with experimental studies that are in a position to utilise the insights obtained.

In the study on the nitration of 6-chloropyrimidine-4(3H)-one (Chapter 3), it was shown that the inductive effect can be employed in some instances to provide a mechanistic explanation for reactivity. This was observed to be relevant where there is a moiety within the molecule, which either withdraws or donates electronic density from or to this group.

In the study on the superelectrophilic activation in amidine dications (Chapter 4), it was shown that relative energetics with respect to formation of reactant/product complexes and transition states can be influenced by the presence or absence of associated counterions.

In the study on the use of iridium based catalysts for hydrogen isotope exchange (Chapter 5) the role of solvent molecules in affecting the reactivity was assessed. This study led to the rationalization and selection of a preferred and beneficial solvent for carrying out these reactions.

In the formation of methanol from CO and CO₂ (Chapter 6) an explanation in terms of relative energetic changes of a series of steps in a novel route to Methanol formation has been reported. It has been shown that the relative energetics of these set of reactions are within a satisfactory range for the process to proceed as represented experimentally.

Abbreviations.

x	Position representation in quantum mechanics
ρ	Momentum representation in quantum mechanics
i	$\sqrt{-1}$
\hbar	$\frac{h}{2\pi}$
γ	4x4 matrices
ψ	4x4 spinor
\hat{H}	Hamiltonian operator
Ψ_j	Wave function
x_N	Electron position representation
E_i	Energy of electronic orbital
R_M	Nucleus position representation
M_A	Mass of nucleus
Z_A	Charge on nucleus A
Z_B	Charge on nucleus B
r_{iA}	Distance between electron i and nucleus A
r_{ij}	Distance between electron i and electron j
R_{AB}	Distance between nucleus A and nucleus B
∇_i^2	Del squared representative of electronic density
∇_A^2	Del squared representative of nuclear density

\hat{T}	Kinetic energy operator
V_{ee}	Potential arising from electronic repulsions
V_{Ne}	Potential arising from electron-nucleus attraction
\hat{O}	Quantum expectation value of an observable
Φ_{SD}	Slater determinant
ϕ_i	Spin electronic orbital
σ_i	Spatial electronic orbital
χ_i	Electronic orbital in Slater determinant
J_j	Coulomb operator
K_j	Exchange operator
\hat{f}	Fock operator
V_{HF}	Hartree-Fock potential
$\rho(r)$	Electronic density
Ω	Conditional probability of observing an electron
E_{ee}	Electron-electron interaction energy between correlation hole and electronic density
T_{HF}	Kinetic energy of a uniform gas of electrons
E_{TF}	Total energy that an atom contains
E_x	Exchange energy
V_{ext}	External potential

r_s	Wigner-Seitz radius
F_{HK}	Hohenberg-Kohn functional
T_s	Non-interacting kinetic energy
F_{HK}	Hohenberg-Kohn functional
E_{xc}	Exchange-correlation energy
V_{xc}	Exchange-correlation potential
V_{eff}	Effective potential
V_s	Potential associated with exchange-correlation energy
φ	Kohn-Sham orbital
π_x	L and R p orbitals
ω_i	Weights of electron densities
Θ_i	Kohn-Sham densities
E	Determinantal energies
$\alpha(\omega)$	Mean polarizability
λ	Coupling parameter
GEA	Gradient expansion approximation
GGA	Generalized gradient approximation
s_σ	Local inhomogeneity of the electron density
V_c	Coulomb potential
C	Vector for orbital expansion

ε	Vector for orbital energies
η_{μ}	Basis function
N	Normalization factor
V_{coul}	Coulomb potential

CONTENTS

ACKNOWLEDGEMENTS.....	III
ABSTRACT.....	VI
ABBREVIATIONS.....	VIII
1. INTRODUCTION.....	4
1.1 HISTORICAL BACKGROUND.....	4
1.2 ROLE OF THEORETICAL CHEMISTRY IN ORGANIC REACTIVITY.....	11
2. METHODOLOGY.....	17
2.1 QUANTUM MECHANICS.....	17
2.2 HARTREE-FOCK APPROXIMATION.....	22
2.3 DENSITY FUNCTIONAL THEORY.....	25
2.4 HOHENBERG-KOHN THEORMS.....	27
2.5 KOHN-SHAM THEORY.....	34
2.6 GENERALIZED GRADIENT APPROXIMATIONS.....	37
2.7 HYBRID FUNCTIONALS.....	38
3.0 THE NITRATION OF 6-CHLOROPYRIMIDIN-4(3H)-ONE.....	42
3.1 INTRODUCTION TO ELECTROPHILIC AROMATIC NITRATION.....	42
3.2 COMPUTATIONAL METHODS.....	47
3.3 RESULTS AND DISCUSSION.....	49
3.3.1 <i>The Concerted Mechanism</i>	49

3.3.2	<i>The Bakke-Based Mechanism</i>	56
3.3.3	<i>Comparison of Various Mechanisms</i>	61
4.0	SUPERELECTROPHILIC AMIDINE DICATIONS	93
4.1	INTRODUCTION TO ORGANIC SUPERELECTROPHILES	94
4.2	COMPUTATIONAL METHODS	96
4.3	RESULTS AND DISCUSSION	97
5.0	HYDROGEN ISOTOPE EXCHANGE WITH IRIIDIUM CATALYSTS	115
5.1	INTRODUCTION TO THE IRIIDIUM CATALYSTS	116
5.2	COMPUTATIONAL METHODS	118
5.3	RESULTS AND DISCUSSION	118
5.3.1	<i>Experimental Results</i>	118
5.3.2	<i>Computational Results</i>	120
6.0	THE FORMATION OF METHANOL FROM CO₂ AND CO	127
6.1	INTRODUCTION TO THE FORMATION OF METHANOL.....	127
6.2	COMPUTATIONAL METHODS	128
6.3	RESULTS AND DISCUSSION	129
6.3.1	<i>The Initiation Mechanism</i>	130
6.3.2	<i>Reaction Enthalpies and Free Energies</i>	133
6.4	CONCLUSIONS AND FURTHER WORK.....	142
7.0	CONCLUSIONS AND FURTHER WORK.....	144
8.0	REFERENCES	148

1. Introduction.

1.1 Historical Background.

Computational chemistry can broadly be described as the application of computer science to assist in solving experimental research problems in the molecular and bio molecular sciences. Theoretical chemistry is mostly concerned with the mathematical solution of the equations that underpin the essential wave mechanical expressions that underpin quantum theory and also with respect to the reduction in computational expense associated with the solution of such equations. Research can be performed in computational/theoretical chemistry which is independent of direct experimental input. This type of research is concerned with, for example, methodological development of Quantum Mechanical (QM)/Molecular Mechanics (MM) approaches and the concomitant reduction of computational expense associated with calculations of this nature.

The mathematical basis of Quantum Mechanics was established in the early part of the 20th century following the publication of Werner Heisenberg's paper 'Über quantentheoretische Umdeutung kinematischer und mechanischer Beziehungen' 'Quantum-mechanical re-interpretation of kinematic and mechanical relations'.¹ This landmark paper was the first description of the essential characteristics of quantum theory, with a particular reference to uncertainty. Central to the re-interpretation of the classical approach of the precise characterization of electron position and period was the description of these descriptors in terms of being unobservable quantities. The

description of the new quantum theory required the characterization of the relations that are in operation between the observables, rather than the actual magnitudes of these quantities. As a consequence of this new postulate, Heisenberg suggested that the time-dependent position coordinate describing the position $x(t)$ should be replaced by a transition probability which describes the likelihood of transition between stationary states of the system. An example of an instance in which difference between observables is represented is with respect to the transition probability that is employed to describe the emitted energy per time. The previous classical description becomes more adequately described according to a transition probability in which the observable is no longer the position and period of the electron, but is adequately described as a difference between two variables which are discrete in nature. This provides a concrete example of the essential difference between the classical kinematic and newly re-formulated quantum kinematic theory.

The development of this formulation of quantum mechanics resulted in the award of a Nobel prize for Heisenberg in 1932. The main characteristic of the approach described by Heisenberg was the description of the quantities in terms of matrices. A year later a concomitant re-formulation of subatomic interactions was postulated by Erwin Schrödinger.² In this paper the foundations of quantum theory were also developed. However, in this approach reference was made to the observation that electrons, previously in the classical sense considered to be particles, could also be described in terms of waves.

Central to the description of the system by Schrödinger was the observation that there must be a representation of the dynamical interactions that are in operation between electrons. Schrödinger made this effect by reference to the geometry of optics. In this approach he argued that if it is possible to apply the theories of geometric optics to light rays, then the reversal of this approach could lead to the description of light rays in terms of an underlying geometry. From this line of reasoning the Schrödinger equation was formulated. A further description of the mathematical details of this expression is presented in the methodology section.

In this description Schrödinger employed partial differential equations to represent the wave equation, which was a more user-friendly mathematical methodology to theoretical physicists at the time, since matrices were not routinely used. As a consequence of the relative similarity of the outcomes of the two approaches employed by Heisenberg and Schrödinger to derive quantum mechanics, it was necessary to determine if these two outcomes were identical or similar. The follow up work carried out by Max Born and Paul Dirac concerned whether the separate formulations were to be regarded as distinct representations, with each describing something different, or whether they were identical in terms of that which they described in physical terms. Arguably the classical text on the underlying mathematical basis of quantum mechanics was that which was written by Paul Dirac 'Principles of Quantum Mechanics'.³ In this text Dirac established that the 2 formulations of quantum mechanics were identical, and that the difference attributed to the mathematical details was a manifestation of the fact that there are a number of

mathematical approaches that could be employed to generate the final form of the theory.

In addition to this fundamental textual contribution to the underlying theory of quantum mechanics, Dirac established that the relativistic contribution to the electron must also be taken into consideration if a complete description of the particle is to be considered. In this description, the electron is considered to be most accurately represented according to an expression that takes into consideration both the spin of the electronic system as well as the spatial component of the system.

The contribution made by Max Born was based on the description of the probabilistic nature of quantum theory. This resulted in the award of the Nobel prize in 1954 to Born. Born described that the electron was spread out in a manner which was not corpuscular in nature, but that the wave like character of the system was emphasized and that there could be a number of possible states of the system. Only under conditions in which the system was measured did it collapse to one of these possible states. This gave rise to the possibility that the probability distribution, itself the product of the wave-function and its complex conjugate, was in a number of possible states before the act of measurement was made. The discontinuous nature of the wave function is therefore emphasized in this description since the probability distribution is also subject to discontinuities. This behaviour was not emphasized in the original Schrödinger equation.

The next most significant contribution to the history of theoretical chemistry was the publication of the π -electron theory postulated by Erich Hückel.⁴ In this theory, Hückel suggested that the stabilization of an aromatic system is enhanced as a consequence of overlap of the π -electron orbitals of the aromatic system. This enhancement of stabilization is the result of the number of π -electrons that are present within the aromatic system. In instances where there is an even number of π -electrons, in the form of singly occupied p orbitals, doubly occupied p orbitals with a concomitant decrease in charge at the atomic centre, or unoccupied p orbitals with zero charge at the centre, then it is proposed that there will be no stabilization since there will be no net overlap of the orbitals.

In 1950 Roothan published a characterization of the approach based on the linear combination of atomic orbitals resulting in the formation of the molecular orbitals. This was based on solution of the pertinent equations based on a self-consistent field theory approach. A good review concerning the nature of this approach is presented by Roothaan.⁵ Subsequent to this approach was the publication of the Pariser-Pople-Parr theory.⁶ The essence of this theory is that the σ -electrons of an aromatic system should be permitted to adjust their position based on the instantaneous positions of the π -electrons of the system. To achieve this, the theory is associated with the assignment of empirical values to the coulombic integrals describing repulsion and penetration. When these values are employed there is an associated decrease in the singlet-triplet splitting and an associated decrease in configuration interaction. In addition there is no associated

complication observed with respect to the mathematics. Based on this ionic structures are subsequently enhanced.

The contributions to theoretical chemistry that were made by the above individuals are pertinent to the application of density functional theory (DFT) methodologies in chemical reactivity studies. There are other fundamental contributions to the history of theoretical chemistry that are also referred to. These include, for example, the earliest calculations carried out in theoretical chemistry based on quantum mechanical theory and were carried out by Walter Heitler and Fritz London in 1927.⁷ There are further numerous contributions that have been made by a wide range of individuals to theoretical chemistry. A detailed analysis of the work that such individuals have carried out is not presented here, however the following individual's contributions are noted. These include the influential textbook on the fundamentals of quantum mechanics to chemistry by Linus Pauling and E. Bright Wilson, *Introduction to Quantum Mechanics-with Applications to Chemistry*.⁸ Further textual contributions to the subject were made by Eyring, Walter and Kimball in 1944, *Quantum Chemistry, Elementary Wave Mechanics-with Applications to Wave Mechanics* by Heitler, written in 1944, as well as Charles Coulson's text, *Valence*, written in 1952. These are not referred to in this thesis as a consequence of the limitations of space, however, their contribution to the subject is noted. The main emphasis in this thesis has been to employ DFT to assist in the elucidation of a selection of reaction mechanisms.⁹ As a result, the fundamental and applied theoretical contributions made towards this field with direct respect to the elucidation of reaction mechanisms will now be discussed in greater detail.

The earliest contribution to DFT was made by Enrico Fermi and L.H. Thomas.^{10,11} In these landmark papers on the theory of DFT, there is use of orbital free approaches to describe the total energy of a molecular/atomic system in terms of the electronic density of the system. Such an expression of the energy is based on the utilization of the simplest functional that makes the energy physically acceptable. Further work was also carried out by Hohenberg¹², Kohn and Sham.¹³ In these papers it was demonstrated that it is possible to derive the ground state density and energy based upon the variation of the total density or the orbitals. Kohn-Sham theory was not widely known until the 1970's, when utilization of the approach by condensed matter physicists to describe the structures of bulk solids as well as their respective surfaces was undertaken. DFT has from that time forward been the dominant procedure for the elucidation of the structures of such materials.

During the period between 1970-1986 there have been several major contributors to the development and application of the theory underpinning DFT. These individuals include Parr,¹⁴ Jones and Gunnarsson,¹⁵ and Levy.¹⁶ Further theoretical work describing the validity of the Local Density Approximation (LDA) to accurately describe the structure of these materials was carried out by Langreth and Perdew.¹⁷ Since the early 90s the use of DFT to accurately describe the structures of a wide range of chemical systems has increased markedly. The frequency of use of the approach in chemistry has been comparable to the growth of DFT in the early 60s by condensed matter physicists. There have been a number of improvements of the functionals employed in DFT applications and these have been principally lead by Becke,¹⁸ and Pople.¹⁹

The continued theoretical development of the approach, such as treatment of the problem associated with dispersion, the continued parameterization of functionals to describe in increasing detail the energies associated with atomic and molecular structures, as well as the associated provision of applicability of the methodology to an increasing number of problems in both solid state physics and chemistry should ensure that the frequency with which the approach is referred to in research publications continues to increase.

1.2 Role of Theoretical Chemistry in organic reactivity.

Prior to the 1960s, before computers were employed to any significant extent to evaluate computational problems in chemistry, the vast majority of computational studies in chemistry were carried out using paper and pencil approaches. Amongst the earliest computational characterizations employed using microprocessor technology was the evaluation of the Urey-Bradley force constants by Overend and Scherer.²⁰ This paper was amongst the first to employ an algorithmic approach to the description of force constants. In this respect it provided a methodological description in computational terms of the details needed to derive these parameters. This paper was significant since Urey-Bradley force constants are used in the calculation of vibrational constants, which form the basis of the derivation of vibrational frequencies. These frequencies are employed to describe the details of the chemical reactivity of the molecule and its relative position on the potential energy surface (PES). The PES is a mathematical hypersurface which is generated as a result of solving the Schrödinger equation for a

number of nuclear geometries. The motion is solved using classical or quantum methods.

The earliest studies carried out with respect to the systematic computational characterization of organic and organometallic reaction mechanisms using DFT were performed by Andezelm.²¹ In this paper the authors employed an approach based on DFT Gaussian-type-orbitals (DGauss), and demonstrated that the resultant indicators of chemical functionality, such as vibrational frequencies, bond dissociation energies, equilibrium geometries as well as reaction barrier energies are significantly closer to experimentally derived values than those based on Hartree-Fock theory. This paper demonstrated that DGauss, itself an implementation of DFT, was found to be of similar accuracy to studies carried out using Hartree-Fock theory. From previous studies, basis sets optimized for utility in Hartree-Fock theory were shown to generate equilibrium structures to a high level of accuracy, however, the use of basis sets optimized in a DFT implementation, which incorporated corrections of a non-local nature to the description of the electronic density, were demonstrated to be essential for the accurate characterization of bond dissociation energies as well as reaction activation barriers.

Recent advances, those that have occurred within the last five years, have been numerous. An influential article documented the application of a stochastic structure searching methodology that selectively evaluated the energies of a number of possible conformers with the aim of identifying the conformer pertaining to the lowest energy on the PES was explained by Saunders.²² This is significant to organic reactivity studies

since the global minimum structure on the PES is that structure which is likely to predominate in nature. The vast majority of chemical optimization packages discern the closest minimum on the PES. This could theoretically correspond to the global minimum, but since this minimum is one amongst a considerable number of minima, then there is a higher level of probability that a non-global minimum will be generated based on such optimization approaches as referred to in the subsequent discussion on transition state optimization procedures. Methodologies which focus on the derivation of such lowest energy equilibrium structures are therefore of high relevance in computational studies of organic reaction mechanisms.

Another significant study involved the description of the quantitative computational indicators that specify aromaticity. Aromaticity and anti-aromaticity, which are qualitative indicators of stabilization and de-stabilization in aromatic groups, can be studied in a quantitative fashion using computational approaches. The essence of the delocalization which gives rise to aromaticity is based upon the π electrons of the aromatic/anti-aromatic group favoring delocalization of the electronic density. In addition the σ electrons also favor delocalization of the electronic density associated with these covalent bonds. The interaction between this delocalization and the tendency of the π orbitals to overlap with one another are the characteristics that give rise to aromaticity. This is the description of aromaticity which is consistent with that of Shaik, Hiberty and other colleagues.²³

Further description of the application of computational chemistry to organic mechanism characterization revolves around the description of the PES. To describe the mechanism of a chemical reaction in complete detail it is necessary to characterize the PES corresponding to the system of interest as a function of the nuclear coordinates. In terms of transition state theory, this is concerned with the evaluation of the region of the PES that surrounds the reactant(s), intermediates(s) and product(s). The saddle point will be first order under conditions in which the vibrational analysis of the geometry yields a single imaginary frequency and this is indicative of the derivation of a potential transition state corresponding to the reaction of interest. A commentary concerning the most significant contributions to transition state theory will follow, with particular reference made to the optimization approaches that are employed in such searches.

To derive the transition state geometry, use of optimization algorithms that calculate the Hessian matrix are employed. This is a matrix of second derivatives that are calculated with respect to the motion of the nuclei. The displacement of the nuclei occurs resulting in either an increase or decrease in the energy of the molecule. Under conditions in which the Hessian matrix contains negative values, then the nuclei are displaced in directions in which there is a decrease in the energy of the system. Under conditions in which the Hessian matrix contains positive values, then the nuclei are altered in directions in which there is an increase in the energy of the system. This optimization approach is referred to as the quasi-Newton technique, where the topology of the PES is quadratic in nature.²⁴ To describe the transition state properly it is helpful to attempt to generate a geometry that is as close to the correct transition state geometry as possible.

The correct selection of the coordinate system is also necessary in this instance. The initial estimate of the Hessian matrix must also be as accurate as possible, as well as the methodology by which the matrix is updated as the calculation proceeds, control of the direction of the search for the transition state and the step size. The use of Quasi-Newton algorithms with respect to the derivation of the transition states are more sensitive to the starting structure than other optimization approaches, such as the synchronous transit approach. Molecular mechanics approaches are generally not employed with respect to the calculation of transition states, since these approaches cannot in general take into consideration the breaking and forming of bonds. As a result minimizations that are based on such approaches are in general not employed when the characterization of transition state geometries are concerned. A number of standard transition state geometries have been published.²⁵ In general terms, however, there is a larger degree of variability in transition state geometries than there is in equilibrium structures.

Certain techniques are employed for the characterization of the transition states. These include, for example, synchronous transit.²⁶ In this approach a linear approximation is initially employed to describe the geometry of the transition state, which is initially computed as a geometry that is midway between the reactants and products. In physical terms this involves representing the transition state geometry by an arrangement in which the atoms are half way between the position at which they started and finished.²⁷ This approach is limited by the fact that there can be large inaccuracies with respect to the generated energies as a consequence of differences in bond length. A similar optimization approach corresponds to the quadratic synchronous transit method. In this

approach the geometry of the atomic coordinates of the atoms that compose the transition state are situated on a parabolic function connecting the reactant and product geometries.²⁸ Other methodologies can also be employed in the characterization of the transition state geometries.²⁹ These include coordinate driving, walking up valleys, and also eigenvector following.²⁹⁻³⁰

2. Methodology.

2.1 Quantum Mechanics.

Central to a discussion of the methodology that underpins Density Functional Theory is a description of the theoretical basis of the approach. The aim of a considerable number of Quantum Mechanical calculations is to generate a non-exact solution to the time-independent, non-relativistic Schrodinger equation represented below in equation 2.1.1³¹

$$\hat{H}\Psi_i\left(\vec{x}_N, \vec{R}_M\right) = E_i\Psi_i\left(\vec{x}_N, \vec{R}_M\right) \quad 2.1.1$$

In the above expression N and M correspond to the upper limits associated with the number of electrons and nuclei that are present within the system. This expression depends on the 3M spatial coordinates of the nuclei. The wave function contains all possible physical information concerning the quantum system. E_i corresponds to an eigenvalue, which represents the numerical value of the energy of the system described by the wave function. The Hamiltonian is a second order differential operator and is represented according to equation 2.1.2 in atomic units,³¹

$$\hat{H} = \frac{1}{2} \sum_{i=1}^N \nabla_i^2 - \frac{1}{2} \sum_{A=1}^M \frac{1}{M_A} \nabla_A^2 - \sum_{i=1}^N \sum_{A=1}^M \frac{Z_A}{r_{iA}} + \sum_{i=1}^N \sum_{j>i}^N \frac{1}{r_{ij}} + \sum_{A=1}^M \sum_{B>A}^M \frac{Z_A Z_B}{R_{AB}} \quad 2.1.2$$

In equation 2.1.2 above, A and B represent the interaction between two nuclei, whereas i and j represent the N electrons present within the system. The first two terms in the above expression represent the kinetic energy that is associated with the electrons and nuclei respectively.

A further simplification of the Schrödinger equation is possible when the difference between the masses of the nuclei and electrons are taken into consideration. This is based on the observation that the mass difference between the electrons and nuclei is of the order of 1800. Taking this difference into consideration results in a representation of the Hamiltonian that is based on the Born-Oppenheimer approximation. The nuclei are considered to be fixed in space with respect to position and the potential energy arising from the nuclei-nuclei interaction is represented by a constant. This results in the reduction of the Hamiltonian given above in equation 2.1.2 to the electronic Hamiltonian represented below in equation 2.1.3.³¹

$$\hat{H}_{elec} = -\frac{1}{2} \sum_{i=1}^N \nabla_i^2 - \sum_{i=1}^N \sum_{A=1}^M \frac{Z_A}{r_{iA}} + \sum_{i=1}^N \sum_{j>1}^N \frac{1}{r_{ij}} = \hat{T} + \hat{V}_{Ne} + \hat{V}_{ee} \quad 2.1.3$$

Solving the Schrödinger equation based on the electronic Hamiltonian generates the electronic wave-function in addition to the electronic energy. The electronic wave function depends upon the electronic coordinates only and the nuclear coordinates don't appear in this representation of the wave function. The total energy is therefore a sum of

the electronic energy and a constant representing the nuclear repulsion term. The form of this nuclear repulsion term is represented according to 2.1.4 below^{31,32}

$$E_{nuc} = \sum_{A=1}^M \sum_{B>A}^M \frac{Z_A Z_B}{r_{AB}} \quad 2.1.4$$

The expectation value of the \hat{V}_{Ne} operator corresponds to the external potential and represents an attractive interaction that is in operation between the electrons and the nuclei. External electric or magnetic fields are also possible sources of an external potential. In the representation given above, however, the external potential is primarily the result of the nuclear-electronic attraction. The square of the wave-function ψ^2 represents a probability distribution, since no physical interpretation can be ascribed to the wave-function alone.

To account for changes in electronic distributions under reaction conditions, alteration of the locations of electrons must be taken into consideration. As a consequence of this, following the switching of the coordinates of any of the electrons, the probability distribution must remain identical to that specified initially. The anti-symmetry principle follows from this and represents the scenario that when the electron coordinates are interchanged then the sign of the wave-function must also change. This condition applies to all fermions including electrons which are particles that possess half-integral spin. A further property of the probability distribution is that there must be a probability of unity

of observing the N electrons at some point in the volume elements represented by the distribution. This is formalized in the following expression³¹

$$\int \dots \int \left| \Psi \left(\vec{x}_1, \vec{x}_2, \dots, \vec{x}_N \right) \right|^2 d\vec{x}_1 d\vec{x}_2 \dots d\vec{x}_N = 1 \quad 2.1.5$$

Wave-functions that satisfy the unity condition given by 2.1.5 above are described as being normalized. To solve the Schrödinger equation for an atomic or molecular system involves the full description of the Hamiltonian \hat{H} . This involves the description of the number of electrons present in the system, N , as well as the external potential. The eigenfunctions are then determined in addition to the eigenvalues E_i of the Hamiltonian operator. All physical values of interest can then be determined via application of the Hamiltonian operator to the wave-function. No precise solution of the Schrödinger equation based upon this approach is currently available, save for a few instances such as the hydrogen atom. In consequence the approach employed is one in which the approximate wave function of the ground state is evaluated. This corresponds to the wave function that generates the lowest energy of the system. Such an approach involving the derivation of the ground state energy using the ground state wave function is termed the variational principle. The expectation value of an observable in quantum mechanics is represented according to the following notation, equation 2.1.6,³¹

$$\left\langle \hat{O} \right\rangle = \int \dots \int \Psi_{trial}^* \hat{O} \Psi_{trial} d\vec{x}_1 d\vec{x}_2 \dots d\vec{x}_N \equiv \left\langle \Psi_{trial} \left| \hat{O} \right| \Psi_{trial} \right\rangle \quad 2.1.6$$

³³The energy that is calculated from the above equation will correspond to an upper bound to the true energy of the system. In terms of formal notation this is represented according to the following expression below³¹

$$\left\langle \Psi_{trial} \left| \hat{H} \right| \Psi_{trial} \right\rangle = E_{trial} \geq E_0 = \left\langle \Psi_0 \left| \hat{H} \right| \Psi_0 \right\rangle \quad 2.1.7$$

The above equality is only true if the value of the trial wave function is identical to the ground state wave function. The approach involved in the variational principle is to derive the ground state energy and involves the minimization of $E[\Psi]$ via a search of all the physically acceptable N -electron wave functions. In terms of physically acceptable values of the wave functions then these must be capable of being quadratically integrable and continuous everywhere. Where these conditions are not satisfied then the normalization of the wave function would not be possible. The lowest energy function will be based on the ground state wave function. Following determination of N and V_{ext} the formation of the Hamiltonian is then possible which then allows the calculation of the ground state energy in addition to all the other values of the system. The ground state energy is then considered to be a functional of the number of electrons N and the nuclear potential V_{ext}

$$E_0 = \min_{\Psi \rightarrow N} E[\Psi] = \min_{\Psi \rightarrow N} \left\langle \Psi \left| \hat{T} + \hat{V}_{Ne} + \hat{V}_{ee} \right| \Psi \right\rangle \quad 2.1.8$$

2.2 Hartree-Fock approximation.

Solution of equation 2.1.8 is not possible by searching for all the acceptable N -electron wave functions. In practice a manageable subset of possible solutions are defined. This subset is obtained by considering the wave function as an anti-symmetrized product of N wave-functions represented as 1-electron systems.^{34,35,36} This is referred to as the Slater determinant. The shortened version of this expression is written below in equation 2.2.1³¹

$$\Phi_{SD} = \frac{1}{\sqrt{N!}} \det\{\chi_1(\vec{x}_1)\chi_2(\vec{x}_2)\dots\chi_N(\vec{x}_N)\} \quad 2.2.1$$

This is further simplified to a representation of the diagonal elements that represent the spin orbitals of the N electron wave function. These spin orbitals are composed of a spatial orbital and 1 of 2 possible spin functions. These are represented in the expression below, equation 2.2.2³¹

$$\chi(\vec{x}) = \phi(\vec{r})\sigma(s), \sigma = \alpha, \beta \quad 2.2.2$$

Such spin orbitals have the property that they are orthonormal. Formally this is represented with respect to the following conditions $\langle\alpha|\alpha\rangle = \langle\beta|\beta\rangle = 1$ and

$\langle \alpha | \beta \rangle = \langle \beta | \alpha \rangle = 0$. This indicates that the spin orbitals overlap when they are identical and there is no such overlap when the spin orbitals are different from each other. The form of the wave-function has been determined with respect to the above expressions. The subsequent aim is to determine the Slater determinant Φ_{SD} that yields the lowest energy value. In formal terms this corresponds to a minimization problem in which the lowest energy of the Slater determinant is derived. In terms of notation this can be written as follows, equation 2.2.3³¹

$$E_{HF} = \min_{\Phi_{SD} \rightarrow N} E[\Phi_{SD}] \quad 2.2.3$$

This characterization of the wave-function in terms of the Slater determinant leads into the determination of the Slater determinant that minimizes the energy of the system. This is another expression of the variational principle and corresponds to the minimization of the energy represented by the Slater determinant via alteration of the spin orbitals. These orbitals are constrained to remain orthonormal. The expectation value of the Hamiltonian is obtained via the expansion of the determinant and formation of the various components with respect to the components of the Hamiltonian. The final Hartree-Fock energy is represented by the following expression, equation 2.2.4.³¹

$$E_{HF} = \langle \Phi_{SD} | \hat{H} | \Phi_{SD} \rangle = \sum_i^N (i | \hat{h} | i) + \sum_i^N \sum_j^N (ii | jj) - (ij | ji) \quad 2.2.4$$

In the above expression, the kinetic energy and electron-nucleus attraction is represented according to the following expression, 2.2.5,³¹

$$\left(i \left| \hat{h} \right| i\right) = \int \chi_i^* \left(\vec{x}_1 \right) \left\{ -\frac{1}{2} \nabla^2 - \sum_A^M \frac{Z_A}{r_{1A}} \right\} \chi_i \left(\vec{x}_1 \right) d \vec{x}_1 \quad 2.2.5$$

The coulomb and exchange integrals are associated with the following expressions. These expressions are representative of the pertinent interactions between two electrons. In the first instance, the coulomb integral represents the contribution to the Hartree-Fock energy that is associated with respect to the repulsive interaction between two electrons, whereas the exchange integral represents the contribution to the Hartree-Fock energy associated with the exchange of position of two electrons in the system. These expressions are given by equation 2.2.6³¹ and 2.2.7³¹ respectively.

$$(ii|jj) = \iint \left| \chi_i \left(\vec{x}_1 \right) \right|^2 \frac{1}{r_{12}} \left| \chi_j \left(\vec{x}_2 \right) \right|^2 \quad 2.2.6$$

$$(ij|ji) = \iint \chi_i \left(\vec{x}_1 \right) \chi_j^* \left(\vec{x}_1 \right) \frac{1}{r_{12}} \chi_j \left(\vec{x}_2 \right) \chi_i^* \left(\vec{x}_2 \right) d \vec{x}_1 d \vec{x}_2 \quad 2.2.7$$

2.3 Density Functional theory.

The wave-function is dependent on $4N$ variables, 3 of which are spatial variables and 1 of which is a spin variable corresponding to each of the N electrons of the system. In bio-molecular and materials science for example, the systems under analysis are typically very large systems containing an unmanageable number of electrons. A consideration of whether the wave-function is needed to gain a complete description of the system indicates that such a complex function may not be required, since the Hamiltonian operator only contains operators that act on 1 or 2 particles at any given time. The wave function may therefore contain information that is not relevant, and a quantity that is less complex may be sufficient to gain information relating to the energy and other relevant properties of the system. The aim in this approach is to identify a property that accurately describes conformational space, in addition to providing a mechanism to generate a solution to the Schrödinger equation. Using a combination of logical arguments, it is possible to demonstrate that the electronic density can be employed to form the Hamiltonian operator for the system. This flow of arguments begins with the observation that the Hamiltonian operator is characterized by the number of electrons in the system, N , the nuclei positions, R_A , as well as Z_A , the charges of the nuclei. The Schrödinger equation can then be solved once all the above information is available and the Hamiltonian operator has been described. The electronic density when integrated generates the number of electrons that are present in the system. This is summarized in equation 2.3.1.³¹

$$\int \rho(\vec{r}_1) d\vec{r}_1 = N \quad 2.3.1$$

The electronic density displays maxima at positions R_A . These regions are cusps. In addition to this, it is also the case that electronic density at the nuclei displays information relating to the charge of the nuclei. Formally this can be summarized in the following equation, 2.3.2³¹

$$\lim_{r_A \rightarrow 0} \left[\frac{\partial}{\partial r} + 2Z_A \right] \rho(\vec{r}) = 0 \quad 2.3.2$$

The above equations indicate that the Hamiltonian operator can be formed from the electronic density. Based on equations 2.3.1 and 2.3.2 it is demonstrated that the electronic density can be employed in the determination of all of the relevant molecular properties. The remaining problem in deriving these properties is centred on finding a solution to the associated Schrödinger equation.

The use of Density Functional Theory as a framework to derive the atomic and molecular properties of the system is centred on the work undertaken by Thomas¹¹ and Fermi.²⁹ Of principal significance in this theoretical approach is treatment of the electrons from a quantum statistical model. The kinetic energy of the electrons are taken into account within this framework, while the positive attractions between the nuclei and

the electrons, as well as the repulsive electronic interactions are treated in an entirely classical fashion.

The above expression for the energy within this model is a characterization of the energy of the system based on electronic density with no reference made to the wave function. The next approach in the accurate characterization of the energy is how to identify the correct electronic density of the system. To achieve this using the Thomas-Fermi model, the variational principle is again employed.

2.4 Hohenberg-Kohn Theorems.

Central to the first Hohenberg-Kohn theorem is the statement that there is an external potential that is associated with an electronic density. The parameters of the Hamiltonian operator are directly affected by the magnitude of the external potential. As a consequence of this interdependency it is observed that the ground state electronic energy is a functional of the electronic density. Two external potentials are considered, V_{ext} and V'_{ext} . The two external potentials are components of two Hamiltonians that differ in the external potential. Formally this can be represented in the following notation,

$\hat{H} = \hat{T} + \hat{V}_{ee} + \hat{V}_{ext}$ representing one Hamiltonian and external potential, and

$\hat{H}' = \hat{T} + \hat{V}_{ee} + \hat{V}'_{ext}$ representing the other Hamiltonian and external potential. These two

different Hamiltonians are associated with two different wave functions, Ψ and Ψ' , which are represented by two different ground state energy values, E_0 and E'_0

respectively. These two separate values for the ground state energy must, by definition, be non-equivalent, since the ground state energy must be unique. It is assumed that both wave functions generate an identical electronic density. This is conceivable, since a process of quadrature determines the mechanism by which a wave function is generated by an electronic density. This can be represented formally in the following expression³¹

$$\rho(\vec{r}) = N \int \dots \int \left| \Psi(\vec{x}_1, \vec{x}_2, \dots, \vec{x}_N) \right|^2 ds_1 d\vec{x}_2 \dots d\vec{x}_N \quad 2.4.1$$

2.4.1 is not a unique specification. When the above is represented in the nomenclature of the previous chapters, this can be represented in the following format,³¹

$$V_{ext} \Rightarrow \hat{H} \Rightarrow \Psi \Rightarrow \rho(\vec{r}) \Leftarrow \Psi' \Leftarrow \hat{H}' \Leftarrow V'_{ext} \quad 2.4.2$$

In equation 2.4.2 the two wave functions Ψ and Ψ' are not identical. Ψ' is employed as a trial wave function for the Hamiltonian operator \hat{H} . The variational principle is then employed to describe the differences in energy associated with the respective wave functions. Formally this is represented in terms of the expectation value of the wave function and is written in the following way³¹

$$E_0 \langle \Psi' | \hat{H} | \Psi' \rangle = \langle \Psi' | \hat{H} | \Psi' \rangle + \langle \Psi' | \hat{H} - \hat{H}' | \Psi' \rangle \quad 2.4.3$$

2.4.3 can be expressed alternatively since the only difference between the Hamiltonian operators is associated with the external potential. This results in an alternative expression represented in 2.4.4³¹

$$E_0 < E'_0 + \langle \Psi' | \hat{T} + \hat{V}_{ee} + \hat{V}_{ext} - \hat{T} - \hat{V}_{ee} - \hat{V}'_{ext} | \Psi' \rangle \quad 2.4.4$$

Using the nomenclature of density functional theory, 2.4.4 can be expressed in the following form, 2.4.5³¹

$$E_0 < E'_0 + \int \rho(\vec{r}) \{V_{ext} - V'_{ext}\} d\vec{r} \quad 2.4.5$$

The external potentials in 2.4.5 can be switched producing the following expression, 2.4.6³¹

$$E'_0 < E_0 - \int \rho(\vec{r}) \{V_{ext} - V'_{ext}\} d\vec{r} \quad 2.4.6$$

When equations 2.4.5 and 2.4.6 are summed, the result is an incompatible outcome in which both the same terms on either side of the inequality are identical, but the right hand side of the inequality is considered greater than the left hand side of the inequality. Formally this can be represented in 2.4.7³¹

$$E_0 + E'_0 < E'_0 + E_0 \quad 2.4.7$$

The conclusion that is to be taken from the above derivation is that two external potentials cannot generate an identical electronic density corresponding to the ground state. The electronic density of the ground state, therefore, characterizes in a completely specified way, the external potential of the system, V_{ext} . The electronic density corresponding to the ground state can be represented as containing details concerning N , Z_A and R_A respectively. This can be summarized accordingly, $\rho_0 \Rightarrow \{N, Z_A, R_A\} \Rightarrow \hat{H} \Rightarrow \Psi_0 \Rightarrow E_0$. The electronic density of the ground state is expressed in terms of being a functional of the electronic density of the ground state. As a consequence of this, the separate parts of the energy of this ground state can also be expressed in terms of these different terms. In a formal sense this can be written as a sum of terms, represented in equation 2.4.8³¹ below,

$$E_0[\rho_0] = T[\rho_0] + E_{ee}[\rho_0] + E_{Ne}[\rho_0] \quad 2.4.8$$

2.4.8 can be written in terms of the parts that are dependent upon the system, and are therefore dependent on the values of N , R_A , Z_A , and those parts of the expression that are independent of the system. The potential energy arising from the interaction of the nuclei and electrons are clearly dependent upon the values of N , R_A and Z_A . This can be represented in the following expression, equation 2.4.9³¹ below,

$$E_{Ne}[\rho_0] = \int \rho_0(\vec{r}_0) V_{Ne} d\vec{r} \quad 2.4.9$$

In terms of the system independent parameters, the energy expression in terms of those parts that are system dependent and independent respectively can be represented in the following expression

$$E_0[\rho_0] = \int \rho_0(\vec{r}) V_{Ne} d\vec{r} + T[\rho_0] + E_{ee}[\rho_0] \quad 2.4.10$$

The parts of the above sum corresponding to the energy of the system that are significant irrespective of the system are $T[\rho_0] + E_{ee}[\rho_0]$. These terms can be collected into another expression. Such an expression corresponds to the Hohenberg-Kohn functional $F_{HK}[\rho_0]$ and is represented in combination with the system dependent parts of the energy according to 2.4.11³¹ below,

$$E_0[\rho_0] = \int \rho_0(\vec{r}) V_{Ne} d\vec{r} + F_{HK}[\rho_0] \quad 2.4.11$$

The significance of the above expression is such that if an electronic density $\rho(\vec{r})$ is considered to be an argument of the Hohenberg-Kohn (HK) functional, then the result of the computation corresponds to the following expectation value $\langle \Psi | \hat{T} + \hat{V}_{ee} | \Psi \rangle$. This

corresponds to a sum of the kinetic energy and a repulsion operator describing the electron-electron interaction operator in addition to the wave function Ψ that is associated with this electronic density. The HK functional is therefore represented in the following expression, 2.4.12²⁸

$$F_{HK}[\rho] = T[\rho] + E_{ee}[\rho] = \left\langle \Psi \left| \hat{T} + \hat{V}_{ee} \right| \Psi \right\rangle \quad 2.4.12$$

2.4.12 is the formal mathematical definition of the HK functional; however the exact composition in terms of energetic parameters remains undefined.

Under conditions where the exact composition of the HK functional were known then it would be possible to find an exact solution to the Schrödinger equation, without the requirement to resort to increasingly accurate approximations of the HK functional. 2.4.12 is equally valid in terms of applicability to molecules that are significantly different in terms of atomic composition. The main uncertainty associated with the HK functional surrounds the composition of the functional describing the kinetic energy and also that which describes the repulsion results as a consequence of the electronic interactions. The Coulomb component $J[\rho]$ of the electron-electron interactions is known from previous discussions and is written according to the following expression, 2.4.13,³¹

$$E_{ee}[\rho] = \frac{1}{2} \iint \frac{\rho(\vec{r}_1)\rho(\vec{r}_2)}{r_{12}} d\vec{r}_1 d\vec{r}_2 + E_{ncl}[\rho] = J[\rho] + E_{ncl}[\rho] \quad 2.4.13$$

$E_{ncl}[\rho]$ is a composite of all terms describing the self-interaction correction, in addition to the exchange and Coulomb correlation that have been described in the previous discussions. The identification of the exact composition of the unidentified functionals $T[\rho]$ and $E_{ncl}[\rho]$ is the main problem that is associated with Density Functional Theory. A significant amount of the published work that is carried out in DFT is associated with describing the interaction between the system independent parts of the energy at increasingly more accurate levels. The Hamiltonian operator is described in a unique fashion by the electronic density that characterizes both the ground and excited states of the system. In this respect then, all of the properties of the system are formally derived from the density of the ground state. It should be noted, however, that to accurately describe the excited state of the system, another functional would be required in addition to the functional that describes the ground state energy. The significance of the ground state density is that it is the only density that contains information concerning the nuclear positions and charges. This information allows the density to be mapped onto the external potential. This cannot occur when the excited state density is employed.

All of the physically relevant properties of the system can be determined from the ground state electronic density. The problem associated with such a scenario is, how can

one determine the density that corresponds to the ground state density? To establish the density corresponding to the ground state, a formal approach, first expounded by Hohenberg and Kohn in 1964¹² is employed. The essence of this theorem is that the ground state energy is obtained only under conditions in which the input electronic density corresponds to the density that describes the ground state. In formal mathematical terms this can be expressed in the following way, 2.4.14,³¹

$$E_0 \leq E[\tilde{\rho}] = T[\tilde{\rho}] + E_{Ne}[\tilde{\rho}] + E_{ee}[\tilde{\rho}] \quad 2.4.14$$

The above expression can be interpreted as stating that if a test electronic density (Density term here) is chosen that is satisfactory with respect to the boundary conditions, these being that the electronic density must be greater than zero, $\tilde{\rho}(\vec{r}) \geq 0$, and that the total electronic density must integrate to the number of electrons present in the system $\int \tilde{\rho}(\vec{r}) d\vec{r} = N$, then an external potential must also be associated with the electronic density, and the energy that is generated from equation 2.5.1 corresponds to an upper boundary with respect to the ground state energy E_0 .

2.5 Kohn-Sham theory

Following the identification by Hohenberg and Kohn regarding the universal functional that relates the density to the ground state, Kohn and Sham carried out work concerning

how to approach the functional in terms of practical utility. The main difficulty associated with the density functionals such as that described by Thomas and Fermi is with respect to the determination of the kinetic energy. Kohn and Sham introduced an electronic system that is non-interacting with respect to the 1-electron functions and was based on the realization that approaches based on orbitals such as the Hartree-Fock method are more effective in describing the kinetic energy. This approach allows the majority of the kinetic energy to be calculated to a very high level of accuracy. Contributions that are non-classical and representative of the electron-electron repulsion are then employed to permit the remaining component of the kinetic energy to be determined. Accurate computation of a considerable amount of the kinetic energy is determined, which then leaves only a small amount of the overall energy to be evaluated via an inexact functional.

The kinetic energy of the non-interacting system is not equal to that of the interacting system, even though the densities could be equivalent. Equation 2.5.1³¹ documents the expression for the computation of the non-interacting kinetic energy.

$$T_s = \frac{1}{2} \sum_i^N \langle \varphi_i | \nabla^2 | \varphi_i \rangle \quad 2.5.1$$

As a consequence of the non-equivalence between the kinetic energies of the interacting and non-interacting systems, irrespective of whether the systems display the same density, Kohn and Sham separated the energies of the functional in the following manner, 2.5.2,³¹

$$F\left[\rho\left(\vec{r}\right)\right]=T_S\left[\rho\left(\vec{r}\right)\right]+J\left[\rho\left(\vec{r}\right)\right]+E_{XC}\left[\rho\left(\vec{r}\right)\right] \quad 2.5.2$$

In the above expression, E_{XC} corresponds to the exchange-correlation energy. This energy is described in the following way, represented below in equation 2.5.3³¹

$$E_{XC}[\rho] = (T[\rho] - T_S[\rho]) + (E_{ee}[\rho] - J[\rho]) = T_C[\rho] + E_{ncl}[\rho] \quad 2.5.3$$

In equation 2.5.3, T_C refers to the difference in kinetic energy between the non-interacting reference system (T_S) and the fully interacting system (T). Since there is no term that describes the details of the exchange-correlation energy E_{XC} as such, this term is subject to approximation using various functionals. The variational principle is applied to generate a minimum with respect to the energy expression given in equation 2.5.3. If the precise forms of E_{XC} and V_{XC} were known in detail, then it would be possible to solve the Schrodinger equation exactly using the methodology of the Kohn-Sham approach.

The Kohn-Sham methodology is, by definition, an exact approach, only where it is necessary to characterize the exchange-correlation energy, and the potential associated with it, is it necessary to introduce a form for the approximate functional describing

these terms. A large part of research in DFT is therefore concerned with developing ever increasingly accurate approximations to this E_{XC} functional.

2.6 Generalized Gradient Approximations.

In a homogeneous system the performance of the local or local spin density functional is satisfactory. The term local is employed to describe the representation of the electronic density of a system in which this property is uniformly distributed throughout the system. As a result of this distribution, each location within the system can be represented identically with respect to the density and no further consideration of the changes in this property out-with this region need be characterized. However, in a non-homogeneous system, in which there is variation in density, the performance of the functional must be improved to take this into account. This is taken into consideration with respect to the introduction of the gradient of the charge density in the region proximal to the reference electron. The structures of the gradient-corrected correlation functionals are more complex with respect to analytical form. These employ empirical parameters and are arguably not fundamentally representative of the physics underlying the exchange-correlation process. An exchange-correlation functional that includes an empirical parameter is included in the correlation equivalent of the functional named after Perdew³⁷, referred to as P or P86. A non-empirical free functional was employed and forms the basis of the PW91 functional. A correlation functional that is employed in calculations in present day DFT work is the functional derived by Lee, Yang and Parr³⁸, LYP. This functional is not based on a homogeneous electron gas, but the correlation

energy of helium is employed in which a precise correlated wave function based on a wave function approach is employed. This functional contains a single empirical parameter. These functionals treat dynamical (short-range correlation effects) but don't treat non-dynamical effects in any way. The combination of exchange and correlation functionals is possible. The component describing exchange is most frequently chosen as Becke's functional. This is combined with the either Perdew's 1986 correlation functional or alternatively the LYP functional.

2.7 Hybrid Functionals.

It has been noted that the contribution from exchange is much larger than that arising from correlation. Correctly representing the functional for exchange is therefore essential for the derivation of results that are meaningful in DFT approaches. The exchange energy can be determined precisely via evaluation of the Slater determinant. To evaluate the total exchange-correlation involves taking the sum of the exact exchange energy and the correlation energy. The correlation energy is approximated using one of the respective functionals referred to above. Performance in atoms is very good, however, this is not reflected in molecules or bonding scenarios. When compared to the G2 set of reference energies there is a mean error of 78 kcal/mol with respect to Hartree-Fock level of theory, in this instance exact exchange is in operation only. Under conditions where a functional that represents correlation is included the error is reduced to 32 kcal/mol.

This contrasts poorly when consideration is given to the exchange-correlation energies of the generalized gradient approximation form, in which both exchange and correlation are represented in an approximate fashion. Exact exchange can be treated in an alternative fashion. The main mechanism to generate the exchange-correlation energy is to vary the level of contribution of the non-classical energy contribution from 0 to 1. This is essentially equivalent to integrating the exchange-correlation hole coupling-strength. In formal terms this corresponds to the energy of the non-classical component of the interaction describing electron-electron interaction with respect to the variation of λ . The kinetic energy is incorporated into the exchange-correlation energy via integration with respect to λ . In formal terms this is represented according to the following expression, equation 2.7.1,

$$E_{XC} = \int_0^1 E_{ncl}^{\lambda} d\lambda \quad 2.7.1$$

When $E_{ncl}^{\lambda=0}$ there is contribution from exchange only. No contribution from correlation is observed. This is equal to the contribution to exchange of the Slater determinant. An exact value for $E_{ncl}^{\lambda=0}$ can be computed provided that the KS orbitals have been made available. Both electron correlation and non-classical contributions are included in the expression for E_{XC} when $\lambda = 1$. This energy is not known, but can be approximated by an exchange-correlation functional of any nature. It is possible to derive the precise energy for $\lambda = 0$ and to approximate the energy for $\lambda = 1$ to a high degree of accuracy.

It is therefore necessary to generate values of the energy ($E_{ncl}^{\lambda=1}$) for values of λ which are intermediate. Solving equation 2.7.1 results in a solution that is “half-and-half”, representative of a combination of exact exchange and exchange-correlation as described elsewhere.²³

$$E_{XC}^{HH} = \frac{1}{2} E_{XC}^{\lambda=0} + \frac{1}{2} E_{XC}^{\lambda=1} \quad 2.7.2$$

Semi-empirical coefficients were subsequently introduced into equation 2.7.3. This produces a weighting of the various contributions of each term of the exchange-correlation, exchange, and correlation terms. The form of this expression is given in equation 2.7.3³⁹

$$E_{XC}^{B3} = E_{XC}^{LSD} + a(E_{XC}^{\lambda=0} - E_X^{LSD}) + bE_X^B + cE_C^{PW91} \quad 2.7.3$$

Exact exchange is given by a, while b and c dictate contributions of the gradients for exchange and correlation. Optimal values corresponding to a=0.20, b=0.72, c=0.81 were determined based on an optimal fit of proton affinities, and atomization/ionization energies to the G2 set of energies. There was a decrease in the amount of exchange energy compared to the half and half scheme. There was a reduction of the absolute error for atomization energies to 2-3 kcal/mol, which is within the accepted chemical accuracy error of 2 kcal/mol. These class of functionals are the hybrid functionals, since

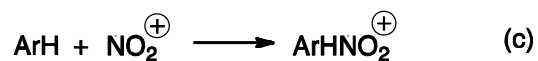
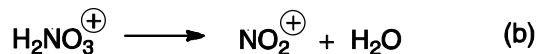
they involve a combination between density functionals for exchange and those describing Hartree-Fock exchange, the latter being an exact representation of the energy. The most popular hybrid functional is B3LYP. The form of this functional is represented in equation 2.7.4,

$$E_{XC}^{B3LYP} = (1-a)E_X^{LSD} + aE_{XC}^{\lambda=0} + bE_X^{B88} + cE_C^{LYP} + (1-c)E_C^{LSD} \quad 2.7.4$$

3.0 The Nitration of 6-Chloropyrimidin-4(3H)-one.

3.1 Introduction to electrophilic aromatic nitration.

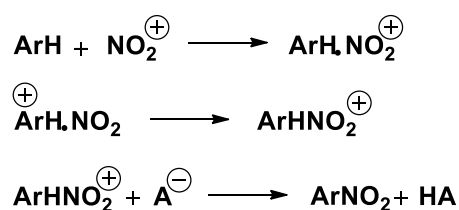
Nitration belongs to the class of reactions corresponding to electrophilic aromatic substitutions. In general mechanistic terms, electrophilic aromatic nitration has been speculated to proceed according to a number of possible schemes. The most widely accepted scheme for the process is the Ingold-Hughes mechanism, represented in the following scheme below.⁴⁰



Scheme 3.1.1. Ingold-Hughes mechanism describing electrophilic aromatic nitration.

The above mechanism is also based on the work carried out by the same authors.⁴¹ The pathways represented by (a)-(d) correspond to the formation of nitrous acid (a), its subsequent dissociation to the nitronium ion and water (b), initial attack on the aromatic molecule by nitronium followed by formation of the Wheland intermediate (c). Pathway (d) corresponds to the generation of the de-protonated nitrated product with regeneration of the molecule composing the solvent system. Central to this mechanism is the formation of a positively charged Wheland intermediate/arenium ion (product of reaction (c), scheme 3.1.1) following electrophilic attack by NO_2^{\oplus} on the π system of the aromatic group. This intermediate has been characterized as a discrete σ complex.

Formation of a π complex, which corresponds to a weakly bound NO_2^+ aromatic system stabilized by $\pi-\pi$ interactions, may occur prior to the formation of this σ complex.^{39-40, 42} In addition to this intermediate there may also be a single electron transfer from the aromatic system to NO_2^+ .⁴³ This is represented according to Scheme 3.1.2. This is also a π system (electron donor complex) and may occur prior to the Wheland ion σ intermediate and then subsequently collapse producing the above σ arenium ion. There is evidence for⁴³ and against⁴⁴ the formation of this complex. This complex is suggested not to be orientated in a definite sense with respect to the position of the nitronium ion in relation to the aromatic ring. There is a high level of electrostatic and charge transfer interactions in operation between these two groups, suggesting that a relatively large number of possible orientations are possible. These interactions explain the highly selective number of positions of attack by the nitronium ion on the aromatic system, with concomitantly low selectivity observed to occur with respect to the aromatic system that is attacked.

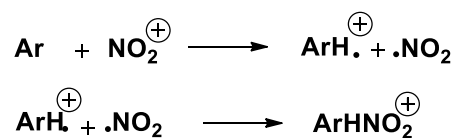


Scheme 3.1.2. Olah's mechanism describing electrophilic aromatic nitration.

The mechanism proposed by Olah is not consistent with an alternative mechanistic proposal in which there is an empirical selectivity rule considered.⁴⁵ The rate constant

for the nitration reaction is very close to the rate constant for diffusional control,⁴⁶ this suggests that the initial complex formed corresponds to an encounter pair, with no discrete complex being formed.

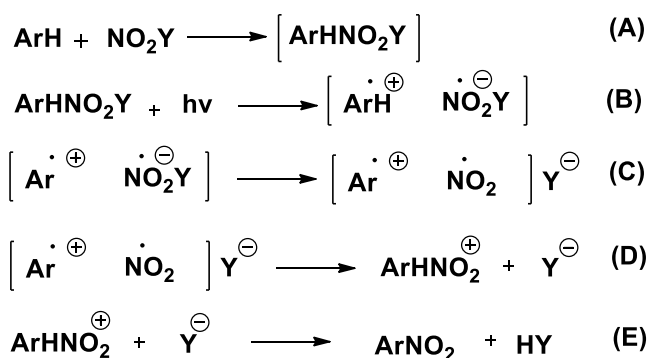
In an alternative proposal, after Schofield,⁴⁷ there is suggested to be an encounter pair formed between the aromatic group and NO_2^+ . The interaction between these two groups in this encounter pair is not covalent in nature; the interacting molecules are proposed to be held together by a solvent cage. This mechanism is represented in the following scheme



Scheme 3.1.3. Schofield's mechanisms for the single electron transfer mechanism of electrophilic aromatic nitration.

The validity of the above mechanism is unclear since it has been observed that there has been high regioselectivity and low substrate selectivity in electrophilic nitration in the gas-phase.⁴⁸ This observation precludes the suggestion by Schofield that the encounter pair is held together in the solvent cage.

The above mechanisms are polar electrophilic aromatic mechanisms in which there is proposed to be a 2-electron transfer process between the interacting molecules. The possibility of a single electron transfer pathway has been suggested by a number of authors.^{45,46,48-55} Central to this suggestion is the proposal that a radical pair is formed as an initial step in the reaction.



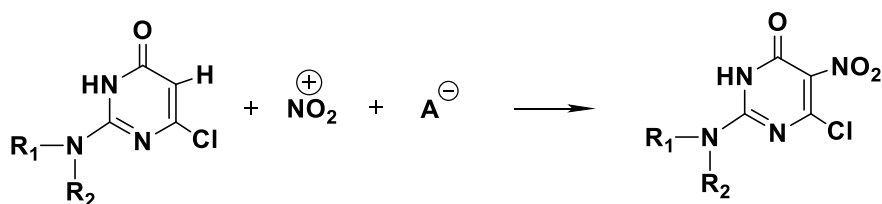
Scheme 3.1.4. Kochi mechanism describing single electron transfer in electrophilic aromatic nitration.

In the above scheme, Y^- is considered to be the anion which is associated with the solvent system. The rate of the above reaction is dictated by the rate at which the ion-pair is formed. In the above scheme this corresponds to step B. This step also defines the substrate selectivity. The spin density that is in operation in the aromatic cation radical governs regioselectivity (positional selectivity) of the reaction. This corresponds to the collapse of the radical complex into the positively charged intermediate, the Wheland intermediate, represented in reaction D, Scheme 3.1.4. The details of this step are uncertain, since the reaction rates as predicted by Marcus theory are significantly lower than those that are observed in solution. In addition the energy that is required to remove an electron from a benzene ring or a less reactive aromatic ring is unfavourably large. In aromatic rings that are more electron rich than benzene, however, the energy becomes increasingly more favourable. Irrespective of which mechanism is in operation, it is considered that the 1 and 2 electron systems combine at a particular point in the

mechanism, resulting in the same product irrespective of which reaction version predominates at intermediate points in the reaction.

3.2 Computational Methods.

The aim of this section of the project has been to account for the difference in reactivity observed between three amine substituted analogues of 6-chloropyrimidin-4(3H)-one, (a) 2-methylamino (b) 2-dimethylamino (c) 2-amino. The 2-amino analogue, represented in reaction with NO_2^+ in Scheme 3.1.1, was observed to generate a satisfactory yield of the nitrated product. Under conditions in which this electrophilic aromatic addition reaction is performed with respect to the 2-methylamino analogue, no yield of product is observed to occur. To account for these differences in reactivity, various mechanisms were evaluated in terms of thermodynamic feasibility, by determining the relative changes occurring with respect to a series of indicators. These included the Gibbs free energy, entropy, electronic energy, enthalpy and zero-point energies respectively. To evaluate these parameters the functional B3LYP and the basis set 6-311G(d,p) were employed. The choice of basis set was based on previous work related to the study of nitration.⁴⁹



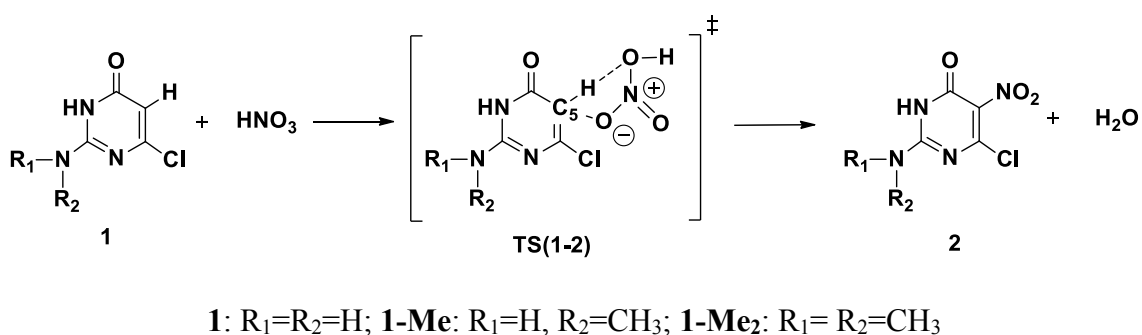
Scheme 3.2.1 Overall reaction scheme corresponding to the addition of NO_2 to analogues of 6-chloropyrimidin-4(3H)-one.

To determine the mechanism(s) by which the above reaction proceeds with respect to the methylated and un-methylated analogues, a series of schemes were proposed, with reference made to addition of nitronium at either the same or different atomic positions in the two different analogues. When the addition of NO_2^+ is proposed to occur at the same position in both analogues, it was observed that there were no energetic differences that would account for the differences in the reactivity, since all changes in free energy were either exergonic or endergonic, thus favoring or dis-favoring both scenarios together. The aim was therefore to attempt to characterize a similar mechanism for both analogues and look for a different energetic change, or alternatively to propose a different mechanism in both instances and observe the differences in energy produced.

3.3 Results and Discussion.

3.3.1 The Concerted Mechanism.

The initial attempt to generate mechanistic data focused on the direct attack on C-5 by HNO_3 . This step involved the proposal that the addition of NO_2^+ and so thought an abstraction of the H atom associated with C-5, producing H_2O , and the concomitant electrophilic attack by NO_2 on the resultant carboanion (Scheme 3.3.1).



Scheme 3.3.1. Mechanistic proposal corresponding to direct electrophilic attack by HNO_3 .

The transition state for the above mechanistic proposal in each of the three cases was established by the presence of a single imaginary frequency. The relative changes occurring with respect to the enthalpy for each of the 3 scenarios (1, 1-Me, 1-Me₂), represented in Table 3.3.1, below, showed that this mechanism was not likely to be competitive.

Transition state	ΔE	ΔH	ΔG
TS(1)	60.71	57.03	68.30
TS(1-Me)	59.88	56.31	68.20
TS(1-Me₂)	59.95	56.36	68.99
TSC₁(1)	49.66	47.74	70.21
TSC₁(1-Me)	—	—	—
TSC₁(1-Me₂)	48.20	46.62	70.80
TSC₂(1)	50.2	47.84	72.26
TSC₂(1-Me)	48.8	46.89	71.82
TSC₂(1-Me₂)	47.3	45.39	71.57

Table 3.3.1. Summary of relative differences in SCF energy, enthalpy, and Gibbs free energy with respect to formation of transition state **TS(1-2)** from reactant analogues **1**, **1-Me** and **1-Me₂** respectively. All values in kcal/mol. The essential features of the **TSC₁** and **TSC₂** geometries correspond to the inclusion of an additional, catalytic water molecule in different orientations.

In the **TSC₂** instance the optimal relative energies are slightly lower with respect to formation of the **1-Me₂** analogue, but higher with respect to formation of **TSC₂(1)**. This is suggested to be the consequence of an alteration in the input geometries in each of the analogues, principally in the reaction centre. Based on the differential between the relative energies corresponding to formation of **TSC₁** and **TSC₂**, these changes are

suggested to favour the stabilization of the TSC_2 complex in the $\mathbf{1-Me}_2$ case and dis-favour formation in the $\text{C}_2(\mathbf{1})$ case.

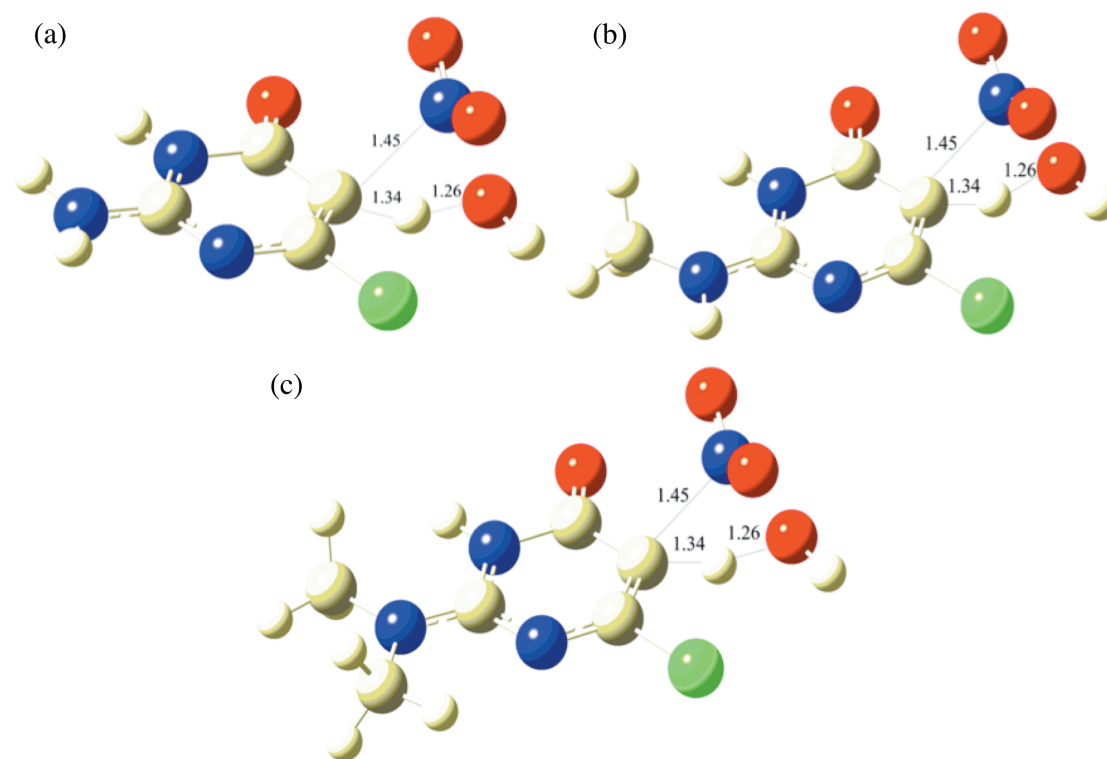


Figure 3.3.1. Molecular representation of optimized transition state structures for (a) **TS(1)**, (b) **TS(1-Me)** and (c) **TS(1-Me₂)**. Distances in Å.

When consideration is given to the relative enthalpies of formation for each of the transition states corresponding to **1**, **1-Me** and **1-Me₂** scenarios represented in Figure 3.3.1 and correlation with the principal inter-atomic distances in operation within the respective TSs it can be seen that in terms of steric considerations there are identical

inter-atomic distances between C-5-N, C5-H, H-OH and in all cases tested. This may indicate that there is a similar level of cumulative electronic density in operation within this region and this can be represented in the relative equivalence of the enthalpies which are observed. This may indicate that the relative enthalpy values pertaining to the formation of these TSs are dependent upon the principal inter-atomic distances within the region at which reactivity is occurring. It is suggested that the inductive effect is not operating within this system of mechanisms.

When an analysis of the charges in these atoms is undertaken it can be seen that there is negative charge associated with the C of the CH₃ group which is bonded to N of **1-Me**. This suggests that there is transfer of electronic charge from N onto C of CH₃, which is consistent with the observation that CH₃ may be functioning to withdraw electron density from N of **1-Me**. This may indicate that there is delocalization of charge within the aromatic nucleus which is contributing to stabilization via the inductive effect arising from the presence of the CH₃ group. When consideration is given to the presence of an additional CH₃ group on the N(CH₃)₂ analogue it can be observed that the presence of an additional group doesn't influence the relative enthalpy change in a significant manner, since these changes are 56.31 kcal/mol in the **1-Me** case and 56.36 kcal/mol in the **1-Me₂** case. There is observed to be a similarly negative charge on the C of the additional CH₃ group, which intuitively suggests that there may be an additive electron withdrawal effect associated with the presence of this group. This is not reflected in the relative changes in enthalpy which have been recorded. From the principal inter-atomic distances represented in Figure 3.3.1 for each of the three analogues, it can be seen that

there is no difference in the C-5-N distance (1.45 Å in all cases). This suggests that the inductive effect is not in operation within these systems, or alternatively there maybe stabilization offered with respect to the presence of the hydroxyl group which prevents any major change in the orientation of this moiety, thereby offsetting any inductive effect.

When consideration is given to the changes in relative energy with respect to the formation of these transition states in each of the scenarios tested (Table 3.3.1), it can be observed that there is a high energetic requirement involved in the formation of each of the respective transition states, with an average change in electronic energy of 60.12 kcal/mol, an average change in the enthalpy of 56.57 kcal/mol and an average change in the Gibbs free energy of 68.5 kcal/mol. From these high energetic requirements for the formation of the transition states **TS(1)**, **TS(1-Me)** and **TS(1-Me₂)**, it is suggested that these mechanisms would not be competitive. As a result another mechanistic scenario was postulated in which there is speculated to be the involvement of an additional water molecule that facilitates proton transfer.

These transition states are represented in Figures 3.3.2 and 3.3.3 respectively. The main differences between these correspond to the input “guess” geometries. The consequence of altering these input “guess” geometries is an alteration in the optimized geometries, producing relative enthalpies which are lower in magnitude. In the geometries represented in Figure 3.3.3, the resultant relative enthalpy changes are observed to be

lower than those corresponding to Figure 3.3.2. This suggests that the latter geometries are either global or nearer to global minima than those reported for Figure 3.3.2.

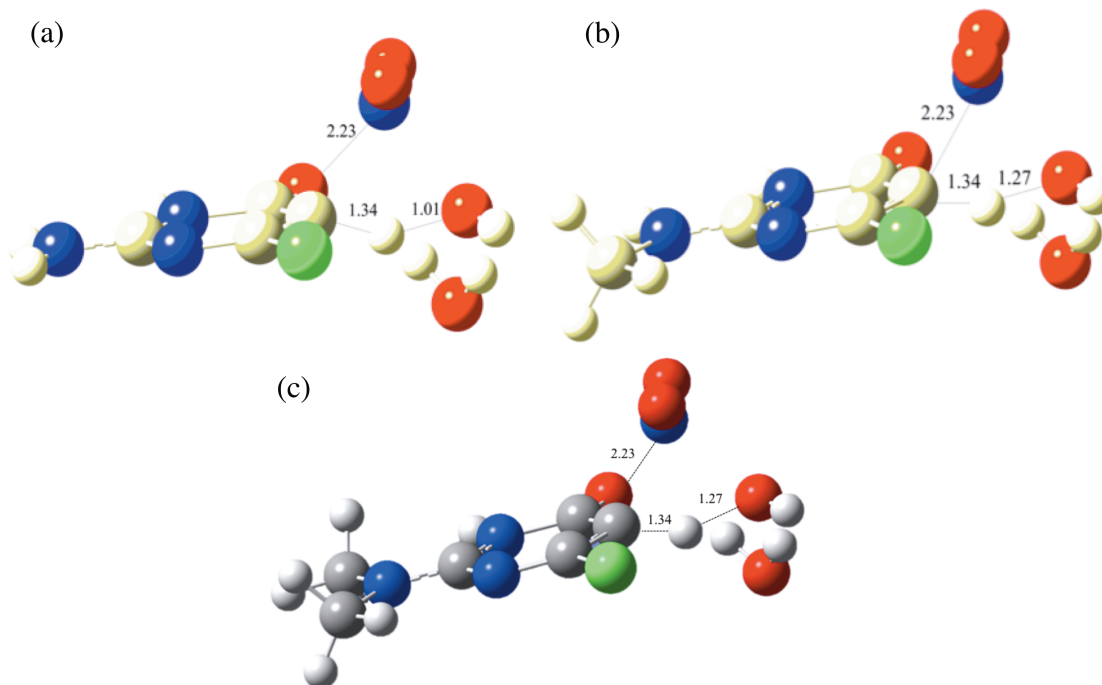


Figure 3.3.2. Molecular representation of optimized transition state structures for (a) $\text{TSC}_1(\mathbf{1})$, (b) $\text{TSC}_1(\mathbf{1-Me})$, and (c) $\text{TSC}_1(\mathbf{1-Me}_2)$. Distances in Å.

From Figures 3.3.2 and 3.3.3 it can be seen that in the transition state in which water is included, enhancing catalysis, the bond distances maybe influenced by the presence of the methyl groups in all cases. In addition the mode referring to the transition state corresponds to the transfer of the proton from C-5 to the hydroxyl group of HNO_3 . From these observations therefore, it appears that the presence of the methyl group doesn't

influence the reaction mechanism to an extent that differs in all of the scenarios tested. Alternative input “guess” geometries, in which the distances and orientations of the principal molecules of interest were altered were set up and subject to the same level of theory (B3LYP) and basis set (6-311G(d,p)). This was performed to attempt to derive a converged geometry in which the activation energies were more favourable. The optimized geometries pertaining to these are represented in the transition state geometries given in Figure 3.3.3.

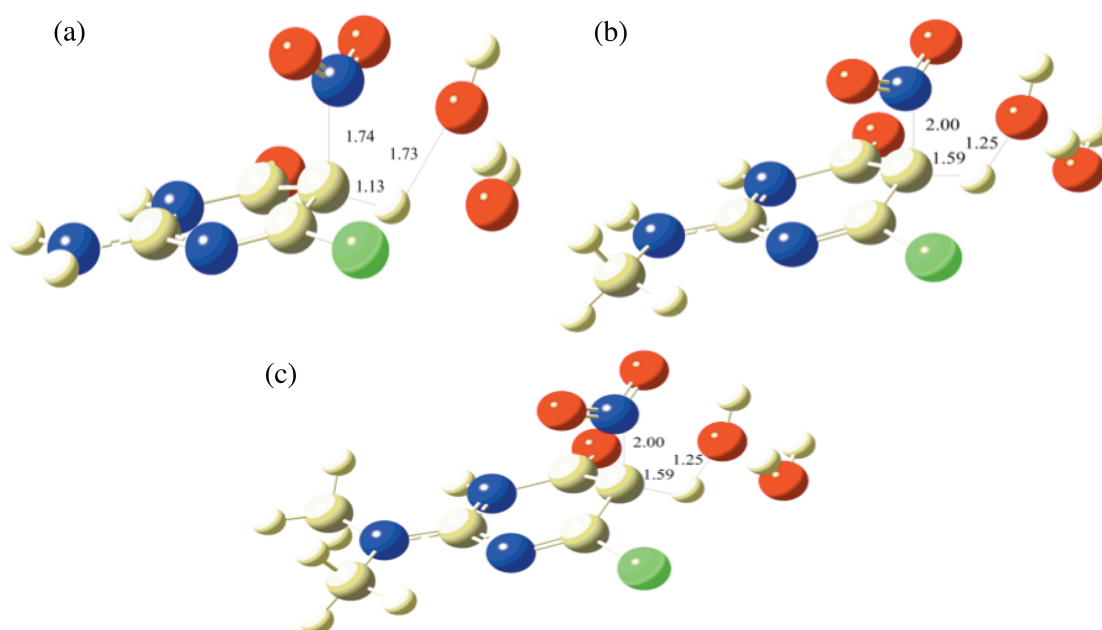


Figure 3.3.3. Molecular representation of optimized transition state structures for (a) TSC₂(1), (b) TSC₂(1-Me), and (c) TSC₂(1-Me₂) using the alternative orientation of the water molecule. Distances in Å.

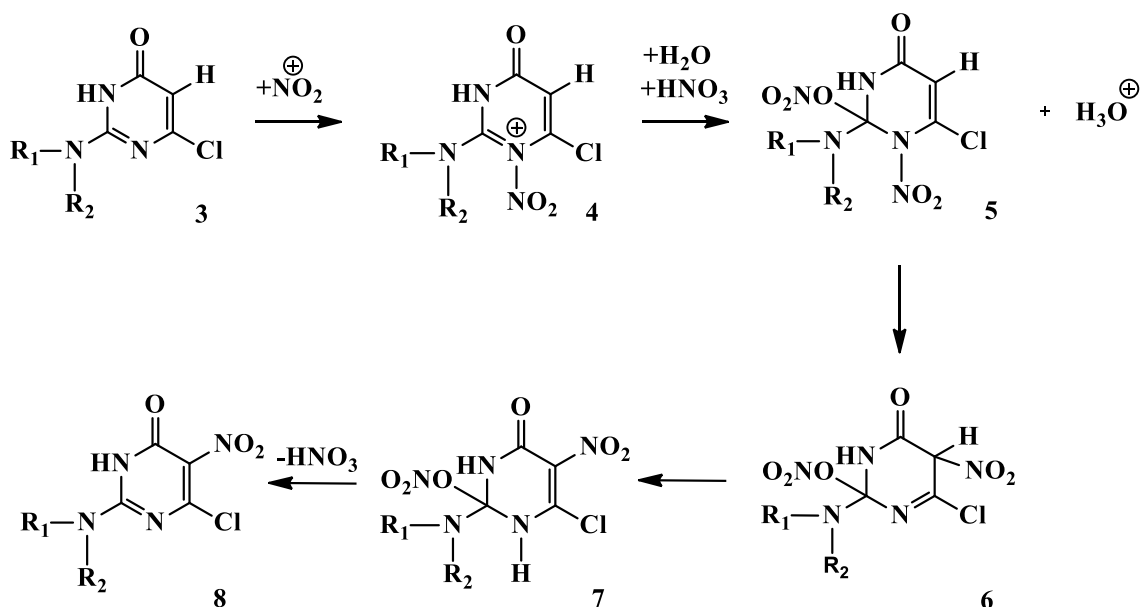
In the case of the NH₂ analogue there is observed to be a shorter inter-atomic distance between C5-N, this may suggest that there is an inductive effect in operation in the methyl and dimethyl cases, but is absent in the NH₂ analogue. This may also account for the smaller C5-H distance in NH₂ and the larger distance in H-OH, these being related to increased electronic density in the inter-nuclear region between H and O and a reduced level of induction to reduce this density, thereby resulting in repulsion. C5-H is also shorter in NH₂ since there is likely to be a favourable interaction between C-5 and H, which has become a proton as a result of the migration of electronic density from this atom.

Instances in which there has been withdrawal of electronic density towards CH₃ have been reported.⁵⁰ It is therefore possible that electronic flow could proceed in the opposite direction in certain scenarios. This could account for situations in which there is increased equivalence between the principal inter-atomic distances in all the analogues tested, such as those reported for TSC₁.

3.3.2 The Bakke-Based Mechanism

As a result of the unfavourable thermodynamic nature of the above reaction, an alternative mechanism was proposed. This mechanism was adapted from a related aromatic electrophilic attack by NO₂.⁵¹ A key point of this mechanism is a NO₂ migration onto C-5 following initial attack of the NO₂ on N-3. This migration is not observed computationally; however, it is assumed that this step occurs via a solvent cage

or via a sigmatropic shift.⁵² The overall mechanism is represented in scheme 3.3.2 below:



Scheme 3.3.2. Alternative reaction scheme based on an adaptation from Bakke.⁵¹

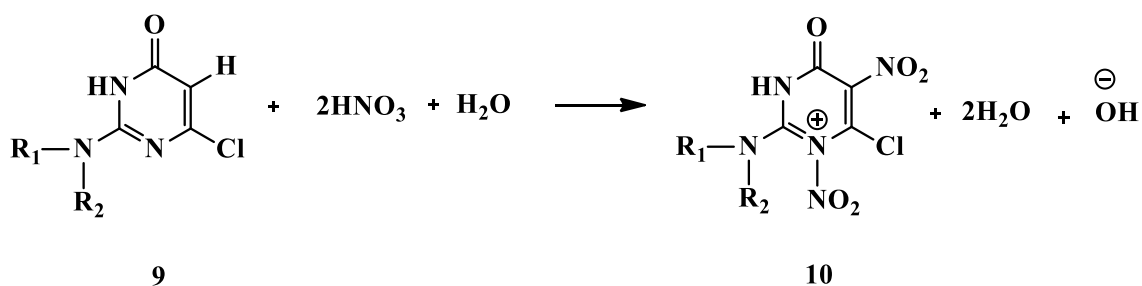
If the migration of the NO₂ moiety onto the C-5 position occurs, then it is proposed to occur via formation of an ionic or radical pair. Again, computational evidence of this effect has not been obtained. No optimization simulation has shown any migration of the NO₂ moiety. The energetic changes occurring with respect to this alternative mechanism (Scheme 3.3.2 above) are represented in the following table (Table 3.3.2).

Reaction	ΔE	ΔH	ΔG
(3)→(4)	-108.9	-106.8	-99.1
(4)→(5)	-51.3	-52.7	0.1
(5)→(6)	-24.2	-23.6	-24.4
(6)→(7)	-17.8	-17.7	-19.5
(7)→(8)	3.6	2.42	-8.0

Table 3.3.2. Energetic changes occurring for each step with respect to Scheme 3.3.2.

Central to the above mechanism is the migration of the nitronium moiety from N-1 to C-5. This is proposed to occur either via the formation of an ionic or radical pair, which then moves via way of a solvent cage. Such a step has been proposed and is central to the mechanism that Scheme 3.3.2 has been adapted from, specifically Bakke.⁵¹ As a consequence of this unfavorable energetic change, it was suggested that the migration of the NO₂ could proceed via a sigma tropic shift. To describe the movement of the nitronium ion from N-1 to C-5 via such a shift in a computational manner, a number of possible minima corresponding to increasingly proximal positions of the nitronium ion to C-5 could be envisioned to occur. The final transition state would involve a direct interaction between the nitronium ion and C-5. Attempts to derive these complexes and transition state were not undertaken within this thesis.

Another possible set of mechanisms was also considered in which a di-nitrated structure is proposed to be involved as a possible intermediate. This involves the addition of nitronium to two positions on the pyrimidine ring system. Such an intermediate is the result of the addition of a second molecule of NO₂ at C-5 following the initial attack by NO₂ at N-1. The mechanism corresponding to this possibility is given in the following scheme below (Scheme 3.3.3):



Scheme 3.3.3. Mechanistic proposal corresponding to addition of NO₂ to N-1.

When an attempt was made to generate the transition state for the above reaction, which was generated according to the following geometry, represented in Figure 3.3.3, the converged structure that was generated was observed to take the geometry represented in Figure 3.3.4 below.

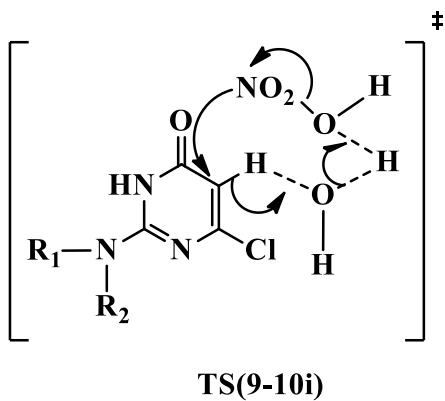


Figure 3.3.4. Proposed direction of electronic flow corresponding to the above reaction with respect to the initial transition state.

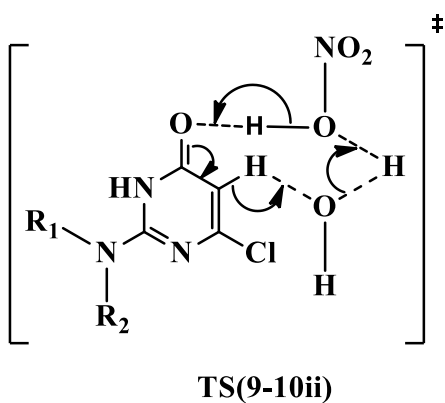


Figure 3.3.5. Transition state corresponding to the above reaction in Scheme 3.3.4 with proposed alterations in electronic flow.

The converged geometry differs from the proposed geometry principally in the direction of the flow of the electronic density. In the proposed geometry the direction of electron flow is towards the re-establishment of the lone pair on the nitrogen atom, this

subsequently favors electrophilic attack by this atom onto the putatively positively charged C-5. The direction of flow in the converged geometry appears to favour the flow of electronic density towards the oxygen of the carbonyl group resulting in the formation of a hydroxyl group. Based on this observation a series of possible reaction mechanisms were proposed that are based on the formation of a hydroxylated intermediate represented below in Figure 3.3.6

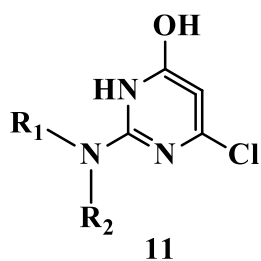
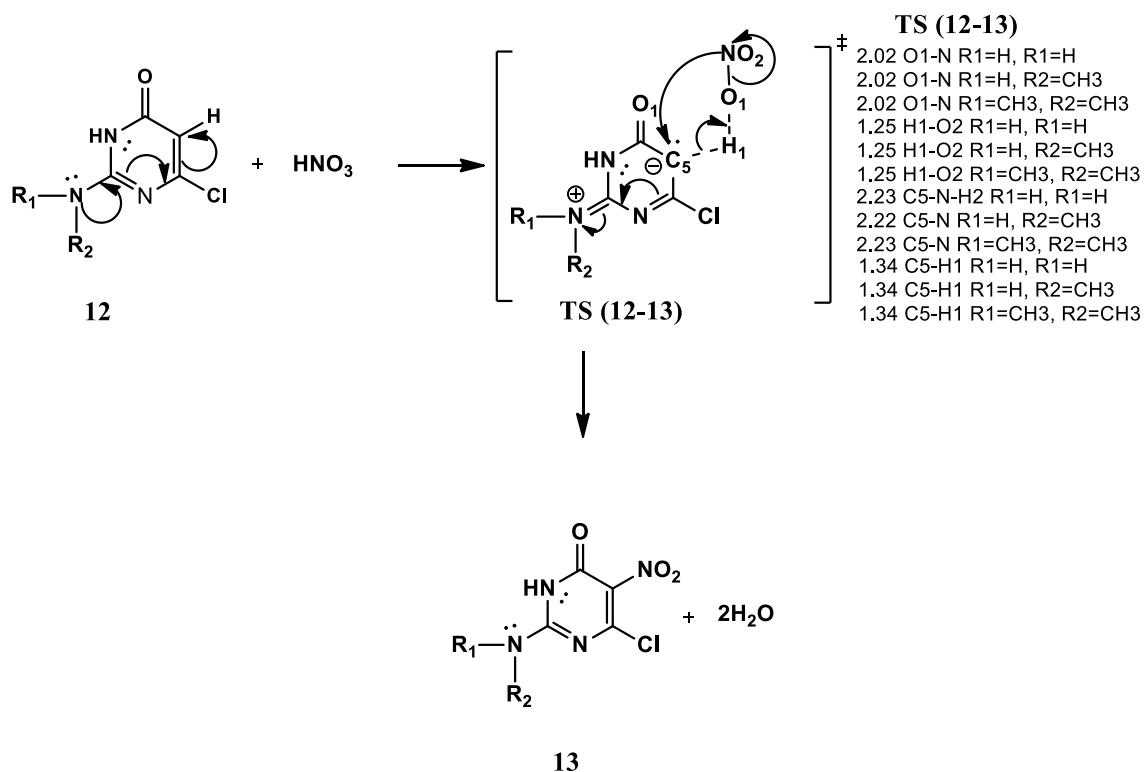


Figure 3.3.6. Proposed hydroxylated intermediate based on the product of the converged transition state given in Figure 3.3.5.

3.3.3 Comparison of Various Mechanisms

The series of proposed reaction mechanisms are represented in the schemes below. These various reaction mechanisms were referred to as (i) the parent system, (ii) the N-NO₂ system. System (i) refers to the direct electrophilic attack on C-5 by HNO₃, with the variant system in each case referring to the formation of the respective hydroxylated intermediate equivalent given above in Figure 3.3.6. System (ii) refers to the addition of a nitronium ion to N-1 in addition to that at C-5. The mechanistic details of these systems are given in Schemes 3.3.7 → 3.3.10. Two versions of these systems were

referred to. These were the variant and non-variant systems respectively. The main difference between each of these mechanistic proposals is associated with the direction of the electron flow as well as the formation of a hydroxylated intermediate in the case of the variant system. These differences are demonstrated in the respective schemes for each of the mechanisms using arrows to represent the proposed direction of the electronic flow. In the representation below in Scheme 3.3.7, the first scenario is presented. This corresponds to the non-variant case with respect to the parent system.



Scheme 3.3.7. Mechanistic proposal corresponding to the non-variant case in the parent system. Inter-atomic distances are given in the adjacent legends.

With respect to the above system represented in Scheme 3.3.7, the proposed mechanism, as indicated with respect to the changes in electronic flow within the transition state, were related to the changes in bond distances in each of the 3 analogues tested. This mechanism doesn't differ in a fundamental sense from that tested in the previous scheme (Scheme 3.3.1). It is included as a control system from which alterations in the addition of moieties and their effect upon electronic migration can be analyzed, since the optimized geometries/structures from this system were amended with the addition of the respective nitronium group (NO_2). The influences of these structural amendments were then assessed with respect to these initial geometries/structures. Any alterations in bond distances/electronic densities can then be assessed with respect to these initial minima/saddle points. This system is not directly equivalent to TS (1-2), since the equilibrium structures/geometries are not identical in energetic terms but is used for comparison within this system of reactions.

The energetic changes occurring with respect to the above mechanism are represented below in table 3.3.3. When consideration is given to formation of the transition state represented above, with analysis of the pertinent bond distances between each of the analogues undertaken it is suggested that the inductive effect is not operating within this system to either stabilize or de-stabilize the final optimized TS geometries. This maybe the consequence of a compensatory influence in operation within the HNO_3 engagement with C-5 and/or offsetting influences within the aromatic nucleus which may result in a neutralization of any inductive effect in operation. When consideration is given to the

energy associated with formation of these TSs it can be seen that there is a marginal increase in stabilization within the methyl and dimethyl analogues. It is suggested that if there is an electronic effect within this system contributing to stabilization then it is marginal, and also that the change in electronic energy is not a function of the chemistry occurring at C-5, given the relative equality of these inter-atomic distances.

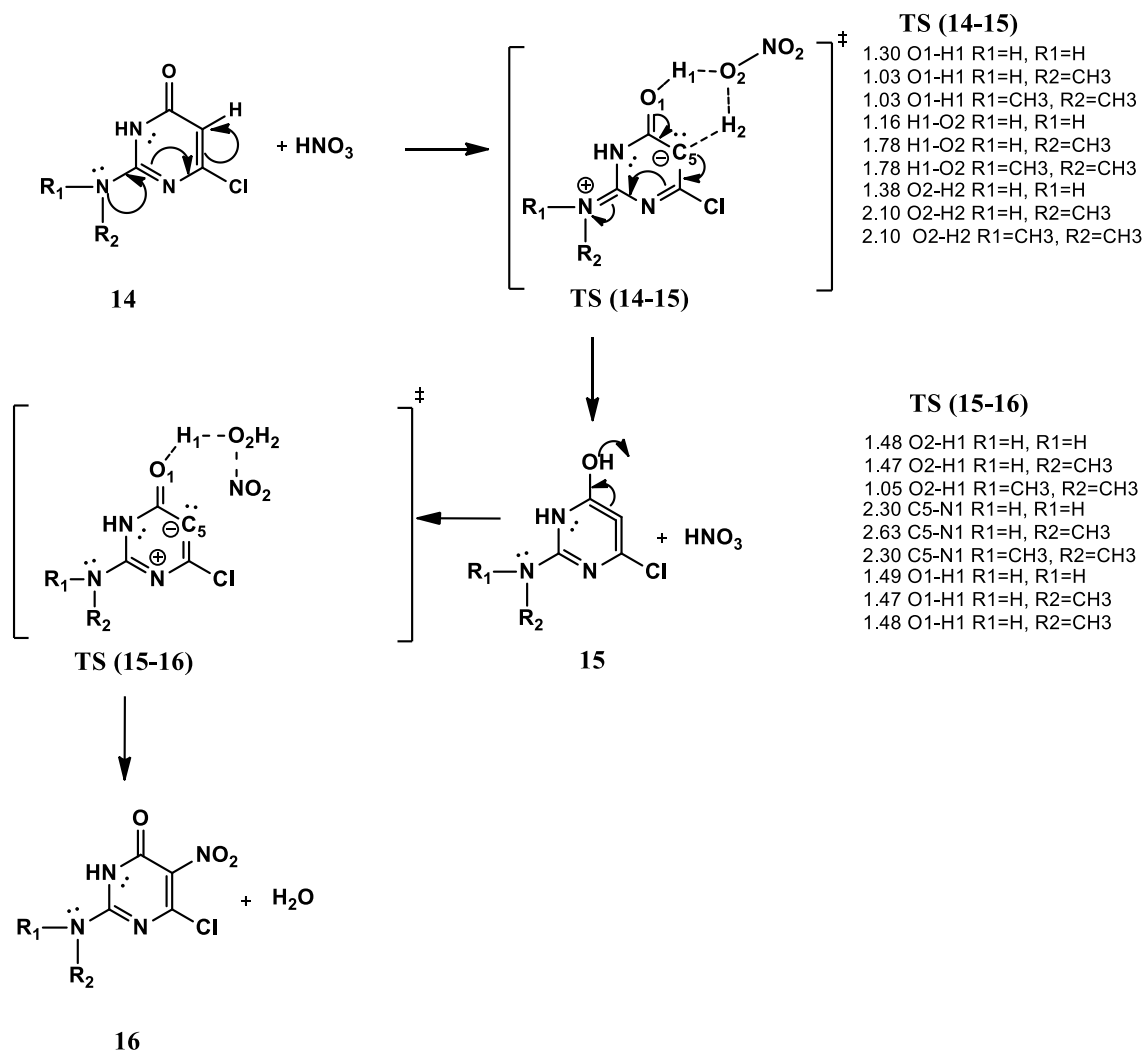
Reaction	ΔE	ΔH	ΔG
NH₂ (12→TS(12-13))	77.4 (55.3)	72.2	75.7
NH₂ (12→13)	-0.2 (-11.6)	-0.3	-1.2
NHMe (12→TS(12-13))	76.4 (49.9)	71.5	94.1
NHMe (12→13)	-0.3 (-11.8)	-0.5	-1.5
NMe₂ (12→TS(12-13))	74.9 (49.9)	71.5	74.8
NMe₂ (12→13)	-0.7 (-12.4)	-0.8	-0.9

Table 3.3.3. Energetic changes occurring with respect to description of the respective steps occurring in the non-variant parent system (Values in parentheses correspond to energies in the presence of solvent, H₂O).

When consideration is given to the energetic changes occurring with respect to formation of TS(12-13) it is observed that there is a large contribution in entropic terms in operation within the single methyl analogue which may indicate that there is a large degree of molecular electronic re-arrangement within the geometry as the optimization

occurred. This could be the result of induction, but the converged geometry, in terms of any differences in the underlying mechanism is suggested to be unaffected by this increase in the number of degrees of freedom within the molecule as a whole.

With respect to the variant case in the parent system, a similar analysis of the respective changes in electronic density was undertaken. The following analysis refers to Scheme 3.3.9 below, describing the mechanism according to the variant case.



Scheme 3.3.8. Mechanistic proposal corresponding to the variant system in the parent case. Inter-atomic distances are given in the adjacent legends.

To determine the feasibility of the above reactions in terms of thermodynamic changes, the relative changes in the free energy, electronic energy and enthalpy were evaluated and are represented in Table 3.3.4 below with respect to the variant parent system. These calculations were carried out in the gas and solvent phases. The solvent chosen for these

analyses was water, with the solvent system being represented within the CPCM model.⁵³

Reaction	ΔE	ΔH	ΔG
NH₂ (14→TS(14-15))	57.0 (52.6)	55.7	56.8
NH₂ (14→15)	6.0 (2.8)	6.0	5.0
NH₂ (15→TS(15-16))	63.6 (65.5)	60.0	64.8
NH₂ (15→16)	-6.2 (-14.4)	-6.3	-6.2
NH₂ (14→16)	-0.2 (-11.6)	-0.3	-1.2
NHMe (14→TS(14-15))	57.2 (52.6)	55.8	56.7
NHMe (14→15)	6.1 (2.6)	6.0	4.7
NHMe (15→TS(15-16))	63.7 (64.8)	60.1	64.9
NHMe (15→16)	-6.4 (-14.4)	-6.5	-6.2
NHMe (14→16)	-0.3 (-11.8)	-0.5	-1.5
NMe₂ (14→TS(14-15))	57.0 (49.9)	55.6	56.9
NMe₂ (14→15)	5.9 (2.4)	5.8	5.3
NMe₂ (15→TS(15-16))	64.0 (65.0)	60.5	5.3
NMe₂ (15→16)	-6.6 (-14.8)	-6.6	-6.2
NMe₂ (14→16)	-0.7 (-12.4)	-0.8	-0.9

Table 3.3.4. Relative changes occurring in the absence and presence, values in parentheses, of solvent for variant parent reaction system.

There is suggested to be pull of electronic density towards C of CH₃ from the lone pair (2p_z) orbital of the adjacent nitrogen. This will result in de-shielding of the positive charge of the nucleus of this molecule resulting in delocalization of the charge towards the C of CH₃. Two possible interpretations with respect to the interaction between N of NHCH₃ and C-2 exist. One is that there is electrostatic attraction between these atoms according to the charges given above. Another is that there is de-stabilization arising from the increase in effective positive charge associated with the N of NHCH₃. In this geometry which is transient between two equilibrium structures, and therefore intrinsically unstable in the energetic terms associated with the eigenvectors (eigenvalues positive) out with the eigenvector associated with the reaction coordinate (eigenvalue negative), it is suggested that there will be less stabilization between these atoms in the transition state than in the equilibrium structure, but there will still be net stabilization given the opposite charges of these atoms. To compensate for this slight decrease in stabilization, it is suggested that there will be transfer of electronic charge from N-1 to C-2, thereby increasing stabilization here.

When analysing the inter-atomic distances which may be pertinent in the description of the reactivity intrinsic within TS (14-15) and TS (15-16), it is observed that the principal distances associated with each of these could be interpreted in terms of the operation of an inductive effect within the methyl and dimethyl scenarios, and an absence of such an effect in the amino scenario. Analysis of the respective distances in more detail and relating these to reactivity and relative free energy changes suggests that in the amino case there is a shorter distance in operation between H₁ and O₂, 1.16 Å compared to 1.78

Å in the methyl and dimethyl cases. This may suggest that there could be a higher level of electronic repulsion between these two atoms as a consequence of electron density being pulled away from O₁, giving rise to a slightly larger positive charge state on this atom resulting in a repulsive interaction between H₁ and O₂ and therefore may account for the larger distance observed in these analogues. This inductive effect may also account for the larger distances in operation between H₁ and O₁ (1.30 Å in NH₂, 1.03 Å in NHMe and N(Me)₂ with a similar effect suggested to be in operation. This may be explained in terms of a slightly smaller negative charge at C-5 in the methyl and dimethyl scenarios through pulling of electronic density from this atom. This will result in a higher level of de-shielding of the positive charge on the nucleus of C-5. This will then cause de-stabilization between C-4, slightly positively charged as a result of polarization and C-5. The inductive effect may operate by pulling electronic density away from O₂ at the opposite side of the ring system, giving rise to a slight increase in positive charge at O₂ and so producing repulsion between O₁ and H₁. This is suggested to be in operation in the methyl and dimethyl scenarios but absent in the amino scenario and hence may account for the larger inter-atomic distances reported here. This effect may also operate in the case of H₂-O₂, where there is reported to be a larger inter-atomic distance between these atoms in the methyl and dimethyl scenarios at 2.10 Å and 1.38 Å in the amino case. Electronic density is suggested to migrate across H₁ from the inter-atomic region between O₂ and H₂, to eventually accumulate at O₁ as per the previous argument to describe the H₁-O₁ distance. This is suggested to have the effect of increasing positive charge on O₂ and so cause a concomitant increase in repulsion between O₂ and H₁ and therefore a larger inter-atomic distance in the methyl and

dimethyl scenarios. As a result of the similarities between the relative electronic energies with respect to formation of TS(14-15) in all the analogues, ca. 57 kcal/mol in all cases, it is suggested that the changes in electronic density which occur within this system occur in a manner in which the surrounding gas phase doesn't contribute to in a different way in each of the analogues.

When the influence of solvation is taken into consideration, it can be seen that there is a decrease in the relative free electronic energy associated with formation of the transition state for the dimethyl analogue, 49.9 kcal/mol compared to 52.6 kcal/mol in the methyl and amino cases. This may indicate that in the presence of an implicit solvent system, H₂O in this instance, there may be a critical interaction between the solvent system and the additional methyl group which could influence electronic migration within the system. The effect of this could be interpreted as being energetically favourable as a result of delocalization of the increased electronic density which will presumably accumulate at this additional methyl group. This may not occur in the single methyl case as a result of either a decreased preponderance of the surrounding water system to coordinate in an energetically favourable manner, or a decreased level of symmetry at this location in the absence of the dimethyl system.

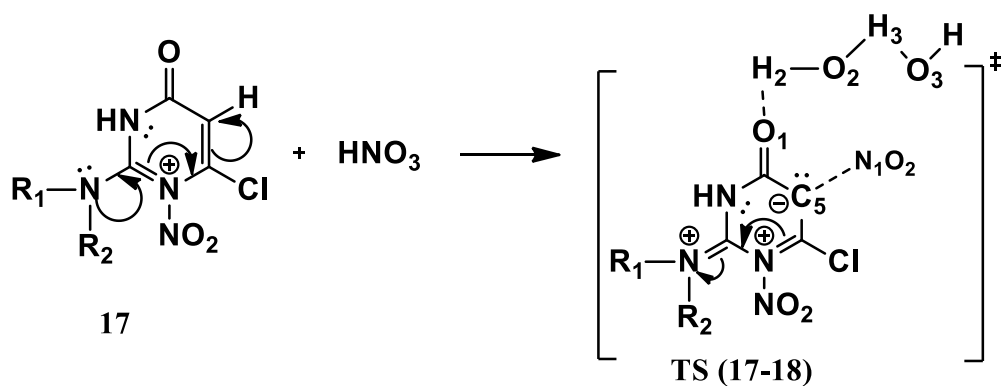
When a similar analysis of the inter-atomic bond distances considered relevant in the second transition state in operation within this reaction proposal ((C-5-N₁-2.30 Å (NH₂), 2.63 Å (NHMe) and 2.30 Å N(Me)₂) (H₁-O₁- 1.49 Å (NH₂), 1.47 Å (NHMe) and 1.48 Å N(Me)₂) and H₁-O₂- 1.48 Å (NH₂), 1.47 Å (NHMe) and 1.05 Å N(Me)₂) corresponding

to TS (15-16) in the above scheme, it can be seen that there are only significant differences in the inter-atomic distances between H₁-O₂ and C-5-N₁ between the methyl and amino/dimethyl analogues. This may indicate that there is an inductive effect in operation with respect to the presence of one methyl group, manifest as the larger distance between C-5 and N of the nitronium moiety. This can be explained by the regeneration of the positive charge on N of NO₂ following dissociation from HNO₃ and the concomitant approach of this molecule to C-5 being inhibited by electron withdrawal from C-5 producing a more positive charge at this location and so preventing the closer engagement of these groups. Of further interest is the observation that the inter-atomic distance between H₁-O₂ is closer to a bonding interaction at 1.05 Å. This suggests that a covalent bond has been formed in this instance to generate H₂O, which is then speculated to release NO₂ in a complete sense from HNO₃. Such an occurrence may not occur in the case of the amino and dimethyl analogues given these pertinent bond distances are essentially identical. The presence of two methyl groups may cause a steric effect which could offset any additional advantages associated with the presence of these groups in close proximity. This could be explained as the transfer of electronic density back through the molecule to reduce repulsion in this region and so generate an electronic condition that is similar to that observed in the amino case. The observation that there is a much smaller relative free energy change associated with formation of TS (15-16) could be explained by the suggestion that there is a re-arrangement of the geometry with a large degree of movement of these methyl groups, driven by electronic transfer away from this region and back through the molecule.

This may indicate that there is only sufficiently large electronic migration towards the methyl groups in the presence of an additional methyl group compared with the mono-methyl analogue. This could be explained by referring to the fact that there is involvement of the carbonyl group which is proposed to pull density away from H₁ towards O₂, and this is further enhanced by a concomitant inductive effect within the ring system which is initiated by migration towards the terminal Nitrogen of the amino moiety. This is further enhanced by the presence of the two methyl groups which need to be present to initiate this effect. The changes occurring with respect to the Gibbs free energy indicate that the reaction would not be competitive, principally as a consequence of the high activation barriers occurring with respect to the formation of TS (17-18) and TS (18-19) respectively. These activation barriers are decreased in the presence of a solvent system for the NH₂ scenario. This is not observed in the NHMe or N(Me)₂ scenarios. In these systems there is a small increase in the magnitudes of the relative Gibbs free energy changes. This may suggest that at a mechanistic level the presence of a methyl moiety singly or doubly and in the presence of the solvent could negatively influence stabilization. The mechanism by which this may occur could not be analysed in terms of the relative changes occurring in electronic distribution between the initial and final transition state geometries, since the solvation energy is a single point calculation which doesn't take the overall optimization into consideration in the same sense as an optimization/frequency and transition state calculation. The magnitudes of these relative free energy changes are of sufficiently high value to indicate that the reaction would not proceed even when the influence of solvation is taken into consideration based on the transition state which has been determined. Conceivably,

employing an Intrinsic Reaction Coordinate calculation to evaluate the correct transition state could provide further insight concerning the accuracy of the transition state which has been elucidated in this instance.

To determine the feasibility of the N-NO₂ system reaction in terms of thermodynamic changes, each of the structures of the proposed reactants, intermediates and products were subject to energy minimization calculations. The mechanistic proposal pertaining to this is represented in scheme 3.3.10. In addition to these calculations, attempts to derive the transition states for each reaction proposal were also performed. The relative changes in the free energy, electronic energy and enthalpy were evaluated and are represented in table 3.3.4. These calculations were carried out in the solvent phase. The solvent chosen for these analyses was water. Further analysis of the electronic changes occurring in the reaction systems encompassing the NO₂ systems in the variant and non-variant cases was also performed.

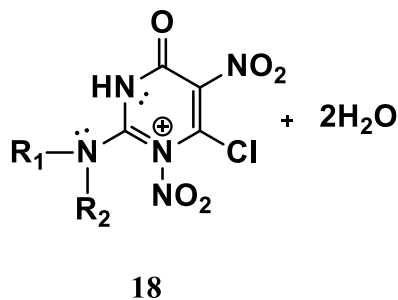


TS (17-18)

O1-H2=1.57, R1=H, R2=H

C5-N= 2.83, R1=H, R2=CH3

O2-C5=3.21, R1=H, R2=CH3

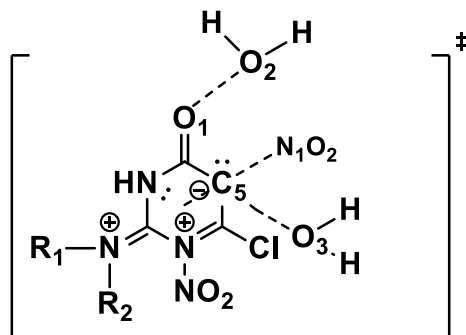


TS (17-18) Methyl case

O1-O2=3.09, R1=CH3, R2=CH3

C5-N=1.47, R1=CH3, R2=CH3

C5-O3=3.1, R1=CH3, R2=CH3



Scheme 3.3.9. Mechanistic proposal corresponding to the N-NO₂ scenario in the non-variant case. Inter-atomic distances are given in the adjacent legends.

The discussion below corresponds to the non-variant case for the N-NO₂ case in scheme 3.3.9. When reference is made to the pertinent bond distances in operation within the transition states represented in TS(17-18) the analogues tested, it can be seen that with respect to the NH₂ scenario the converged outcome of the calculation is not geometrically similar to that represented in the N(Me)₂ case. In the NH₂ scenario it can be seen that there is a larger distance between C-5 of the aromatic nucleus and N₁ than is observed in the N(Me)₂ case, with the relevant values corresponding to 2.83 Å and 1.47 Å respectively. This is suggested to be the result of the presence of the CH₃ groups which are suggested to produce a larger degree of polarization within the ring system compared with the NH₂ scenario. Further stabilization is also offered with respect to the presence of the water molecule which is interactive with O₁. The presence of this molecule is proposed to delocalize the electronic density associated with O₁, thereby leading to a decreased level of shielding of the nuclear charge of this atom. Further, it is suggested that the presence of the additional water molecule may cause an enhancement of the delocalization of the electronic charge within the water system, thereby offering further stabilization within the system. Further stabilization is suggested to be in operation with respect to the negative charge associated with C-5, which may contribute to delocalization of the positive charge at C-4 which has been introduced as a result of the migration of electronic density away from O₁ and the subsequent transfer of electronic density away from C-4 as a result of the inductive effect. This will cause an increased level of de-shielding of the positive charge of C₁ which will destabilize the

carbonyl group, but this may be offset with respect to the presence of the negative charge at C-5, which is suggested to contribute to delocalization and therefore lower the energy of this complex. This inductive effect is suggested to be a smaller effect compared to that which may operate in the presence of the CH₃ groups, in which there is a larger level of intrinsic delocalization in operation within the aromatic ring. This may account for the observation that the distance between N₁ and C-5 is larger in this instance, since there is likely to be a larger repulsion between these atoms as a result of lone pair interactions. This stabilization is consistent with the overall level of reactivity which is observed in the NH₂ scenario.

When a similar analysis is carried out with respect to the N(Me)₂ scenario it is observed, firstly, that there is no water system stabilizing the carbonyl group. Indeed, in this instance, the only water molecule is further away from the carbonyl group, with an inter-atomic distance between O₁ and O₂ of 3.09 Å. This larger distance is suggested to be the result of repulsion between the lone electron pairs of these atoms and is likely to contribute to further stabilization. The presence of the CH₃ groups is suggested to produce induction which will result in a decrease in negative charge at C-5, thereby allowing a closer approach of N₁ towards C-5. The additional water molecule is not permitted to gain access to the reactive centre in the complex as a result of steric repulsion introduced as a result of the presence of NO₂. This is evidenced by the larger distance in operation between O₃ and C-5 (3.1 Å). These destabilizing interactions lead to a higher energy in the complex, even although this seems to favour the approach of

the nitronium moiety. This is consistent with the overall observation in energetic terms for the CH₃ systems.

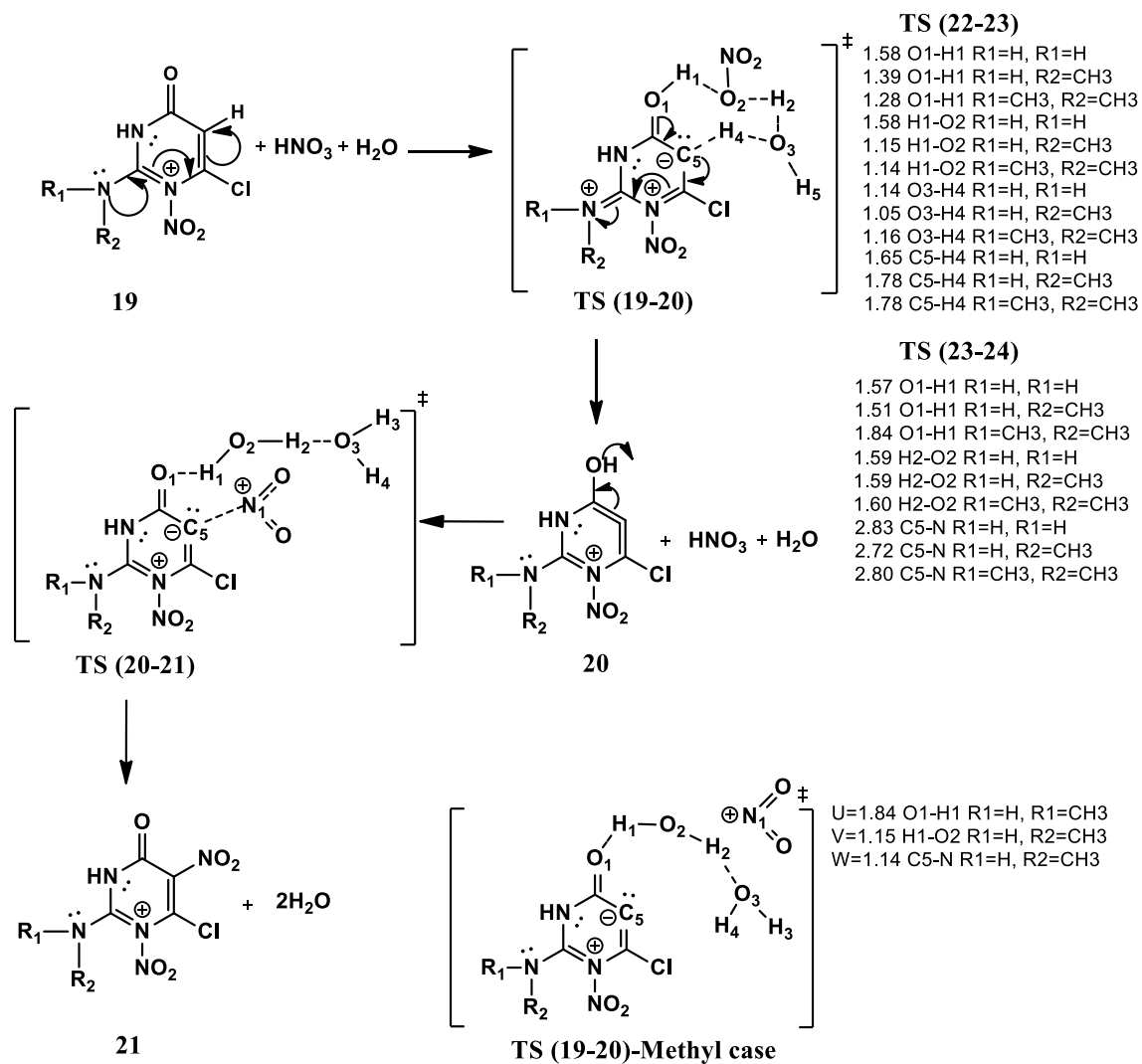
Reaction	ΔE	ΔH	ΔG
NH₂ (17→TS(17-18))	44.8	42.5	46.9
NH₂ (17→18)	-2.8 (-12.8)	-2.9	-0.2
NHMe (17→18)	0.7 (-9.4)	0.5	3.0
NMe₂ (17→TS(17-18))	52.0	47.4	52.2
NMe₂ (17→18)	-2.8 (-9.4)	-2.9	-1.0

Table 3.3.5. Relative changes occurring for non-variant N-NO₂ system. (Values in brackets indicate the relative changes in electronic energy occurring in the solvent phase). TS could be located for the NHMe scenario.

From the above relative changes in electronic energy it can be seen that the scenario with respect to the methyl analogue is such that the overall reaction would not proceed in the gas phase as a consequence of the endergonic changes in electronic energy that are occurring. When solvation is taken into consideration it can be seen that there are exergonic changes in all instances with respect to the overall reaction. As a result this mechanism would not be satisfactory with respect to a description of the experimental observations. In all instances, in the presence and absence of solvent, the activation barrier is too large to allow the reaction to proceed via this mechanism.

Further analysis was performed with respect to the N-NO₂ system in the variant case.

The scheme describing this mechanism is represented in scheme 3.3.11 below.



Scheme 3.3.10. Mechanistic proposal corresponding to the N-NO₂ scenario for the variant case. Inter-atomic distances are given in the adjacent legends.

When consideration is given to the N-NO₂ variant scenario represented in Scheme 3.3.11, in the first transition state represented by TS(19-20) for the NH₂ scenario it is observed that the distances between H₁ and O₁ correspond to 1.58 Å, 1.39 Å in the NHMe case and 1.28 Å in the N(Me)₂ case, while that observed with respect to C-5-H₂ is observed to correspond to 1.65 Å. In the NHCH₃ scenario the C-5-H₂ distance is observed to correspond to 1.78 Å, while that corresponding to the N(Me)₂ case is found to correspond to 1.78 Å. In the case of O₂-H₃ in the NH₂ scenario the distance is observed to correspond to 1.01 Å, whereas in the NHMe and N(Me)₂ cases the distances are 1.15 Å and 1.14 Å respectively. The distances between O₃-H₄ in the NH₂, NHMe and N(Me)₂ cases were optimized to 1.14 Å, 1.05 Å and 1.16 Å respectively.

In the case of the second of the transition states for this scheme, it is found that the pertinent bond distances in the NH₂, NHMe and N(Me)₂ case for O₁-H₁ are 1.57 Å, 1.51 Å and 1.84 Å and those pertaining to O₂-H₂ are 1.59 Å, 1.59 Å and 1.60 Å respectively. The C₅-N₁ distances are found to correspond to 2.83 Å for the NH₂ case, 2.72 Å for the NHMe case and 2.80 Å for the N(Me)₂ case. To account for these distances reference is again made to the operation of an increased inductive effect in the CH₃ cases, with an enhancement suggested to be in operation in the case of the N(Me)₂ scenario. In addition there is a smaller non-covalent interaction between one of the terminal H atoms and one of the O atoms associated with the NO₂. This may produce an increased delocalization of charge, which could alter stabilization within this complex via alteration of the influence of the inductive effect. In general terms the smaller distance in the NHMe case pertaining to the C₅-N₁ distance is suggested to result as a consequence of decreased

electronic density at this location. The increased distance between O_1 and H_1 is assumed to be the result of an inductive effect which results in an increase in charge at N-1, this causes the need of C-1 to decrease positive charge, this is accomplished by pulling electronic density away from O_1 , increasing the charge here and so causing repulsion between O_1 and H_2 , manifest as a larger distance between these atoms.

Reaction	ΔE	ΔH	ΔG
NH₂ (19→TS(19-20))	36.9 (53.1)	31.7	37.5
NH₂ (19→20)	35.4 (36.7)	34.1	38.3
NH₂ (20→TS(20-21))	10.1 (21.9)	8.9	8.7
NH₂ (19→20)	-38.2 (-49.5)	-37.1	-38.5
NH₂ (19→21)	-2.8 (-12.8)	-2.9	-0.2
NHMe (19→TS(19-20))	41.8 (41.7)	36.4	42.1
NHMe (19→20)	40.3 (41.6)	39.0	42.6
NHMe (20→TS(20-21))	11.6 (17.9)	11.0	12.8
NHMe (20→21)	-39.6 (-9.4)	-38.5	-39.7
NHMe (19→21)	0.7 (-9.4)	0.5	3.0
NMe₂ (19→TS(19-20))	38.1 (41.7)	32.8	38.7
NMe₂ (19→20)	36.4 (40.2)	35.3	39.3
NMe₂ (20→TS(20-21))	12.9 (19.4)	12.2	13.2
NMe₂ (19→20)	-39.2 (-49.6)	-38.2	-40.3
NMe₂ (19→21)	-2.8 (-9.4)	-2.9	-1.0

Table 3.3.11. Relative changes occurring in the absence and presence of solvent, values in parentheses, for variant N-NO₂ reaction system.

With respect to the above mechanism it can be seen that there is moderate activation energy in all cases with respect to formation of the transitions states TS (22-23) and TS

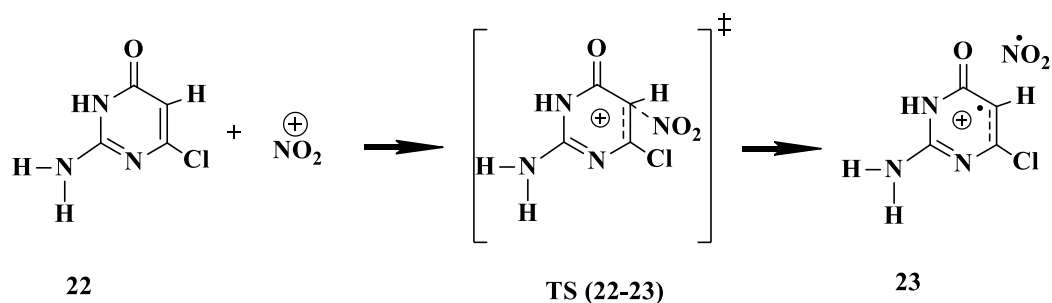
(23-24). These calculations have been carried out in the gas phase. When consideration is given to formation of these transition states in the presence of solvent, it can be observed that in all instances, except in the case of 22→TS (22-23), there is a significant increase in the activation barriers. This suggests that the presence of the NO₂ moiety influences the nature of the activation barrier. This may be the consequence of alterations in the flow of electrons in the pertinent region of the molecule.

From the energetic changes occurring with respect to the above reaction, represented in table 3.3.11, the relative changes occurring for the above reaction for the amino case indicated that the reaction was favourable from an energetic perspective. When consideration was given to the methyl case it was also observed that the changes were favourable. The above reaction is therefore a candidate for the description of the reaction mechanism in terms of the amino case with the alternative methylated scenario unlikely to proceed via scheme 3.3.10, based on the energetic changes occurring.

The above changes in relative electronic energy, enthalpy and Gibbs free energy suggest that this reaction would not be competitive as a consequence of the very high activation energy needed for formation of the transition states in all of the scenarios tested. The above changes in relative electronic energy, enthalpy and Gibbs free energy between the reactants and products are sufficiently different to suggest that there may be a different mechanism in operation between the NH₂, NHMe₃ and N(Me)₂ systems, producing a different electronic distribution between the reactants and products. These changes are observed across the enthalpy and Gibbs free energy, suggesting that these electronic

differences are reflected in terms of the changes in entropy and heat content of the system respectively. In terms of the formation of the transition state pertaining to NHCH_3 for this system, the entropy change is positive in this instance, corresponding to 4.3 Cal/mol-Kelvin (not shown). This suggests that there is a high statistical probability that this transition state would form based on entropic considerations. The associated change in the entropy, which is observed to be negative in both the NH_2 and $\text{N}(\text{CH}_3)$ cases (-9.5 Cal/mol-Kelvin and -4.7 Cal/mol-Kelvin) (not shown) indicates that the formation of the NH_2 and $\text{N}(\text{CH}_3)$ analogues are unfavourable from a statistical perspective. The entropic changes are not considered to be the primary drivers in this instance since the overall change associated with the Gibbs free energy is not significantly different between the NHCH_3 and $\text{N}(\text{CH}_3)$ cases.

With respect to the energetic changes occurring for these variant and non-variant steps, there is no obvious difference between the systems tested between the NH_2 , NHCH_3 and $\text{N}(\text{CH}_3)$ cases. In addition there is an increase or no increase in the Gibbs free energies when solvation is taken into consideration in all instances regarding formation of both transition states with respect to the NH_2 , NHCH_3 and $\text{N}(\text{Me})_2$ cases in the variant case. This suggests that the presence of the NO_2 moiety contributes in a neutral or destabilizing fashion to the system when the solvent is introduced in this system. This may be the consequence of either an electron donating or withdrawing effect of this moiety influencing the ability of other atoms in the molecule to form hydrogen bonds to the solvent water system, thereby having no measurable effect on the solvent system to stabilize the molecule.



Scheme 3.3.11. Scheme proposed for the formation of a radical complex involving NO_2 and the aromatic system.

The mechanism represented in scheme 3.3.11 is a further consideration to attempt to account for the previous observations related to reactivity. It is to be viewed separately to any of the mechanisms presented before this point. The relative electronic energetic changes corresponding to this proposal are represented in table 3.3.12.

Reaction complex description	ΔE
$22 \rightarrow \text{TS (22-23) (NH}_2\text{)}$	-20.2
$22 \rightarrow \text{TS (22-23) (NHMe)}$	26.2
$22 \rightarrow \text{TS (22-23) (N(CH}_3\text{)}_2\text{)}$	57.0

Table 3.3.12. Relative changes occurring with respect to formation of transition state geometries in description of scheme 3.3.11.

In the case of the methyl analogue it can be observed that the free energy change is not favourable with respect to the formation of the aromatic: NO_2 analogue. In this respect,

therefore, it appears that representation of the total system in terms of a complex with an overall multiplicity of 3, which is speculated to involve a transfer of electronic density from the aromatic system to the electrophile, generating two free electrons in the overall complex, one in each component of the system, could proceed as a result of intersystem crossing. This phenomenon has been reported to be responsible for the formation of the triplet state from the singlet in a number of aromatic systems.⁵² In this instance it is proposed that there is a transfer of electronic density between both components of the complex, resulting in generation of the triplet state, corresponding to a total of two free electrons for the whole complex. The transition state corresponding to this proposed process has been suggested to involve the approach of the electrophile towards the aromatic system, the subsequent transfer of electronic density from the aromatic group onto the electrophile and the resultant formation of a complex in which both the aromatic moiety and the electrophile are separated by a measurable distance. Attempts to describe the transition states for these processes were undertaken for all analogues. The imaginary frequency corresponding to this saddle point was found to correspond to -46.17 cm^{-1} , which in general terms would not be considered to be of sufficient magnitude to properly describe a transition state. In this instance, however, it is proposed that this frequency, corresponding to a rotation of the NO_2 group, may account for the transfer of the electronic density from either the aromatic group to the electrophile, or from the H atom which has migrated from the main aromatic nucleus with a concomitant transfer of the associated electronic density onto the positively charged NO_2 . This is speculated to cause an associated shift in electronic density within the electrophile, resulting in the eventual attack of this group onto C-5, producing the

final nitrated product given above. The transfer of the electron occurs with respect to a nuclear framework that is essentially stationary.⁵⁴ This is likely to be manifest as an initially unaltered nuclear framework, with a small re-arrangement of the nuclear coordinates occurring following the transfer of the electron from the donor (aromatic group) to the acceptor (NO₂ electrophile). This small frequency would be consistent with such an outcome. Such a scenario is observed in these transition states, there is initial approach of the electrophile towards the aromatic group, followed by association of the NO₂ group at C-5, and then an alteration in the rotational state of the NO₂. This gives rise to the imaginary frequency that was reported. With respect to the methyl-amino case, the same transition state was also generated, with an imaginary frequency of -44.85 cm⁻¹. Again a similar mechanism is proposed corresponding to this scenario. In the case of the dimethyl scenario, a similar transition state with an imaginary frequency of -44.05 cm⁻¹ was reported. With respect to the pertinent changes in the relative Gibbs free energies for the formation of these transition states it can be observed that there is an overall change with respect to the formation of the complex with a triplet multiplicity which is exergonic in the case of the amino analogue (-20.18 kcal/mol) and endergonic in the case of the methyl-amino analogue (26.18 kcal/mol). When the formation of these complexes is considered with respect to the presence of the solvent, the relative free energies for formation are reduced accordingly. In the amino case the free energy change is reduced to -25.09 kcal/mol, whereas the methyl-amino free energy change is reduced to 10.40 kcal/mol.

A further effect to account for the reduced activation of the C5-H bond with respect to the triplet state in the methyl analogue of the aromatic system may be associated with the increased electron excitation energy of the aromatic system being lost to the surrounding medium, in this instance, the solvent system. With respect to a lattice system it has been reported that in the triplet state, there has been transfer of excitation energy from the constituent system.⁵⁵ A similar effect may occur with respect to the methyl analogue, since the electronic density associated with C-5 could be decreased as a consequence of the electron withdrawing effect of the methyl group. This may decrease the level of activation in the methyl analogue to such an extent that there is no transfer of electron density between the aromatic system and the electrophile, thereby preventing formation of the transition state and subsequently the aromatic : NO₂ complex. The inductive effect and the influence of the electron withdrawing effect of the methyl group could be employed to explain the effects that are speculated to operate with respect to the methyl analogue. The presence of the methyl group is proposed to withdraw the electron density from the aromatic group via the inductive effect. This may inhibit the transfer of the free electron from the aromatic group onto the NO₂ electrophile. With respect to the relative free energy changes occurring in the dimethyl analogue, it can be observed that the formation of the transition state from the dimethylreactant is exergonic, with a change of -5.82 kcal/mol reported for this step. In this instance, the formation of the transition state is favourable from the dimethyl reactant analogue. The electron withdrawing effect of the dimethyl groups cannot therefore be invoked to explain the inhibition of electron transfer in this instance.

When analysis of the pertinent bond distances ($C_5:NO_2= 1.77 \text{ \AA}$, $C_5:H= 2.04 \text{ \AA}$) in the NH_2 , $NHMe$ and $N(Me)_2$ scenarios are considered it is suggested that in the case of the $C_5:H$ distance, the reason for the larger distance in this instance may be the result of a reduced level of electronic transfer between H and NO_2 arising as a result of the electron withdrawing influence of the distant methyl group, producing an inductive effect within the molecule. The shorter distance between $C_5:NO_2$ in $N(Me)_2$ maybe the consequence of increased positive charge at C-5 as a result of the increased electronic withdrawal, producing reduced density at this location. This is suggested to be associated with the presence of the additional methyl group. The larger distance between $C_5:H$ could be the result of increased electrostatic repulsion between between the positively charged NO_2 group and the newly acquired positive charge associated with the dissociated proton, thus forcing the proton further away from this reactive centre.

In all instances reported with respect to the attempt to characterize electrophilic aromatic substitution in terms of the electronic flow occurring in the transition state, no definitive solution can be found when this methodology is employed. As a consequence of the transient quantum nature of the transition state geometry it is suggested that relativistic effects should be taken into account to correctly characterise the reduction of this state in the correct way. In the final example presented in the above discussion, corresponding to formation of a defined complex with a multiplicity of 3 and the concomitant changes in relative free energy favouring formation of the NH_2 analogue and dis-favouring the $NHCH_3$ analogue, there is not observed to be a defined difference in the electronic changes which may inhibit formation of the complex in the case of the $NHCH_3$ analogue

but favour formation of the NH_2 analogue. A description of the mechanism based on such electronic considerations in this way is therefore not proposed to account for differences in the reactivity between both analogues. In a previous study of the reactivity of a Janus aromatic system⁵⁶ it has been reported that there is formation of a worm-hole type structural feature within the system. This is proposed to link regions of the molecule, via orbital interactions, which would not be linked under normal circumstances. It is conceivable that such interactions could provide an alternative pathway by which electronic density could proceed within the transition state. If such structural elements were in operation within the NHCH_3 analogue but absent within the NH_2 analogue, and was principally operational at a location which could influence the mechanism, then it is suggested that electronic flow could be inhibited/altered in a fashion which would dis-favour the mechanism in the NHCH_3 case but not in the NH_2 case. The possibility of identifying such structural elements within orbitals in the transition state for the reaction was not performed in a quantitative sense since the necessary analysis of the orbitals was not undertaken within this study, however it is suggested that such analysis could proceed as a possible future study.

It has been demonstrated within the set of reaction systems proposed to account for the differential level of reactivity reported between the methylated and un-methylated analogues, that there may be an inductive effect in operation with respect to formation of several of the transition states. This effect is suggested to account for alterations in inter-atomic distance in instances where electrostatic considerations become significant, for example where there are obvious de-stabilizing influences in operation within the

molecule. That such differences in inter-atomic distance are observed in the amino case but not the methyl and dimethyl cases appears to provide evidence that this effect is operational, as the mechanism associated with the reaction system is essentially identical in all cases. These differences are therefore suggested to occur as a consequence of an inductive effect of some description. Conceivably there could be electron donation from CH_3 towards N of the N-R_2 to initiate the reaction, thereby forcing donation of the lone pair into the adjacent bonding region. This is suggested to produce further electronic transfer towards C_5 , resulting in either a reaction complex or transition state in which there is a defined negative charge on C_5 . There is then suggested to be associated changes in inter-atomic distances to re-generate an equilibrium state electronic configuration in CH_3 , which is suggested to have become negative as a result of acquisition of electronic density from the proximal hydrogen atoms. This is suggested to occur as a consequence of compensation for the decrease in electronic density associated with electronic transfer away from this group to initiate the reaction. Inter-atomic bond distance differences are suggested to be the result of this inductive effect, and this may explain why there are differences between the amino and (di)-methyl cases. Where there is increased stabilization within the molecule, or there is another mechanism to reduce repulsion within the aromatic group, for example by direct electronic transfer to another group, as in scheme 3.3.12, it is suggested that the bond distances will be similar in all three analogues. In instances in which there is no mechanism to transfer electronic density away from the aromatic group, then there will be a relatively large degree of re-orientation within the reaction system, to decrease repulsion. Where no inductive effect is operational, as is suggested in the case of mechanistic proposals where the principal

inter-atomic bond distances are similar between each of the analogues, then there is suggested to be no major increases in repulsion within the molecule as the reaction occurs. Studies in which the relative lateness of the reaction along the reaction coordinate could also be carried out, this involves the quantitation of the lateness of the reaction using a dimensionless quantity⁵⁷. This analysis is based on the Hammond principle⁵⁸, which indicates that the transition state geometry will be closest in geometry to the product structure(s) when an endothermic reaction is in operation and will be closest to the reactant(s) structure(s) when an exothermic reaction is operating. To confirm whether the transition states are correct in the formal chemical sense, it may be possible to perform intrinsic reaction coordinate calculations.⁵⁹ Reaction rate studies could also be performed to complement the thermodynamic analyses which have been undertaken. This could involve using the rate theory of Eyring.⁶⁰

4.0 Superelectrophilic Amidine Dications.

There has been one published outcome generated with respect to the undertaken in this section of the thesis. The work undertaken in this section of the thesis forms the basis of the computational analysis of the reaction system included in the paper.

Superelectrophilic Amidine Dications: Dealkylation by Triflate Anion.

Luka S. Kovacevic, Christopher Idziak, Augustinas Markevicius, Callum Scullion, Michael J. Corr, Alan R. Kennedy, Tell Tuttle, and John A. Murphy. *Angew. Chem. Int. Ed.*, **2012**, *51*, 8516.

4.1 Introduction to Organic Superelectrophiles.

Electrophilic compounds display a significant role in many aspects of chemistry. Such compounds are electron deficient and are therefore extremely reactive towards centres of high electronic density. A characteristic of superelectrophiles is the high level of reactivity of such compounds when reacted with nucleophiles that are of limited strength. The first reported instance of superelectrophilic activation was observed for the increased reactivity of nitronium and acetylium salts in superelectrophilic media⁶¹ but the first instance of carbocations can be traced to 1901 with triphenylmethyl alcohol ionization reported in sulphuric acid as well as triphenylmethyl chloride with aluminum and tin chlorides.⁶²

Carbocations have been extensively characterized as intermediates in a wide range of reactions, using various kinetic, stereochemical and a varied array of experimental approaches. As a consequence of the high reactivity of these species towards a range of solvation media, the need to find suitable approaches to ensure their stability was of fundamental experimental importance. This was accomplished in the early 1960s by George Olah, for which the Nobel Prize was awarded to him in 1994.

Electrophilic reactivity is a significant driver in many reaction systems. Understanding the kinetic, thermodynamic and ultimately mechanistic details of the increased reactivity of these compounds is therefore essential. The main mechanism underpinning the enhanced reactivity of these species is centered upon hydrogen bonding (protosolvation).

In this mechanism, there is transfer of hydrogen as either the proton or hydride to centres of negative or positive charge respectively. To provide an example of the mechanism underpinning such activation, consideration is given to the protosolvation of the nitronium ion within a superacidic medium. Superacidic media are acids which display high hydrogen ion concentration to facilitate protonation, in addition to being of low nucleophilicity, so that there is no, or limited reaction with the resultant superelectrophiles. In the formation of the protonitronium ion (NO_2H^{++}) from the acid H-A, there is the introduction of an additional positive charge into the nitronium ion. This is responsible for the increased reactivity/superelectrophilicity which is observed in the protonitronium ion. Such superelectrophilic activation is proposed to be the contributory factor to the mechanism of activation of previously less reactive groups in molecules. Such activation can cause a large change in the associated reactivity of interacting groups. This is the basis of the work that has been carried out in this project, and a description of the changes in reactivity of amidine dications towards triflate anion forms the following discussion.

The system that was studied in this instance corresponded to a series of amidine dications with varying levels of activation of the C-Me bond. This system was studied since there is a close association in primary and secondary metabolism between the transfer of methyl groups and the associated activation of sp^3 -nitrogen. Examples of the importance of methylation in biochemical control processes include chemotaxis in *Bacillus subtilis*,⁶³ genetic control in prokaryotes and eukaryotes⁶⁴ and also in the biosynthesis of homocysteine. The activation of the sp^3 -(nitrogen)- sp^3 -(carbon) bond is

central to the formation of this secondary metabolite, and proceeds via transfer of a methyl group from N⁵-methyltetrahydrofuran to methionine. A specific example of a high-energy barrier with respect to demethylation is provided by the de-methylation of a methyldialkylamine.⁶⁵

4.2 Computational Methods.

To characterize C-N bond activation in the presence of solvent in greater detail, a series of syntheses were performed in which the level of activation operating in the amidine dication intermediates were altered with respect to variations in electron delocalization. These levels of activation are primarily the consequence of the charge differential and distance between the electronic densities of the associated carbon and nitrogen of the pertinent C-N bond. A more comprehensive understanding of the mechanism of bond activation in the presence of solvent was the principal focus of these activation studies. The computational approach to evaluate these levels of activation and subsequent changes in free energy was to employ the functional M06⁶⁶ and the basis set 6-311G.⁶⁷ The conductor-like polarizable continuum model was used to model the influence of the dichloromethane solvent. A secondary focus was to evaluate if there was a functional dependence on the relative free energy changes by evaluating the reaction scheme with three different functionals. These functionals were B3LYP⁶⁸ M06⁶⁶ and B97D.⁶⁹ B97D incorporates the influence of long-range dispersion into consideration through an empirical term which is added to the mean-field energy.⁶⁹ The form of this expression is written below:

$$E_{disp} = -S_6 \sum_{i=1}^{N_{at}-1} \sum_{j=i+1}^{N_{at}} \frac{C_{ij}}{R_{ij}^6} f_{dmp}(R_{ij}) \quad 4.1.1$$

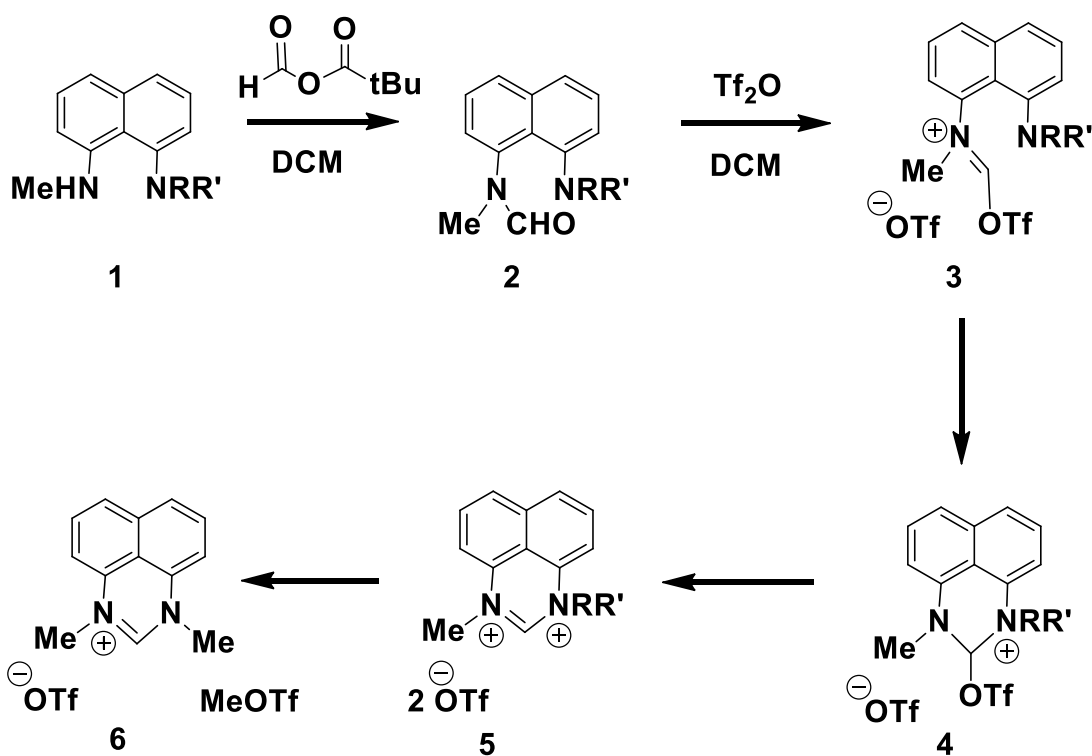
The functional form of the damping term is represented according to equation 4.1.2 below⁶⁵:

$$f_{dmp}(R_{ij}) = \frac{1}{1 + e^{-d(R_{ij}/R_r - 1)}} \quad 4.1.2$$

Equation 4.1.2 is incorporated into the dispersion term to prevent the formation of singularities at short interatomic distances. The advantage of this expression is that there is likely to be a more representative description of weakly bound systems in which non-bonded interactions are responsible for stabilization, such as systems involving dispersion interactions, for example π stacking

4.3 Results and Discussion.

Scheme 4.3.1, displays the main inter-conversions that were subject to solvation calculations. The calculations were performed with respect to the Conductor like Continuum Polarization Model (CPCM) solvation model.⁷⁰ The relative free energy changes are presented in the following table with respect to Scheme 4.3.1 below.



Scheme 4.3.1 Representation of the steps associated with the proposed mechanism in terms of synthesis of intermediates 1-6.

The relative changes in free energy were evaluated in terms of each of the above conversions, in addition to those corresponding to the formation of the respective transition states. These free energy changes are represented succinctly in Figure 4.3.1, which is adapted from the paper on which this work is based.⁷¹

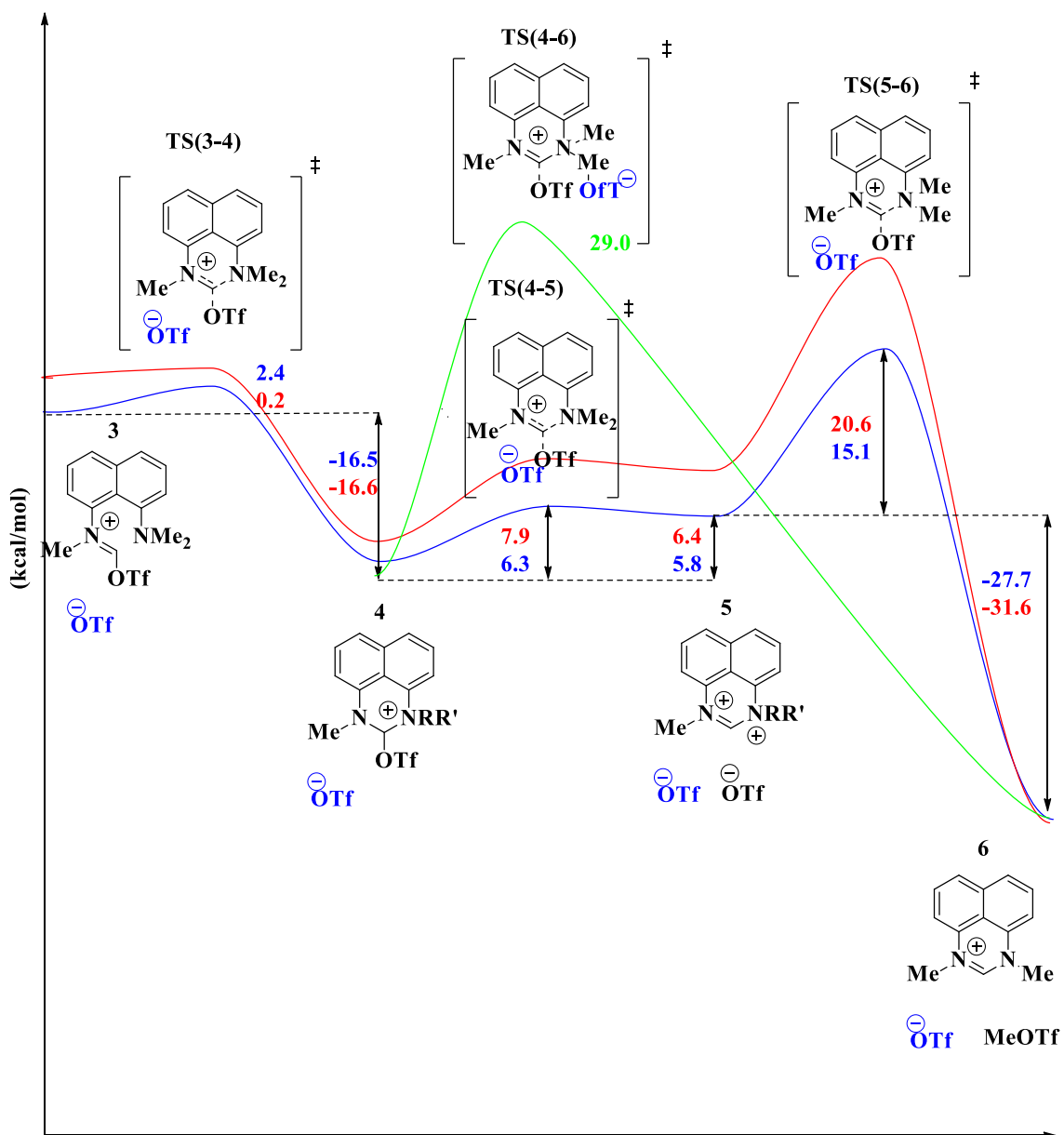


Figure 4.3.1. Relative free energy changes occurring with respect to formation of the intermediates 3→6 from the previous TS's and intermediates respectively. These changes are represented with respect to the gas-phase.

The blue lines correspond to the presence of OTf in the reaction complex. The red line corresponds to the absence of OTf in the complex, with the green line corresponding to

the energy change occurring with respect to the concomitant dissociation of the two methyl groups.

With respect to Figure 4.3.1 it can be observed that two possible mechanistic scenarios are presented, those in which the triflate counter anion is proposed to be an active component of the transition state geometry or reactant/intermediate/product complex, and those instances in which this anion is proposed to be absent from these geometries/complexes. The relative free energy changes can be explained with respect to the proximity or otherwise of the triflate counter anion. The presence of the counter anion is represented in Figure 4.3.1 by the blue line and absence represented by the red line. In instances in which the triflate ion is present, it can be seen that there is either a measurable stabilization of the resultant transition state geometry/intermediate complex, a small increase in the resultant transition state geometry/intermediate complex, or no stabilization. To account for these changes, reference is made to the electrostatics and relative proximity of the interactions between the counter ion and the positively charged aromatic system. In the first inter-conversion (**5**→**TS(5-6)**) it can be observed that the change in relative free energy corresponds to 2.4 kcal/mol in the presence of the counterion and 0.2 kcal/mol in the absence of the counterion. There doesn't appear to be any stabilization observed in the presence of the counterion in this instance. In effect there is a de-stabilization observed with respect to the presence of the counterion. This may be the consequence of a repulsive interaction between the negatively charged triflate and the π system of the aromatic group.

From Figure 4.3.1 it is clear that the proximity of the triflate ion to the aromatic group is such that there is likely to be relatively significant interactions between the π system of the aromatic group and the delocalized negative charge of the triflate ion. The distance of the oxygen atom of the triflate ion from the nitrogen of the 6-membered ring of the triflate ion (2.86 Å) is proposed to be optimal with respect to repulsion and attraction, with the repulsive force being dominant in this example. The repulsive term corresponding to this interaction is proposed to dominate as a result of the observation that no stabilization is offered in the presence of the counter-ion. Stabilization in the absence of the counter-ion is observed and is proposed to be the consequence of a favourable electrostatic interaction between the double bond and the positively charged nitrogen of the unconstrained 6-membered ring system.

With respect to the subsequent step in the reaction pathway (**5**→**6**) it is observed that there is no difference between the relative free energies associated with the presence and absence of the triflate. This can be speculated to be the result of the increased distance between the ion and the positively charged nitrogen that has migrated from the initial nitrogen location, moving across the 6-membered ring and being finally localized on the other side of the ring system. The counter-ion on this occasion has not altered location, and so stabilization is not observed with respect to this scenario. Any stabilization is therefore speculated to be localized to the 6-membered ring system, with a favourable interaction occurring between the positively charged nitrogen and the partial double bonds which will be generated as a result of delocalization of the aromatic system and

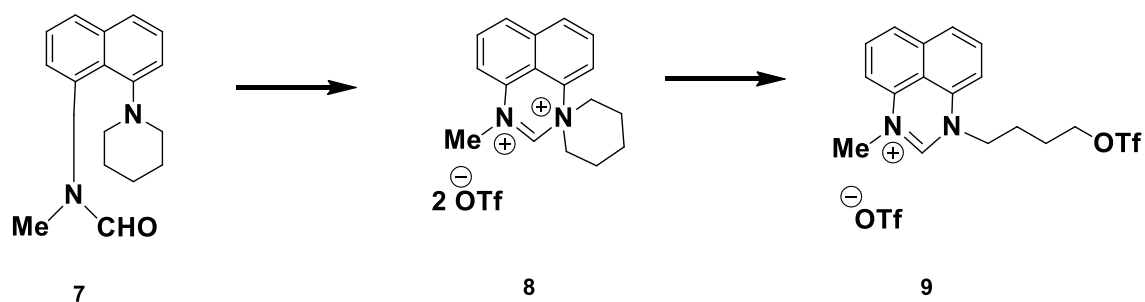
the subsequent incorporation of partial and/or full double bond character in the adjacent 6-membered ring.

Formation of the subsequent transition state **TS(4-5)**, from intermediate **4**, is slightly more favourable with respect to the presence of the counterion (6.3 kcal/mol) compared to the absence of the counterion (7.9 kcal/mol). On this occasion it is suggested that the partially dissociating triflate from the 5-membered ring system may be associated with decreased electronic density with respect to the covalent scenario. As a consequence there is speculated to be less repulsive interaction between the counterion and the previous transition state **TS(5-6)**, in which there is a full covalent bond in operation between the 6-membered ring system and the triflate, with the associated electronic density of this covalent bond. The transfer of this electronic density from the 6-membered ring onto the triflate is speculated to account for enhancement of the stabilization in the presence of the triflate, since the electronic density is decreased in this instance and so there is more likelihood of a favourable interaction between the counterion and the more distant positively charged nitrogen atom.

In terms of the formation of intermediate **5** from **4**, there is a small amount of stabilization in the presence of the counterion, 5.8 kcal/mol compared with 6.4 kcal/mol in the absence of the counterion. This is the result of already favourable interactions in operation within the 6-membered ring system leading to the level of stabilization already produced in the absence of the counter-ion. A slight increase in stabilization is observed in the presence of the counter-ion. This is the result of the presence of two counter-ions

in the geometry producing favourable attractive interactions. In the final step it is observed that there is a large stabilization in the presence of the counterion (15.1 kcal/mol) compared to 20.1 kcal/mol. This is proposed to be the result of a directly favourable interaction between the counterion and the 6-membered ring system, which is proximal to the positively charged nitrogen atom of the 6-membered ring system.

In the final instance of the inter-conversions represented in Figure 4.3.1, that involving the synthesis of intermediate **6** from intermediate **5**, it can be observed that the relative free energy change for this step was calculated as -27.7 kcal/mol with respect to the step involving the presence of the counterion in the product complex, whereas the absence of the counterion resulted in a relative free energy change of -31.6 kcal/mol. In this example it is clear that there is less stabilization produced with respect to the presence of the triflate ion, which has undergone methylation. The reasoning behind this step was to establish the mechanism by which demethylation proceeds. The main interconversions are represented in scheme 4.3.2, adapted from the main paper on which the work is based.⁷¹



Scheme 4.3.2. Alternative mechanism test to establish operation of S_N2 mechanism.

The intent was to establish whether the mechanism tested previously was operative with respect to terminal C at to non-terminal C atoms. The observation that an alkyl triflate (9) was produced instead of intermediate 8 indicated that the reaction must proceed via a S_N2 mechanism, since if this was not the case the corresponding alkene product would be generated following dissociation of the 6 membered ring substituent associated with compound 7. Evidence of a S_N2 was further suggested based on the observation that a C-OTf bond was generated in the product compound as opposed to a separate, dissociated alkene product.

Further analyses were carried out with respect to the characterization of the above mechanism in Scheme 4.3.1 with respect to the inclusion of solvent. Experimentally the reaction mechanism was studied in dichloromethane. The functionals B97D and B3LYP were employed in order to evaluate the influence of both solvent and functional on the relative free energies generated. The same polarization model (CPCM)⁷⁰ was employed in this study. Comparison with respect to the relative change in free energy of M06 was

also made. The outcomes of these calculations are represented in Table 4.3.1 below. To determine whether the choice of the functional influences the generated change in the relative electronic energy (ΔE), separate calculations were carried out with respect to M06 and the other two functionals, B97D and B3LYP, referred to earlier.

Reaction	ΔG_{M06}	ΔE_{M06}	ΔE_{B97D}	ΔE_{B3LYP}
3→TS(3-4)	0.23	1.22	0.84	1.70
3→TS(3-4)	2.45	3.52	1.83	5.42
3→4	-16.61	-21.66	-15.97	-16.83
3→4	-16.48	-22.80	-17.92	-18.77
4→TS(4-5)	7.87	9.24	10.55	13.27
4→TS(4-5)	6.35	7.04	1.95	3.09
4→5	6.42	9.06	4.75	4.17
4→5	5.82	9.59	4.90	5.55
5→TS(5-6)	20.64	22.41	17.04	16.44
5→TS(5-6)	15.12	18.69	14.05	12.64
5→6	-31.55	-30.98	-28.70	-30.24
5→6	-27.69	-27.23	-25.27	-29.62

Table 4.3.1. Relative free energy changes occurring with respect to formation of intermediates and transition states when B97D, B3LYP and M06 were employed.

Values which are further down the table for each inter-conversion correspond to the presence of the triflate counter ion.

With respect to the energies represented in Table 4.3.1 above pertaining to the inter-conversions represented in Figure 4.3.1 for M06 as well as the intermediate structures and transition state geometries represented in this figure, it is clear that in the first step when triflate is present, there is a de-stabilization observed with respect to the value obtained for the relative change in ΔG , since the change is 1.22 kcal/mol in the case of triflate being absent from the complex, whereas the value corresponds to 3.52 kcal/mol in the case when triflate is present. This change in energy is consistent with that which is observed for ΔG in M06 and is explained in electrostatic terms with respect to the previous commentary given for this step for M06. In terms of ΔE occurring in B3LYP, there is a large change in the energy of 5.42 kcal/mol reported with respect to the complex involving triflate and the 6-membered ring. It is suggested that this is an overestimation of the energy of the resultant complex. Such overestimations have been reported in instances in which B3LYP has been employed before to evaluate the energies in operation in systems where dipole-dipole and/or dispersion are in operation.⁷² From the generated structures in figure 4.3.1 associated with formation of **TS(3-4)** it can be observed that there is generation of a partial bond associated with the 6-membered ring system. This can be viewed as early stage formation of a single covalent bond, resulting in the generation of a closed ring system. Such a scenario presents the possibility that there could be delocalization of the π electrons from the

adjacent bond associated with the aromatic ring, producing an interaction between the cation in the 6-membered ring and this region of delocalized π electronic charge density. This could cause the increase in stabilization that is observed with respect to this functional in the absence of the counter-ion. This would be expected to be the case for both the presence and absence of the counterion, with this intramolecular interaction being responsible for the stabilization of the 6-membered ring system. In the presence of the counterion there is most likely to be a repulsive effect associated with the presence of the triflate counterion and the π system of the 6-membered ring system. This would most likely further increase the instability in **TS(3-4)**. In the absence of the counterion the energy is enhanced to a small extent with respect to B97D and M06. This is presumed to be the result of the favourable interaction energy between the cationic nitrogen of the 6-membered ring system and the newly introduced delocalized π electronic system.

A comparison of the relative changes in energy (ΔG and ΔE) associated with the formation of each of the transition state geometries and intermediates respectively was undertaken. From Figure 4.3.1 it can be seen that ΔG with respect to the formation of **TS(3-4)** from **3** indicated that there was no stabilization observed when the triflate counter ion was included in the complex. This is the consequence of the observation that there is an increase in ΔG from 0.2 kcal/mol in the absence of triflate, to 2.4 kcal/mol in the presence of triflate. The geometry in **TS(3-4)** is such that there is proposed to be formation of a π bond as this step proceeds. This is proposed to account for the increase

in ΔG that is associated with the presence of triflate, specifically, the repulsion between the triflate and the π bond system which is in the process of forming in this geometry, may contribute to this de-stabilization. This level of de-stabilization is also observed with respect to ΔE in the case of M06, B97D and B3LYP. In the case of M06 it can be observed that there is an increase from 1.22 kcal/mol in the absence of triflate to 3.53 kcal/mol in the presence of triflate. This is proposed to be the consequence of a negative correlation repulsion of the type expounded upon with respect to ΔG . In the case of ΔE with respect to B97D, there is an increase from 0.84 kcal/mol to 1.83 kcal/mol. This increase is not as large as is observed in the case of B3LYP, where there is a large increase in ΔE from 1.70 kcal/mol to 5.42 kcal/mol. This differential is assumed to be the consequence of an overestimation in the case of B3LYP, since such overestimations have been reported on previous occasions with respect to this functional. There is a short-range interaction in operation within this transition state. As a result there will be a correction in the dispersion term, which has been specifically written to account for short-range interatomic distances. The larger increase in ΔE in B3LYP will be accounted for by the overestimation which occurs in this functional in the description of cationic interactions.⁷²

With respect to the formation of structure **4** from **3**, it can be observed that ΔG is not influenced by a large extent with respect to the presence of the triflate counter-ion. This is assumed to be the consequence of there being no significant dispersion interaction between the triflate counter-ion and the positive charge of the nitrogen in the 6-

membered ring system. Since the formation of this structure is exergonic it can be assumed that this structure will predominate in terms of stability. As a result it will predominate with respect to **3**. As a consequence there is only a small probability that the positive charge will migrate back onto the other nitrogen of the 5-membered ring and so no increased stabilization with respect to the proximal location of the triflate counter-ion in terms of electrostatic stabilization of **3** will be observed. There is a slight stabilization of the complex with respect to ΔE as measured by M06, which indicates a weak correlation effect in the presence of this counter-ion. There is no major stabilization with respect to B97D (-15.97 in the absence of triflate and -17.92 kcal/mol in the presence of triflate), which indicates that the dispersion is intermediate in range and relatively small in magnitude. As a result there is no dispersion correction observed in this instance. A slight stabilization is also reported with respect to measurement by B3LYP. This indicates that there is a small level of correlation in operation in all instances and that this correlation is likely to be intermediate in distance, consistent with the distal location of the counter-ion with respect to the positively charged nitrogen of the 6-membered ring.

The subsequent step in the reaction pathway corresponds to formation of **TS(4-5)** from **B**. ΔG in these steps corresponded to 7.9 kcal/mol in the absence of triflate and 5.8 kcal/mol in the presence of triflate. The triflate counter-ion is distal with respect to the positively charged nitrogen of the 6-membered ring. This would seem to suggest that any correlation/dispersion would be minimal. This is reflected in the small stabilization observed in the value of ΔG . The small stabilization in the case of M06 (9.24 kcal/mol

in the presence of triflate and 7.04 kcal/mol in the absence of triflate) can be explained in terms of an intermediate range correlation effect. To account for the increased stabilization in operation with respect to ΔE in the case of B97D it is proposed that the much larger difference between the presence and absence of triflate can be ascribed to a shorter range interaction between the triflate and the positive charge on the 6-membered ring. In this instance, even though the positive charge is distal to the triflate, it is suggested that there will be migration of the positive charge across the 6-membered ring to a position at which there is a large degree of electrostatic interaction between the triflate and the positively charged nitrogen. This can be represented in terms of the following resonance structures for **TS(4-5)**, Figure 4.3.2 below.

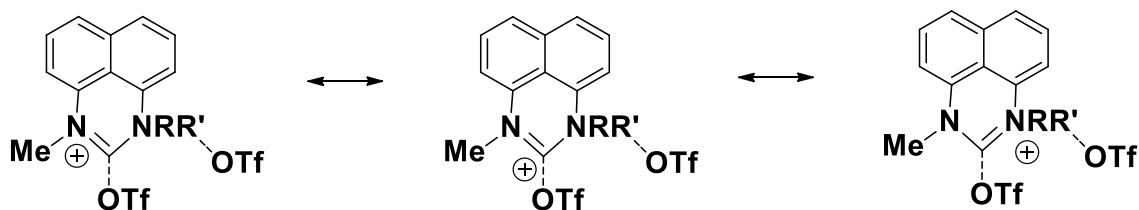


Figure 4.3.2. Proposed interaction in operation between triflate and the 6-membered ring system.

A large degree of dispersion is then indicated in this instance. This would account for the increased interaction between the triflate and the 6-membered ring system, giving rise to the smaller ΔE with respect to B97D. It is proposed that there is no correction for dispersion in this instance, since there is a large degree of stabilization in the

presence of triflate. It is proposed that there is relative proximity in operation between triflate and the 6-membered ring system as indicated above. This proximity is not sufficient, however, to give rise to a large correction for dispersion. It is proposed that there is no underestimation in the case of the interaction between the counter-ion and the 6-membered ring system in the case of B3LYP since there is a similar degree of stabilization observed in the case of B3LYP and B97D.

In terms of the following step in the pathway, formation of **5** from **4**, it can be seen that ΔG is stabilized by the presence of the triflate counter-ion by a small degree (6.42 kcal/mol in the absence of triflate and 5.82 kcal/mol in the presence of triflate). Such stabilization is also observed in the case of ΔE for M06, with a small degree of stabilization observed (9.06 kcal/mol in the absence of triflate and 9.59 kcal/mol in the presence of triflate). This level of stabilization is also offered in the case of B97D, with a small level of stabilization offered with respect to B97D (4.75 kcal/mol in the absence of triflate and 4.90 kcal/mol in the presence of triflate). It is assumed that the similar level of stabilization offered in this instance is the consequence of there being a stabilizing influence in the 6-membered ring between the positive charge of the nitrogen and the π electrons. Significantly increased stabilization is not offered with respect to the presence of the triflate anion. The major stabilization is therefore offered with respect to the 6-membered ring system. A similar magnitude of ΔE is observed in all functionals in this case.

With respect to the following step, that involving formation of **TS(5-6)** from **5**, there is an increase in the entropy with respect to formation of the neutral transition state ($\Delta S = 5.1$ in the presence of triflate and -1.7 in the absence of triflate, not shown). This reflects the fact that there is an increase in disorder following the dissociation of the triflate moiety. This is then reflected in a favourable change in ΔG (20.64 kcal/mol in the absence of triflate and 15.12 kcal/mol in the presence of triflate). In terms of ΔE for each of the functionals it can be observed that there is a level of stabilization offered with respect to the presence of triflate, with a similar magnitude of $3-4$ kcal/mol in terms of stabilization observed in all cases. Correlation/dispersion is suggested to operate in this instance as there is a moderate level of stabilization observed in the presence of triflate in all cases. It is suggested that even although a level of stabilization is likely to be observed with respect to electrostatic interactions in the 6-membered ring between the positive charge on nitrogen and the π system, further, significant stabilization is offered by the increase in entropy. In the case of the presence of triflate with respect to ΔE , there is a moderate level of stabilization in all cases. This is the consequence of correlation, but not a large degree of correlation is observed in this instance. There is not a dispersion correction of any description with respect to B97D. This indicates that the level of correlation is relatively small and is not corrected to a large degree by the correction in B97D.

In the last step in the pathway, it can be observed that there is a de-stabilization observed with respect to the complex involving triflate/methyltriflate/**6**. This is reported in all

cases with respect to both ΔG and ΔE . This may indicate that the complex containing these 3 molecules is de-stabilized relative to the absence of triflate as a consequence of steric hindrance in this complex. A similar effect may be in operation in **TS(4-5)**. This transition state geometry corresponds to the concomitant dissociation of the two triflate moieties. This resulted in a large ΔG of 29.0 kcal/mol. No major stabilization occurs in this instance with respect to the presence of the counter-ion, and coupled to a possible steric effect in the region at which dissociation occurs this maybe contributing to the large ΔG observed. A similar effect is therefore suggested to describe the de-stabilization observed with respect to the formation of complex **6**. The main steric interaction is proposed to involve the methyl moiety of methyltriflate and either of the 6-membered ring or the adjacent triflate anion. In this instance, even although there should be a stabilizing effect with respect to the presence of triflate to some extent, as this has been observed in previous complexes, it is suggested that this will be offset to some extent by steric effects in the resultant complex. The relative contribution or otherwise of the electronic and/or steric effect to the stabilization or otherwise of the system could be analysed using an ONIOM approach in which the relative importance is attached to either of the steric or electronic effects.⁷³

It has been shown within this section of the thesis how it is possible to alter the typical reactivity of a particular molecule by altering the electrostatic characteristics of an interacting species. In this instance the triflate ion has been shown to exhibit nucleophilic behavior as a consequence of the requirement to decrease electrostatic

repulsion within an amidine dication. The mechanism by which this is achieved is via the demethylation of the 6-membered ring system of the amidine dication and the associated decrease in repulsion which results.

It has also been demonstrated that there are concomitant increases in stabilization as a consequence of the presence of the triflate counter ion within the reaction system. In the majority of instances this stabilizes the complex; however the presence of this ion should be taken in the context that such stabilization is only likely to occur when it is proximal to the 6-membered ring system and / or there are no electronic repulsions to dis-favour this interaction.

5.0 Hydrogen Isotope Exchange with Iridium Catalysts.

A manuscript summarizing the combined experimental and computational work relating to the Iridium catalysts has been prepared. The work undertaken in this section of the thesis forms the basis of the computational analysis included in the manuscript.

The Use of Alternative Solvents in Iridium-Catalysed Hydrogen Isotope Exchange

Alison R. Cochrane, Christopher Idziak, William J. Kerr, Bhaskar Mondal, Tell Tuttle, Shalini Andersson, and Göran N. Nilsson. *To be submitted.*

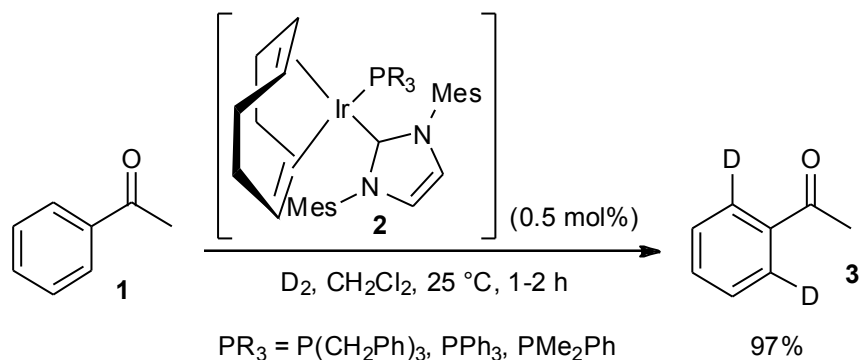
5.1 Introduction to the Iridium Catalysts.

There remains a fundamental requirement to characterize the rates of failure of potential drug candidates at an earlier level in the drug discovery process. The cost of running such projects is formidable. As a consequence of this high level of costing and the associated observation that drug failure rates are at such levels,⁷⁴ the need to identify methodologies that characterize compounds not likely to be successful at earlier stages in the process must be identified.

One such approach that could contribute to increased awareness concerning the reactivity of a potential drug candidate is the isotopic labeling of molecules. Based on such an approach it is possible to incorporate such labeled molecules into biological systems and observe the rates of change associated with metabolism, stability and toxicity. To achieve this aim as easily as possible, a hydrogen isotope exchange provides a method by which this can be accomplished in a single step.

The fundamental step associated with this procedure involves the incorporation of deuterium within the molecule. This has traditionally been achieved using Crabtree's catalyst, whose general structure corresponds to the following $[\text{Ir}(\text{COD})(\text{PCy}_3)(\text{py})]\text{PF}_6$.^{75,76} Although this compound was identified as the complex that affected deuterium incorporation optimally, there remained problems concerning the specificity of the stoichiometry required to generate this transformation as well as the long time periods needed for the reaction. It has previously been demonstrated that

complexes of the form $[\text{Ir}(\text{COD})(\text{PR}_3)(\text{IMes})]\text{PF}_6$ could effect the isotopic labeling process to a very high level in a number of substrates.⁷⁷ In addition it was also shown that these complexes could be employed at low concentrations and with respect to shorter reaction times.



Scheme 5.1.1 Isotopic Labelling with Ir(I) complexes (**2**).

The main difficulty associated with the use of this catalyst is the utility of dichloromethane (DCM) as the medium in which the reaction is performed. Such a solvent is both highly carcinogenic and displays a high vapour pressure. As a consequence of this, there is a focus within the pharmaceutical industry towards employing solvents that are less toxic.⁷⁸ In practical terms, potential drug candidates also display a low level of solubility in this particular solvent. As a result of these various unfavourable characteristics of DCM, there has been an increased level of research effort directed towards identification of alternative solvents that could be employed in the hydrogen isotope exchange reaction.⁷⁹

5.2. Computational Methods.

Density functional theory (DFT)⁸⁰ was employed to calculate the relative energies for the iridium complexes. Initial pre-optimisation of the structures was carried out with the gradient corrected BP86 functional,⁸¹ in order to take advantage of the resolution-of-the-identity (RI)-DFT approach,⁸² as implemented in TurboMole.⁸³ Calculations involving the iridium atom employed a large-core, quasi-relativistic, effective core potential⁸⁴ with the associated basis set; all other atoms were described with the def2-TZVP or def2-SVP basis set.⁸⁵ The final optimisation of structures and their characterisation was performed with the Gaussian 09 program suite.⁸³ These calculations have been performed at the M06 level of theory⁶⁶ in conjunction with the 6-31G(*d,p*) basis set⁶⁷ for all main group elements, and the Stuttgart RSC effective core potential and the associated basis set for Ir.⁸³ Frequency calculations were performed at the same level of theory to characterise the minima and the first order saddle points.

5.3 Results and Discussion.

5.3.1 Experimental Results

The experimental investigations involved the screening of a number of solvents in reactions performed under the standard conditions employed within our collaborator's laboratory. The isotopic labeling of the simple substrate acetophenone **1**, using 5 mol% of complex **2a** (R = CH₂Ph) and a reaction time of 16 hours, proceeded to varying degrees of deuteration in the selected reaction media. As illustrated by the results displayed in Table 5.3.1, the first attempt at HIE reactions in an alternative solvent, Et₂O,

delivered the isotopically enriched product **3** in a level of deuterium incorporation comparable to that obtained previously in DCM. Such a high degree of isotope exchange was maintained upon moving to the more sterically hindered and less volatile *t*-BuOMe. Unfortunately, but perhaps somewhat expected, the reaction performed in acetone produced only a moderate deuterium loading of 45%. Finally, the use of 2-MeTHF as an alternative reaction medium for HIE reactions was examined. The use of this solvent in the pharmaceutical industry has increased greatly over recent years following its identification as a potential replacement of DCM in other areas of chemistry due to its high polarity but low miscibility with water. Pleasingly, the use of this solvent in H-D exchange reactions proceeded without incident, furnishing the desired product in an excellent 95% deuteration.

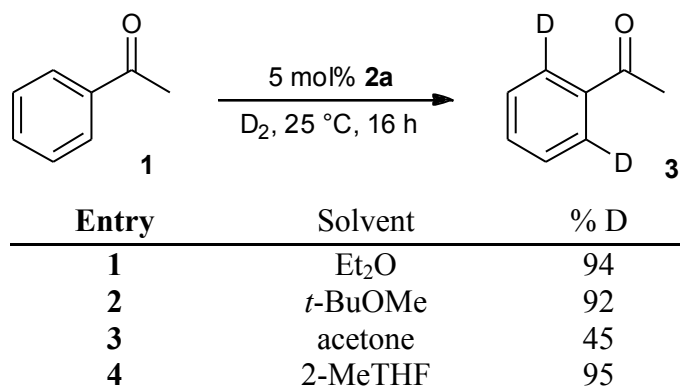
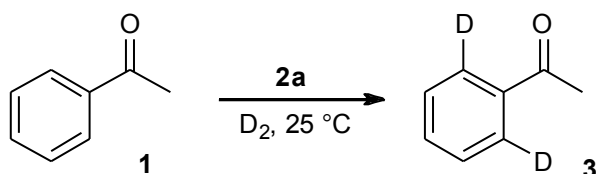


Table 5.3.1 Solvent Screening. The tabulated data represented above was produced by the experimental group working on the reaction system.

In view of these findings, three of the four solvents examined were selected for further investigation, namely Et₂O, *t*-BuOMe and 2-MeTHF. As mentioned, our Ir(I) complexes display exceptional activity in HIE reactions performed in DCM.⁷² It was therefore of

interest to determine if such an efficient catalytic procedure could be retained in systems utilising alternative solvents. Following a short series of optimisation studies, the most favourable conditions for the isotopic labeling of acetophenone **1** were identified (Table 5.3.2).

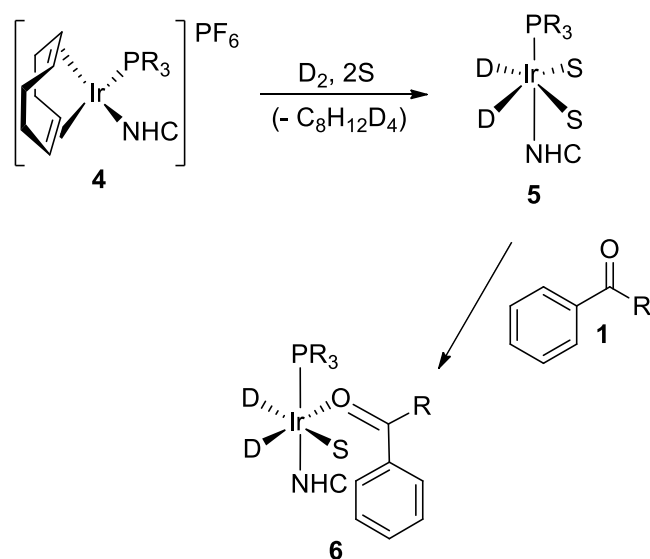


Entry	Solvent	Catalyst Loading (mol%)	Time (h)	%D
1	Et ₂ O	3	1	97
2	<i>t</i> -BuOMe	5	2	94
3	2-MeTHF	3	1	96

Table 5.3.2. Optimised conditions for HIE in alternative solvents.

5.3.2 Computational Results

To gain further insight into our observations regarding the performance of HIE reaction in alternative solvents, a series of theoretical studies were undertaken. In accordance with the proposed mechanism by which isotope exchange occurs, it was assumed that following activation of our Ir(I) complexes through loss of d₄-cyclooctadiene, the resulting coordinatively unsaturated Ir species would be stabilised by the coordination of two solvent molecules (**5**, Scheme 5.3.1).



Scheme 5.3.1. Proposed solvent coordination

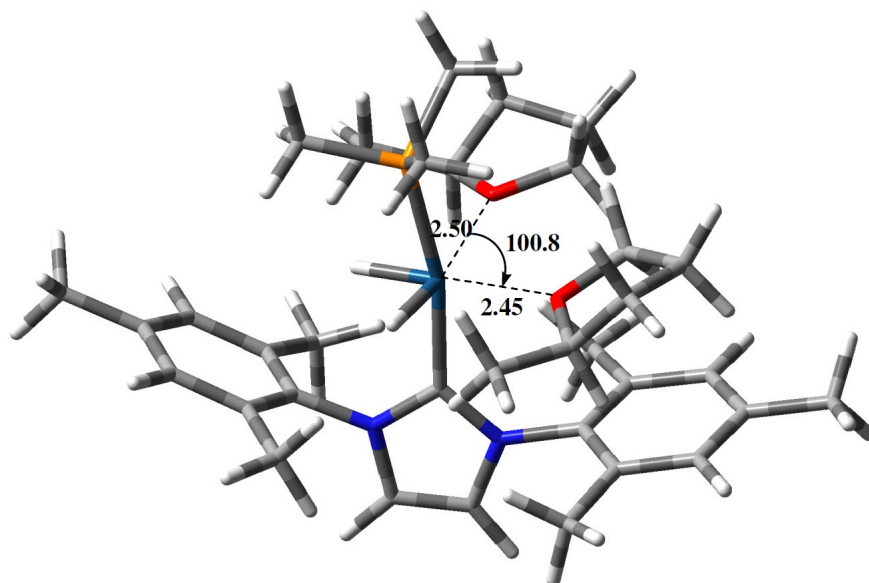
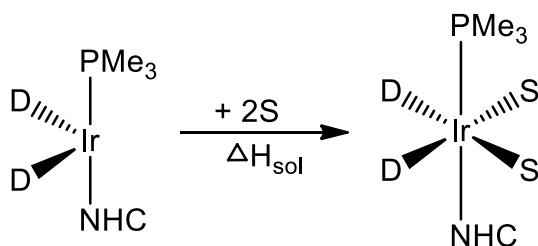


Figure 5.3.1. Optimised structure of the Ir species with two solvent (2-MeTHF) coordination (distances are in Å and angle in degrees).

The R groups on the axial ligand were trimmed down from -PPh₃ (experimental system) to -PMe₃ (computational system) in order to minimize computational cost. The R group bound to the acetophenone substrate is envisioned to correspond to the associated drug candidate molecule, for example, to be employed in the deuteration study. This approximation has no significant effect on the solvent binding enthalpies (ΔH_{sol} , for acetone) as calculated -38.60 and -41.44 kcal/mol for -PMe₃ and -PPh₃ respectively. In parallel, the absolute substrate binding enthalpies (for acetophenone) are calculated to be -23.48 and -21.41 kcal/mol for -PMe₃ and PPh₃ respectively.

Stable bi-solvent complexes for the five different solvents investigated (optimised structure of 2-MeTHF coordinated complex is shown in Figure 5.3.1) were obtained. In order for the reaction to progress, the dissociation of these solvent molecules from the metal centre must be a favourable process to enable subsequent coordination of the incoming substrate molecules. We therefore examined the explicit binding enthalpies of the solvent molecules (ΔH_{sol}), calculated as illustrated below.



Scheme 5.3.2. Calculation of solvent binding enthalpy (ΔH_{sol})

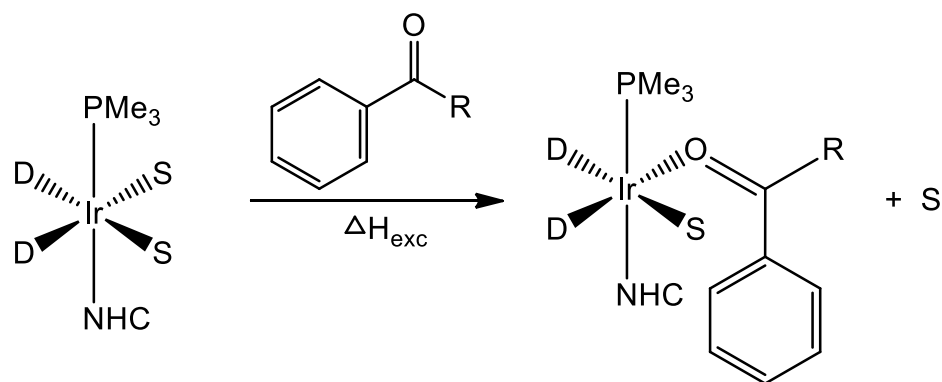
For each solvent investigated, the binding enthalpies (ΔH_{sol}) were found to be exothermic (Table 5.3.3). The variation in the deuteration yields between different

solvents, can be affected by the strength of the interaction between the solvent molecule and the iridium centre, with a larger binding enthalpy having a negative effect on %D. Of the solvents investigated, DCM was found to have the lowest binding enthalpy and the most weakly coordinating of the ethereal reaction media was found to be *t*-BuOMe, followed by Et₂O and then 2-MeTHF, with acetone having the highest binding enthalpy. Nonetheless, while acetone was found to have the highest binding enthalpy and DCM the weakest, there is no direct correlation between the other solvent molecules investigated and the experimental deuteration yields (%D). However, this initial investigation indicates only the ability of the solvent molecules to bind to the metal centre, which, as mentioned, is in all cases favourable. The ability for the substrate (**1**) to undergo deuteration will depend on the equilibrium between **5** and **6** (Scheme 5.3.1).

Entry	Species	ΔH_{sol}
1	Ir(D) ₂ (PMe ₃)(IMes)(DCM) ₂	-13.12
2	Ir(D) ₂ (PMe ₃)(IMes)(<i>t</i> -BuOMe) ₂	-17.48
3	Ir(D) ₂ (PMe ₃)(IMes)(Et ₂ O) ₂	-26.81
4	Ir(D) ₂ (PMe ₃)(IMes)(2-MeTHF) ₂	-33.03
5	Ir(D) ₂ (PMe ₃)(IMes)(acetone) ₂	-38.59

Table 5.3.3. Solvent binding enthalpies (ΔH_{sol} , kcal/mol) for five different solvents

The second step of the reaction, as presented in Scheme 5.3.1, is the exchange of one solvent molecule with the substrate at the metal centre. We therefore investigated the binding enthalpies (ΔH_{exc}) associated with the exchange of one solvent molecule with the substrate. The following scheme (Scheme 5.3.3) illustrates the calculation of the corresponding binding enthalpies (ΔH_{exc}).



Scheme 5.3.3. Calculation of substrate binding enthalpy (ΔH_{exc})

As expected, the substrate binding enthalpies follow the reverse order as that observed previously for the solvents (Table 5.3.4). That is, the solvent molecules that bound most strongly to the Ir centre are most destabilised by the exchange of the solvent molecule with the substrate and *vice versa*. However, importantly, the calculation of the ΔH_{exc} provides a much clearer indication of the solvents which will promote deuteration of the substrate. Specifically, the exchange of the DCM, the ethereal solvents and 2-MeTHF by the substrate all occur in an exothermic reaction (i.e., the equilibrium is shifted towards the substrate coordinated complex, which is then able to undergo deuteration). On the other hand, exchange of acetone occurs in a thermoneutral (slightly endothermic) reaction. As such, the substrate will only be available for deuteration 50% of the time or less, resulting in a much lower efficiency of the catalyst (lower %D).

Entry	Species	ΔH_{exc}
1	$\text{Ir}(\text{D})_2(\text{PMe}_3)(\text{IMes})(\text{PhCOMe})(\text{DCM})$	-13.26
2	$\text{Ir}(\text{D})_2(\text{PMe}_3)(\text{IMes})(\text{PhCOMe})(-t\text{BuOMe})$	-12.81
3	$\text{Ir}(\text{D})_2(\text{PMe}_3)(\text{IMes})(\text{PhCOMe})(\text{Et}_2\text{O})$	-7.30
4	$\text{Ir}(\text{D})_2(\text{PMe}_3)(\text{IMes})(\text{PhCOMe})(2\text{-MeTHF})$	-3.70
5	$\text{Ir}(\text{D})_2(\text{PMe}_3)(\text{IMes})(\text{PhCOMe})(\text{acetone})$	0.30

Table 5.3.4. Enthalpies of exchange (ΔH_{exc} , kcal/mol) associated with the exchange of one solvent molecule with the substrate

The difference in the direction of the equilibrium, as shown by the calculated ΔH_{exc} , in the presence of acetone and the other four solvents align with the difference between the levels of H-D exchange observed in the reactions. This delicate balance between solvent and substrate binding enthalpies is clearly important in determining the ability of the reaction to occur. However, once bound the solvent may also affect the activity of the catalyst through polarizing the medium in which the reaction occur. These more subtle effects of the solvent on the reaction mechanism may account for the differences in deuteration observed between DCM, the ethereal solvents and 2-MeTHF.

In this section of the thesis it has been demonstrated that the yield of deuteration which proceeds in the presence of an acetophenone substrate is directly related to the strength of the interaction in operation between the iridium complex and the solvent molecules which bind to this complex. This is related to an overall catalytic complex in which there are a series of deuterium / hydrogen, acetophenone and solvent exchange steps with the iridium complex. The calculated percentage of deuteration of the acetophenone substrate is inversely proportional to the binding enthalpies of the solvent molecules, with larger

values of the binding enthalpies observed for deuteration yields which are smaller in value. The enthalpies associated with binding of acetophenone to the iridium complex are inversely proportional to those which are observed with respect to the solvent interaction enthalpies. This is consistent with the observation that it is more energetically expensive to dissociate a strongly binding solvent molecule with the substrate. A less obvious effect may also be associated with a polarization effect in the surrounding implicit solvent system that is rooted in the explicit interaction of the solvent molecule with the iridium complex. This secondary effect may also influence the level of deuteration which is observed in a less quantitative / measurable fashion.

Further work could take the form of endeavoring to determine in a more exact fashion the nature of the interactions in operation between the iridium complex and the bound solvent molecules. This could take the form of explicitly including a larger number of solvent molecules at varying locations and orientations within the complex and attempting to observe if there are any changes in energetics which occur. This could then lead to determinations concerning whether there is a polarization effect in operation within the implicit medium as a consequence of these additional explicit solvent molecules.

6.0 The Formation of Methanol from CO₂ and CO.

6.1. Introduction to the Formation of Methanol.

There is a large commercial significance attached to the synthesis of methanol. This molecule functions as a fuel and building block in a number of synthetic routes. Alternative routes to the formation of this molecule are therefore of fundamental importance, with traditional industrial approaches relying heavily on extremes of both temperature and pressure. The formation of methanol occurs from syngas at temperatures of between 250-300 C and pressures of between 50-100 atm. To facilitate more environmentally friendly approaches, an alternative mechanism has been proposed.⁸⁶

In this mechanism hydrogenation of carbamates, carbonates and formates has been accomplished under catalytic conditions. This has been accomplished at significantly more favourable conditions, with both lower temperatures and pressures employed compared with the previously referred to excesses of such parameters. In addition the syntheses have been accomplished in the absence of a discrete solvent system, with measurable yields having been reported in the presence of the principal reactant dimethylcarbonate. These moieties can be employed as precursors in the formation of methanol, and can be formed from CO and CO₂.

In the original paper,⁸⁶ formation of alcohols from organic carbonates has been reported. This is suggested to be the first instance of such a synthesis based on this moiety. The

catalytic details of this mechanism are based upon a series of Ru (II) pincer complexes, which have undergone de-aromatization/aromatization. This is the principal mechanistic driver for the cooperation that is in operation between the core Ru and the associated aromatic nucleus surrounding this metal centre. In this thesis, a computational analysis of the mechanistic details of a proposed route involving the synthesis of methanol from these previously referred to precursor moieties has been undertaken. The experimental work that has been undertaken previously,⁸⁶ combined with the computational work undertaken in this thesis, contributes in a positive fashion to the elucidation of both a greener and more commercially viable synthetic route to methanol formation at more favourable temperatures and pressures.

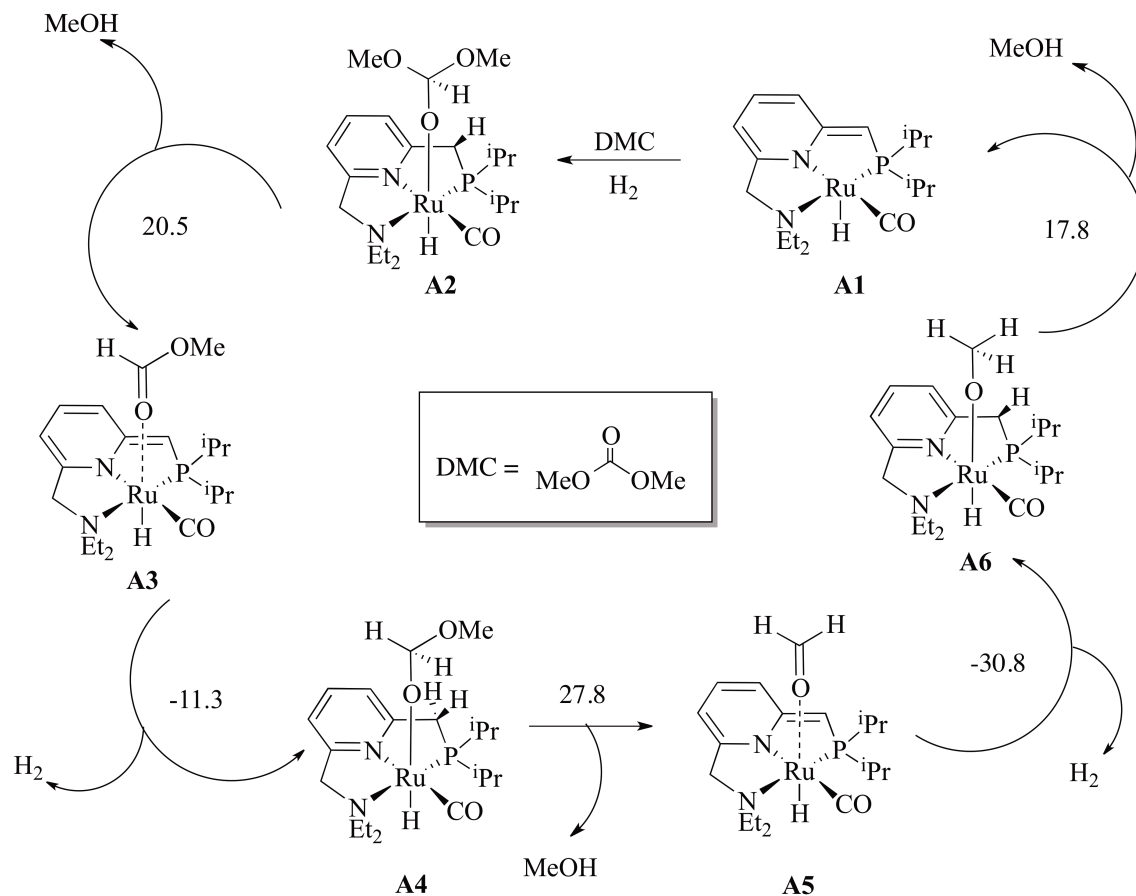
6.2 Computational Methods

DFT calculations were performed to attempt to describe the mechanistic details of another cyclic organometallic reaction system involving the aromatization-de-aromatization of a series of ruthenium complexes in which there are alternate additions of molecular hydrogen and dissociation of methanol respectively.⁸⁶ Optimization/frequency and saddle point calculations were set up for each of the respective intermediates, transition state and product/reaction complexes. These were carried out with respect to the Stuttgart Effective Core Potential⁸⁴ to describe the relativistic effects in operation in Ru. The functional that was employed in these calculations was M06⁶⁶ and the basis set was 6-31G(d).⁶⁷ M06 was again employed

since this functional provides good performance for the characterization of reaction barrier heights.

6.3 Results and Discussion.

The generation of methanol from the catalyst **A1** is proposed to occur via the mechanism outlined in Scheme 6.3.1.

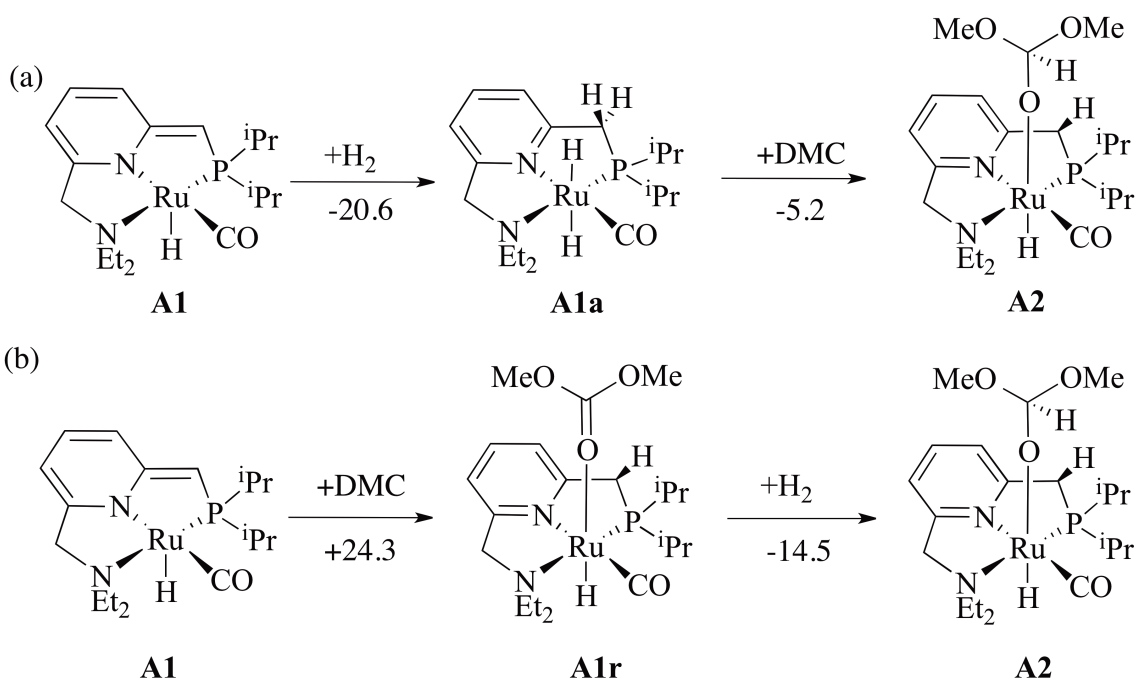


Scheme 6.3.1. Proposed mechanism for the formation of methanol based on catalyst **A1**.

Relative reaction free energies (ΔG , kcal/mol, 298.15 K) between the intermediates shown are given.

6.3.1 The Initiation Mechanism.

There are two routes proposed to account for formation of intermediate **A2**. In the first route the catalyst **A1** is first hydrogenated (Scheme 6.3.2a) followed by the addition of dimethylcarbonate (DMC). The alternative mechanism involves the initial addition of DMC followed by hydrogenation (Scheme 6.3.2b)



Scheme 6.3.2. Alternative mechanisms for the formation of **A**. Relative reaction free energies (ΔG , kcal/mol, 298.15 K) between the intermediates shown are given.

While the first mechanism (i.e., initial hydrogenation followed by addition of DMC) was found to be exergonic (ΔG -25.8 kcal/mol), the barrier associated with the addition of DMC to the hydrogenated intermediate (**A1a**) was found to be prohibitively high ($\Delta G^* =$

71.5 kcal/mol). The transition state geometry associated with the first mechanistic proposal is represented in Figure 6.3.1. Therefore, the second mechanism (i.e., the formation of **A2** from the addition of H₂ after the reactant complex is formed (Scheme 6.3.2b)) is predicted to be the favoured mechanism. Although the reaction is overall endergonic ($\Delta G = 9.8$ kcal/mol) the maximum barrier for this mechanism is associated with the latter addition of H₂, where the barrier is +18.9 kcal/mol.

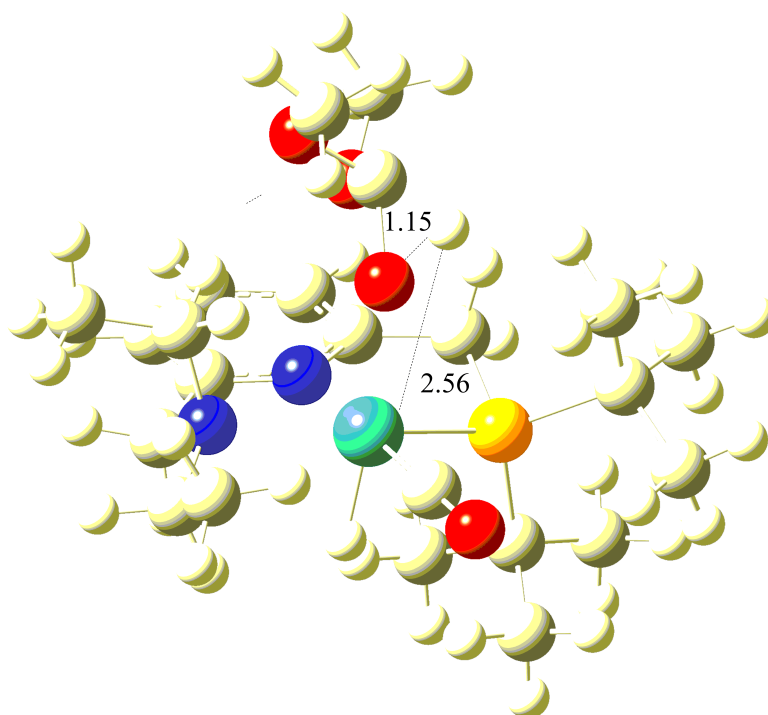


Figure 6.3.1. Optimized geometry corresponding to **TS(A1a-A2)**. Distances in Å.

With respect to the transition state geometry corresponding to formation of **TS(A1a-A2)**, the change in relative electronic energy corresponding to this step corresponds to

an unfavourable endergonic value of 71.5 kcal/mol. The reaction coordinate indicative of the step giving rise to this prohibitive relative electronic energy change corresponds to the incorporation of the hydride into the carbonyl group of dimethyl carbonate by the bound hydride associated with the Ru centre. The initial guess corresponding to this transition state was based on the approach of this terminal hydride towards the oxygen of the carbonyl group. Following a number of attempts to derive this converged geometry, the resultant imaginary frequency was found to correspond to -1405 cm^{-1} . The magnitude of this imaginary frequency provides an indication of the length of the barrier associated with a hydrogen atom that can undergo quantum tunneling. This is represented according to the following equation⁸⁷

$$\kappa_i^\ell(T) \approx \frac{\beta}{\beta - \alpha_i^\ell} \left[e^{(\beta - \alpha_i^\ell)V_i^{\text{TS}}} - 1 \right] \quad 6.3.1$$

where

$$\beta = \frac{1}{k_B T},$$

$$\alpha = 2\pi / (\hbar\omega),$$

V_0 = Parameter of potential,

ω = Parameter of potential,

k_B = Boltzmann's constant

In instances where the energy barrier is unlikely to permit the reaction to proceed in classical terms, it may be possible that a quantum tunneling effect may be in operation. The magnitude of the imaginary frequency is given according to Equation 6.3.1 above. In instances where the imaginary frequency is small then the barrier corresponding to quantum tunneling is likely to be represented by barriers that are both broader and gentler in shape. Similarly in instances where the imaginary frequency is larger in value, then the barrier is likely to be taller and narrower with respect to geometry. As a consequence of the relatively large magnitude associated with this particular transition state it is suggested that there is an increased probability of quantum tunneling in this instance.

6.3.2 Reaction Enthalpies and Free Energies

From the relative Gibbs free energy changes pertaining to Scheme 6.3.1, it can be seen that dehydrogenation is exergonic for all steps. These steps are **A3** → **A4** and **A5** → **A6** respectively. With respect to the first of these steps (**A3** → **A4**) the free energy change is -11.3 kcal/mol, and for **A5** → **A6** it is -30.8 kcal/mol. These exergonic changes for dehydrogenation are considered to be exergonic as a consequence of the introduction of aromaticity into the products of the relevant steps (**A4** and **A6** respectively). The introduction of aromaticity occurs as a consequence of adherence to Hückel's $4n+2$ rule that describes the level of π bonding necessary to characterize a molecule in aromatic terms. In the relevant intermediates, this is the consequence of the introduction of an additional π bond in the 6-membered ring, the relevant structural feature being obtained from the adjacent 5-membered ring system. In contrast to the introduction of

aromaticity in the hydrogenation steps, dissociation of methanol is associated with a reduction in aromaticity via transfer of the relevant π bond from the 6-membered ring to the adjacent 5-membered ring. This removal of aromaticity is assumed to account for the associated free energy changes occurring for the relevant steps. In the above mechanism these steps are **A2** \rightarrow **A3**, **A4** \rightarrow **A5**, and **A6** \rightarrow **A1** respectively. The Gibbs free energy changes were found to correspond to 20.5, 27.8 and 17.8 kcal/mol respectively. Again the $4n+2$ Huckel rule is considered to account for the observation that there is a reduction in aromaticity following dissociation of the methanol moiety from the respective reactants.

A number of enthalpy diagrams were produced to reflect intermediate formation of methanol along the reaction pathway described in Scheme 6.3.1. From these figures below (Figures 6.3.2 – 6.3.4) it can be observed that there a number of steps which are favourable from an energetic perspective. It can also be observed that there are a number of conversions in which the relative changes in electronic energy with respect to formation of the transition states could conceivably proceed.

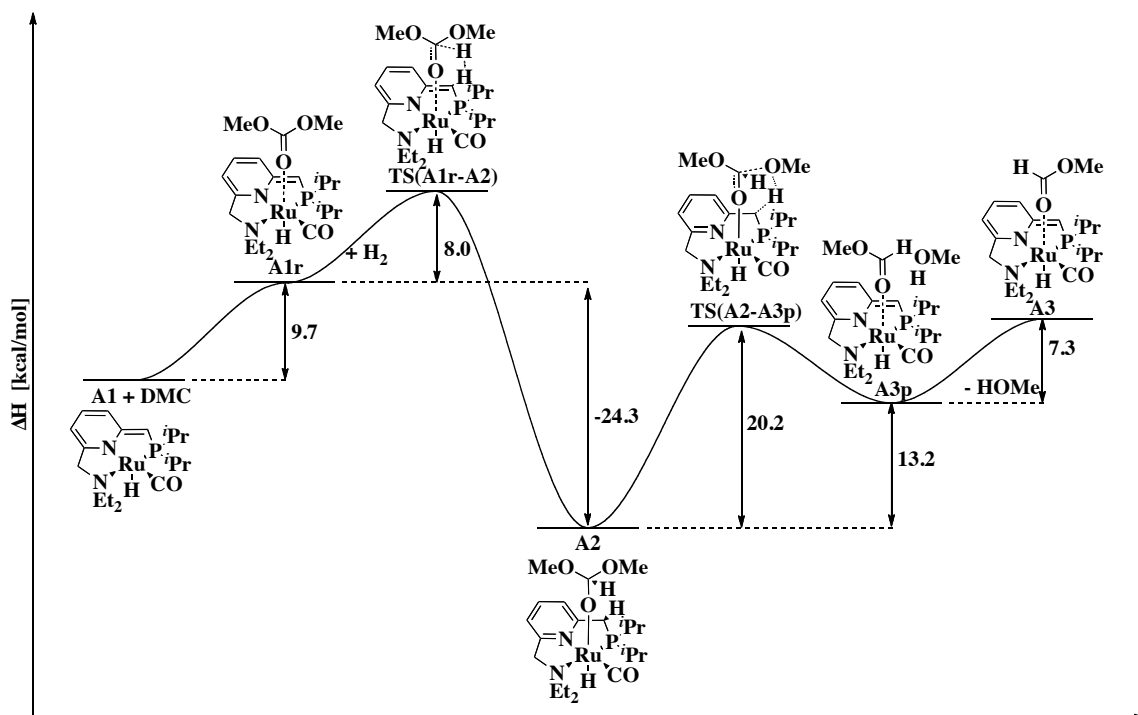


Figure 6.3.2. Relative enthalpy changes occurring with respect to steps A1 → A3 incorporating TSs and reaction/product complexes.

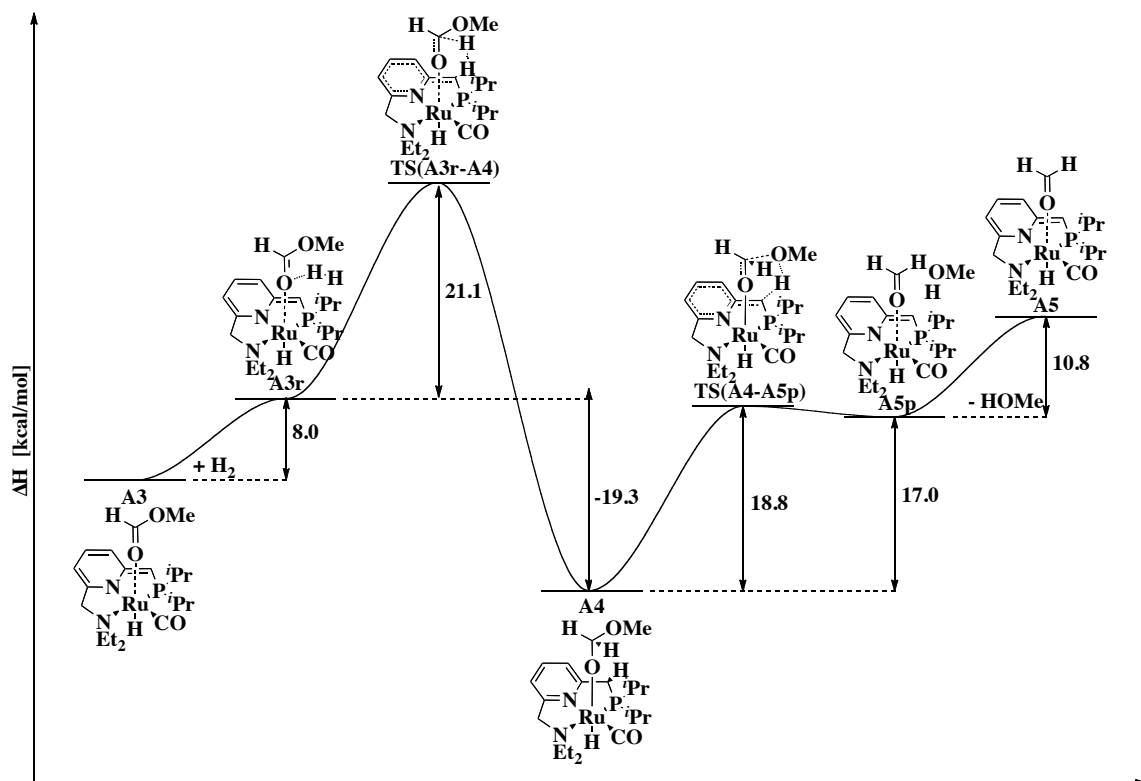


Figure 6.3.3. Relative enthalpy changes occurring with respect to steps A3 → A5 incorporating TSs and reaction/product complexes.

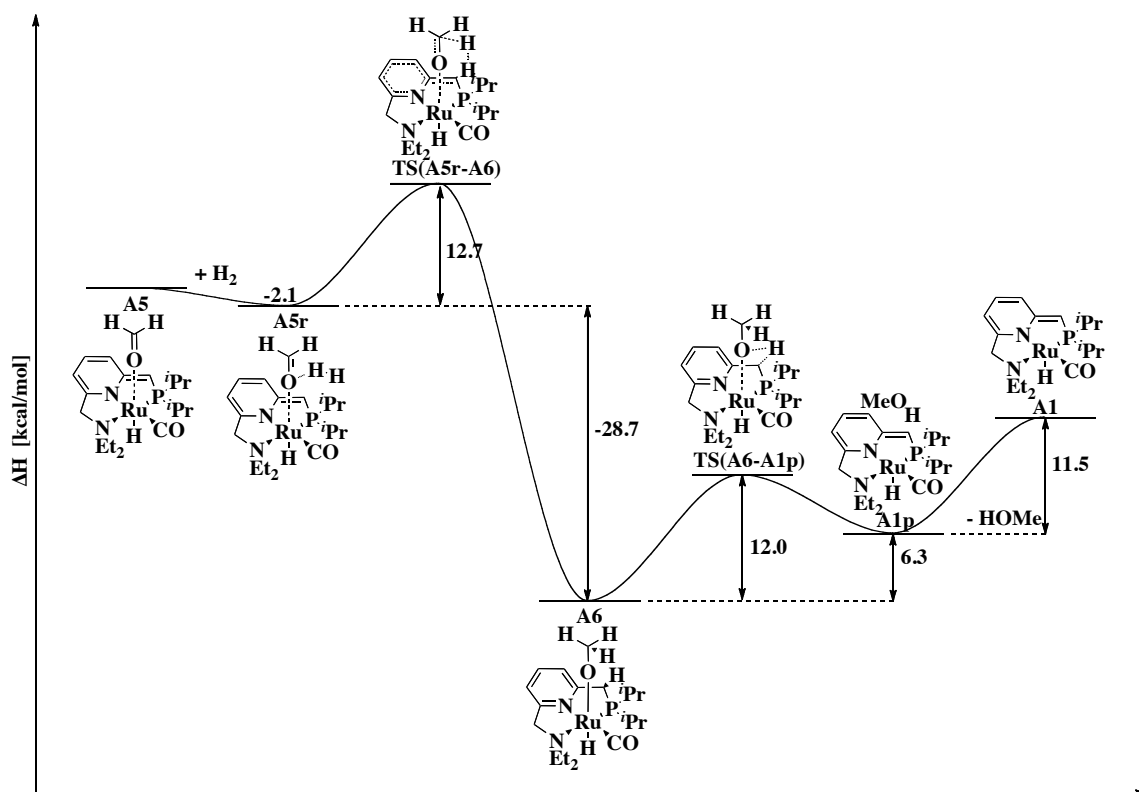


Figure 6.3.4. Relative enthalpy changes occurring with respect to steps A5 \rightarrow A1 incorporating TSs and reaction/product complexes.

From an analysis of the energetic changes occurring with respect to formation of the transition states, reaction and product complexes in suggested to form, represented in the enthalpy diagrams Figures 6.3.2-6.3.4, but not shown in Scheme 6.1.1, there are a number of steps which were of sufficient magnitude to allow the reaction to proceed. These are assumed to be those steps in which the activation barrier is of a reasonable magnitude. Such instances of endergonic (with respect to Gibbs free energy) transition state activation barriers that are conceivably possible to overcome given the temperature

and acidic conditions referred to in the paper, are as follows **A1** → **TS (A1r-A2)**, **A2** → **TS (A2-A3p)**, **A3** → **TS (A3r-A4)**, **A4** → **TS (A4-A5p)**, **A5** → **TS (A5r-A6)**, **A6** → **TS (A6-A1p)**. The magnitudes of these changes are 18.8 kcal/mol, 21.3 kcal/mol, 22.9 kcal/mol, 19.2 kcal/mol, 14.4 kcal/mol and 11.9 kcal/mol respectively. From the magnitudes of these changes it is suggested that each of the activation barriers are of a sufficiently low value to permit the reaction to proceed via direct formation of these geometries from the preceding intermediates. The probability of this is further enhanced since there are increased temperatures and acidic conditions under all scenarios tested in the paper. Such analyses were carried out and are represented in the subsequent discussion. Comparison with computation could only be made under conditions in which the solvation effects could be incorporated into the DFT calculations. Under such conditions it may be possible to demonstrate how large the influence of the solvent is likely to be on the energetics of the reaction. Further effects as a result of the influence of temperature and pressure are unlikely to be directly comparable between computations and experiment since these cannot easily be taken account of in a computational sense. It is suggested, however, that these effects will further enhance the energetics of the reaction.

With respect to Scheme 6.3.1, the formation of the respective reactant and product complexes from the intermediates occurring prior to and after these molecules are represented below in Table 6.3.1.

	ΔG (kcal/mol)
A1 \rightarrow A1r	24.3
A2 \rightarrow A3p	12.8
A3 \rightarrow A3r	17.0
A4 \rightarrow A5p	14.7
A5 \rightarrow A5r	5.3
A6 \rightarrow A1p	5.1

Table 6.3.1. Tabulation of the relative free energy changes occurring with respect to formation of reactant and product complexes based on transition states for Scheme 6.1.2

With respect to the relative enthalpy changes occurring in the formation of the reactant complexes (Figures 6.3.2 – 6.3.4) it can be observed that there is a favourable change occurring with respect to **A5 \rightarrow A5r**, although typically the formation of these complexes is unfavourable, particularly when the entropic effects are taken into account in the free energy (Table 6.3.1).

Inclusion of the entropic effects, for the reaction **A5 \rightarrow A5r** results in an endergonic reaction (+ 5.3 kcal/mol, Table 6.3.1). The entropic change associated with this step is a large decrease in this parameter (-24.9 Cal/Mol-Kelvin). This is consistent with the observation that there is a decrease in disorder associated with formation of this complex, since there is decreased randomness with respect to molecularity following

association of dihydrogen with **A5**. When these are taken into consideration, the outcome will be an endergonic value corresponding to the relative change in the Gibbs free energy under conditions in which the magnitude of $T\Delta S$ is more negative than ΔH .

Formation of **A1r** from **A1** with respect to the relative enthalpy change was observed to correspond to 9.7 kcal/mol (Figure 6.3.2). In terms of the entropy change for this step it can be observed that there is a very significant decrease in the relative magnitude of this parameter (-49.1 Cal/mol-Kelvin). This is consistent with the association of DMC with **A1**, and a resultant decrease in the disorder associated with the **A1r** complex. This large change in the relative entropy is a factor in the significant increase in the relative change in the Gibbs free energy, the final value corresponding to 24.3 kcal/mol. As a consequence of this unfavourable value for the relative change in entropy it is suggested that the relatively small change in the enthalpy corresponding to this step and the concomitant stabilization of this complex is the consequence of increased electrostatic interactions occurring upon the association of **DMC** with **A1**.

A similar analysis of **A2** \rightarrow **A3p** indicates that the relative enthalpy change associated with this step was evaluated to correspond to 13.2 kcal/mol. The relative change in entropy was determined to correspond to 1.4 Cal/mol-Kelvin. This produced a Gibbs free energy change that was again endergonic (12.8 kcal/mol). This suggests that the dissociation of methanol was a contributory factor to this step proceeding, but was not of sufficient magnitude to produce a favourable outcome in terms of the Gibbs free energy.

This suggests that this step is driven by changes in the Gibbs free energy and is not altered sufficiently by the entropic changes occurring.

With respect to the next step, that pertaining to formation of **A3r** from **A3**, it is clear from Figure 6.3.3 that the relative change in the enthalpy for this step is 8.0 kcal/mol. When consideration is given to the relative change in entropy for this step it can be observed that there is an unfavourable change in this relative value (-30.1 Cal/mol-Kelvin). This is a negative contribution with respect to the step and is again indicative of a decrease in the number of degrees of freedom in going from **A3** to **A3r**. This is then reflected in the relative change in the Gibbs free energy corresponding to an endergonic value (17.0 kcal/mol, Table 6.3.1). The relative change in entropy and enthalpy therefore act concomitantly to increase the relative change in Gibbs free energy for the step.

Consideration of the formation of **A5p** from **A4** indicates that the relative enthalpy change for this step corresponds to 17.0 kcal/mol (Figure 6.3.3). The relative change in the entropy for this step was evaluated as 7.6 Cal/mol-Kelvin, which is again consistent with the dissociation of a methanol moiety from this product complex, resulting in an increase in the number of degrees of freedom in the resultant complex. This increase is favourable from an energetic perspective and offsets the unfavourable increase in the enthalpy by decreasing the relative change in the Gibbs free energy to 14.7 kcal/mol (Table 6.3.1).

When a similar analysis is performed with respect to the formation of **A1p** from **A6**, it can be observed that the relative enthalpy change for this step was determined to

correspond to 6.3 kcal/mol (Figure 6.3.4). The relative entropy change is positive, 4.0 Cal/mol-Kelvin, indicative of an increase in disorder in the complex relative to the undissociated state. This increase in entropy is again of sufficient magnitude to offset the relative enthalpy change, resulting in a relative Gibbs free energy change corresponding to 5.1 kcal/mol at 298K.

With respect to the remaining steps, corresponding to dissociation of methanol (formation of **A3p**, **A5p** and **A1p**) it can be observed that the relative entropic changes occurring in these instances are 1.4 Cal/mol-Kelvin with respect to **A3p**, 7.6 Cal/mol-Kelvin with respect to **A5p** and 4.0 Cal/mol-Kelvin with respect to **A1p**. These changes in the entropy are favourable from an energetic perspective, since they will function to minimize the Gibbs free energy. The unfavourable Gibbs free energy changes for these steps are therefore suggested to be the consequence of the removal of aromaticity within the aromatic nucleus following dissociation of the methanol moiety. There may also be enhanced stabilization offered with respect to the presence of the methyl group that may function to withdraw/donate electrons from/to the surrounding groups, thereby increasing the inductive effect within this region. Removal of the methoxy group may decrease this effect and decrease stabilization.

6.4 Conclusions and Further Work

With respect to the overall context in which the work was carried out in, there has been a related study which has been undertaken based on the experimental work presented in

the original paper.⁷⁸ This study which postulates an alternative mechanism documenting the dehydrogenation of methanol.⁸⁰ In the latter paper, a ruthenium-triphenylphosphine catalyst was employed to evaluate the influence of this moiety on the activation energy associated with the dehydrogenation steps. In further studies based on this paper, the influence of the substitution of the PPh₃ moiety by a more electron donating phosphine moiety demonstrated that there was a decrease in the activation energy associated with the presence of this phosphine group. This suggested that electron donation was a significant driver in the minimization of the reaction rate in this instance.

A possible explanation in terms of relative energetic changes of a series of steps in a novel route to Methanol formation has been reported. Possible transition states for these steps have been determined and the energies of each transformation evaluated. It has been shown that the relative energetics of these set of reactions are within a satisfactory range for the process to proceed as represented experimentally.

Finally, the calculations described in this work have all been carried out in the gas phase. Under conditions in which the system has been perturbed via inclusion of a solvent, there are likely to be associated decreases in free energy for each of the respective inter-conversions. Since the experimental conditions were principally carried out in the solvent phase using tetrahydrofuran, 1,4-dioxane and under neat conditions the effect of these solvents on the mechanism are also of interest.

7.0 Conclusions and Further Work

In this thesis the use of DFT has been employed within the context of the partial elucidation of a number of reaction mechanisms. The computational work which has been undertaken has provided evidence concerning whether the experimental observations which have been reported can be rationalized in terms of the energetic changes associated with the underlying reactions. Such studies can be employed to provide evidence in favour of, or against, a particular mechanistic proposal.

A possible explanation for the experimental observation which was reported in the nitration system has been provided. The exact details, in terms of possible orbital interactions within the pyrimidine ring system which could account for this mechanistic proposal were not undertaken within this study. The potential for further work within this context is therefore suggested. Further work could also focus upon the use of Intrinsic Reaction Coordinate calculations to provide further details relating to the transition states which have been suggested to connect the respective reactants, intermediates and products of these systems. In addition it could be possible to calculate the energy of TS (22-23) for the singlet state in scheme 3.3.12 to determine if this is more or less stable than the triplet state. This could increase or decrease evidence for the operation of this mechanism. Additionally a different combination of functional and / or basis set could be used to evaluate the energies obtained for the mechanisms.

The main conclusion from the work undertaken on superelectrophilic dications has been that it was possible to alter the chemical reactivity of a molecule whose typical chemical functionality has been established in previous studies. In this study it has been shown that accepted modes of reactivity, established from previous studies and accepted, can be altered if a rational approach is taken to the design of the interacting molecules. Such methodology could be employed, for example, in the design of potential drug candidates, where a novel type of reactivity would be of benefit within an active site region. The need to minimize the energy of the system has been demonstrated to be of paramount importance in the behavior of a system in which electrostatic considerations are of most importance. It has further been demonstrated that in a system in which electrostatic repulsions must be reduced, there can be alternative atypical, complementary, electrostatic behavior within an interacting species. The main driver within the system is the maintenance of molecular cohesion within the de-stabilized system. This indicates the fundamental electrostatic considerations in operation within the molecule should be viewed as the driving force for reactivity. It has also been demonstrated that electrostatic considerations can be rationalized with respect to the geometries of the transition states to which they refer. These observations can provide further explanations for the energies which have been produced. Further study could be undertaken which attempts to rationalize the differences in energies between each

of the functionals that were employed in the study. This was beyond the scope of the work undertaken here.

With respect to the main findings from the work undertaken in the study of iridium catalysts it has been shown that a direct relationship exists between the strength of the solvent: iridium complex interaction and the extent to which deuteration proceeds in a catalytic system which is coupled to this substrate. This could have significant value to studies in which the toxicity of potential drug candidates towards biological material are to be assessed, since the suitability of a particular solvent system could be specifically optimized for the system. An intuitive, inversely proportional energetic relationship has also been shown to operate with respect to the dissociation of the respective solvent molecules by the acetophenone substrate. These findings could be employed to form the basis of a general model for the selection of an appropriate solvent system in which the extent of deuteration associated with a particular molecule could be optimized for the nature of the study, whether this is with respect to toxicity or whatever. This is suggested as a possible future study. In addition the iridium complex that is utilized within this study may not be as hazardous to health as Crabtree's catalyst.

The main finding from the work undertaken within the methanol project has been principally connected to the elucidation of the experimentally presented reaction mechanism, and has demonstrated that that it may be a feasible route to a more

environmentally friendly mode of methanol synthesis. To facilitate this synthesis, it has been shown that a different order of approach of DMC and H₂ may be required in order to ensure that the energies of the cycle are more consistent with those which are consistent with the environmentally friendly overview of the paper. Further work which could be undertaken may be associated with the calculation of the energies of the steps within the catalytic cycle under scrutiny using a different functional or basis set combination. In addition it could be constructive to compare the experimentally derived energies with those generated using computational approaches in order to make the comparison between these two approaches more meaningful.

8.0 References.

1. Heisenberg, W., *Z.Phys* **1925**, 33, 879-893.
2. Schrodinger, E., *Ann. Phys. (Berlin)* **1926**, 79 (4), 361-U8.
3. Dirac, P. A. M., *Principles of Quantum Mechanics Fouth Edition*. Oxford Science Publications: 1930.
4. Huckel, E., *Z. Phys* **1931**, 70 (3-4), 204-286.
5. Roothan, C. C. J., *Rev. Mod. Phys.* **1951**, 23 (2), 69.
6. Pariser, R., and Parr, R., *J. Chem. Phys* **1953**, 21, 466.
7. Heitler, W., and London, F., *Z. Phys* **1927**, 44, 455-472.
8. L. Pauling and E. Bright Wilson, *Introduction to Quantum Mechanics With Applications to Chemistry*. Dover Books: New York, 1935.
9. Burke, K., *J. Chem. Phys* **2012**, 136, 150901.
10. Fermi, E., *Z. Phys* **1928**, 48 (73).
11. Thomas, L. H., *Proc. Cambridge Philos. Soc* **1926**, 23, 542.
12. Hohenberg, P., and Kohn, W., *Phys. Rev* **1964**, 136 (B864).
13. Kohn, W., and Sham, L.J., *Phys. Rev* **1965**, 140 (A1133).
14. Parr, R. G., and Yang, W., *Density Functional Theory of Atoms and Molecules*. Oxford university Press: Oxford, 1989.
15. Gunnarsson, O., and Jones, R.O., . *Rev. Mod. Phys* **1989**, 61, 689-746.
16. Levy, M., *Proc. Nat. Acad. Sci. USA* **1989**, 61, 689.
17. Langreth, D. C., and Perdew, J.P., *Solid. State. Commun* **1975**, 17, 1425.
18. Becke, A. D., *Phys. Rev. A* **1988**, 38, 3098.

19. Gill, P. M. W., Johnston, B.G., Pople, J.A., and Frisch, M.J., , *Chem. Phys. Lett* **1992**, *197*, 499-505.
20. Overand, J., and Scherer, J.R., *J. Chem. Phys* **1960**, *32* (1296).
21. Andzelm, J., and Wimmer, E., *J. Phys. Chem* **1992**, *97*, 4664.
22. Saunders, M. J., *J. Comput. Chem* **2004**, *25*, 621-626.
23. Shaik, A., Danovich, D., and Hiberty, P.C., **2001**, *101*, 1501-1540.
24. Peng, C. Y.; Ayala, P. Y.; Schlegel, H. B.; Frisch, M. J., *J. Comput. Chem* **1996**, *17* (1), 49-56.
25. Cotton, F. A., Wilkinson, G., Gaus, P.L., *Basic inorganic Chemistry. 2 ed.* John Wiley & Sons: 1976.
26. Halgren, T. A., and Lipscomb, M.N., *Chem. Phys. Lett* **1977**, *49* (2), 225-232.
27. Jensen, F., *Introduction to Computational Chemsitry*. Second Edition ed.; 2007.
28. Peng, C., and Schlegel, B, *Israel. J. Chem* **1993**, *33*, 449-545.
29. Simons, J., and Nichols, J., Int. J. Quantum Chem. In *Quantum Chem. Symp*, 1990; Vol. 24, p 263.
30. Baker, J., and Hehre, W.J., *J. Comput. Chem* **1991**, *12*, 606.
31. Koch, W., and Holthausen, M.C., *A Chemist's Guide to Density Functional Theory second edition*. 2002.
32. Born, M., Oppenhiemer, R., *Ann. Phys. (Leipzig)* **1927**, *84*.
33. Overand, J., and Scherer, J.R., *J. Chem. Phys* **1960**, *32* (5), 1289.
34. Hartree, D. R., *Proc. Cambridge. Phil. Soc* **1928**, *24*, 89-110.
35. Hartree, D. R., *Proc. Cambridge. Phil. Soc* **1928**, *24*, 111-132.
36. Hartree, D. R., *Proc. Cambridge. Phil. Soc* **1928**, *24*, 426-437.

37. Langreth, D. C., and Perdew, J.P., *Phys. Rev B* **1977**, *15*, 2884.
38. Lee, C. T.; Yang, W. T.; Parr, R. G., *Phys. Rev B* **1988**, *37* (2), 785-789.
39. Ebersson, L., and Radner, F., *Acta. Chem. Scand* **1984**, *B38*, 861.
40. Ingold, C. K., Structure and Mechanism in Organic Chemistry. Ingold, C. K., Ed. Cornell University Press: New York., 1969.
41. Ingold, C. K., Hughes, E.D.J., *J. Chem. Soc* **1950**.
42. March, J., *Advanced Organic Chemistry*. John Wiley: New York, 1985.
43. Aschi, M.; Attina, M.; Cacace, F.; Ricci, A., *J. Am. Chem. Soc* **1994**, *116*, 9535.
44. Peluso, A., and Del Re, G., *J. Phys. Chem* **1996**, *100*, 5303.
45. Johnson, C. D., *Chem. Rev* **1975**, *75* (6), 755-765.
46. Coombes, R. D., Moodie, R.B., Schofield, K.J., *J. Chem. Soc. B* **1968**, 800.
47. Lund, T., Ebersson, L.J., *Chem. Soc., Perkin Trans. 2* **1997**, 1435.
48. Olah, G. A., Kuhn, S., and Flood, S.H., *J. Am. Chem. Soc* **1961**, *83*, 4571.
49. Esteves, P. M., Carneiro, J.W.M., Cardoso, S.P., Barbosa, A.G.H., Laali, K.K., Rasul, G., Prakash, S. and Olah, G.A., *J.Am.Chem.Soc* **2003**, *125*, 4836-4849.
50. Teixidor, F., Brabera, G., Vaca, A., Kivekas, R., Sillanpaa, R., Olivia, J., and Vinas, C., *J. Am. Chem. Soc* **2005**, *127*, 10158-10159.
51. Bakke, J. M., *Pure. Appl. Chem.* **2003**, *75* (10), 1403-1415.
52. Li, R., and Lim, E.C., *J. Chem. Phys* **1972**, 605-612.
53. S. Miertuš, E. S., and J. Tomasi, *Chem. Phys. Lett* **1981**, *55*, 117-129.
54. Atkins, P. W., and Friedman, R.S., *Molecular Quantum Mechanics, Third edition*. Oxford University Press: 1997.
55. Dexter, D. L., *J.Chem. Phys* **1953**, *21* (5), 836-850.

56. Hartree, D. R., *Proc. Cambridge Phil. Soc.* **1928**, *24*.
57. Manz, T. A., Scholl, D.S., *J. Comput. Chem* **2010**, *31*, 1528-1541.
58. Hammond, G. S., *J. Am. Chem. Soc* **1955**, *77*, 334-228.
59. Foresman, J. B.; Frisch, A., *Exploring Chemistry with Electronic Structure Methods*. 2nd ed.; Gaussian Inc.: Pittsburgh, PA, 1996.
60. Glasstone, S., Laidler, K. and Eyring, H., *The Theory of Rate Processes*. McGraw-Hill: New York, 1941.
61. Nenitzescu, C. D., Olah, G., and Schleyer, P.v.R, John Wiley: New York, 1968; Vol. 1.
62. Olah, G. A., *Carbocation and Electrophilic Reactions*. VCH-Wiley, Weinheim, New York: New York, 1973.
63. Thaelke, *J. Bacteriol* **1990**, *172* (2), 1148-1150.
64. Doerfler, W.; Toth, M.; Kochanek, S.; Achten, S.; Freisemrabien, U.; Behnkrappa, A.; Orend, G., *Febs Letters* **1990**, *268* (2), 329-333.
65. Callahan, B. P.; Wolfenden, R., *J. Am. Chem. Soc* **2003**, *125* (2), 310-311.
66. Zhao, Y., Truhlar, D.G., *Theor. Chem. Account* **2008**, *120*, 215-241.
67. McLean, A. D.; Chandler, G. S., *J. Chem. Phys* **1980**, *72* (10), 5639-5648.
68. Becke, A. D., *J. Chem. Phys* **1993**, *98* (2), 1372-1377.
69. Grimme., S., *J. Comput. Chem* **2006**, *27* (15), 1787-1799.
70. Miertus, E. S., Tomasi, J., *Chem. Phys. Lett* **1981**, *55*, 117-129.
71. Kovacevic, L. S., Idziak,C., Markevicius, A., Scullion,C., Corr,M.J., Kennedy,A.J., Tuttle,T., and Murphy,J.A., *Agnew. Chem* **2012**, *124*, 1-5.

72. Schneebeli, S. T., Bochevarov, A.D., Friesner, R.A., *J. Chem. Theory. Comput.* **2011**, *7*(3), 658-668.
73. Ananikov, P. A., Musaev, D.M., Morokuma, K, *Eur. J. Inorg. Chem* **2007**, 5390-5399.
74. Kola, I., and Landis, J., *Nature. Rev* **2004**, *3*, 711-716.
75. Crabtree, R. H.; Felkin, H.; Morris, G. E., *J. Organomet. Chem* **1977**, *141* (2), 205-215.
76. Crabtree, R., *Accounts. Chem. Res* **1979**, *12* (9), 331-338.
77. Brown., J. A. I., S.; Kennedy., A.R.; Kerr., W.J.; Andersson., S.; Nilsson., G.N., *Chem. Commun* **2008**.
78. Henderson., R. K. J.-G., C.; Constable., D.J.C.; Alston., S.R.; Inglis., G.; Fisher., J.; Sherwood., S.P.; Binks., Curzons., A.D., *Green Chem* **2011**, *13*, 854-862.
79. Salter., R. B., J, *J. Labelled Compd. Radiopharm* **2003**, *46*, 489-498.
80. Ziegler, T., *Chem. Rev* **1991**, *91* (5), 651-667.
81. Perdew, J. P., *Phys. Rev. B* **1986**, *33*, 8822-8824.
82. Cerny. P, J. P., Hobza. P, and Valdes. H, *J. Phys. Chem A* **2007**, *111*, 1146-1154.
83. M. J. Frisch, G. W. T., H. B. Schlegel, G. E. Scuseria,; M. A. Robb, J. R. C., G. Scalmani, V. Barone, B. Mennucci,; G. A. Petersson, H. N., M. Caricato, X. Li, H. P. Hratchian,; A. F. Izmaylov, J. B., G. Zheng, J. L. Sonnenberg, M. Hada,; M. Ehara, K. T., R. Fukuda, J. Hasegawa, M. Ishida, T. Nakajima,; Y. Honda, O. K., H. Nakai, T. Vreven, J. A. Montgomery, Jr.,; J. E. Peralta, F. O., M. Bearpark, J. J. Heyd, E. Brothers,; K. N. Kudin, V. N. S., R. Kobayashi, J. Normand,; K. Raghavachari, A. R., J. C. Burant, S. S. Iyengar, J. Tomasi,; M. Cossi, N. R., J. M. Millam, M. Klene, J. E.

Knox, J. B. Cross,; V. Bakken, C. A., J. Jaramillo, R. Gomperts, R. E. Stratmann,; O. Yazyev, A. J. A., R. Cammi, C. Pomelli, J. W. Ochterski,; R. L. Martin, K. M., V. G. Zakrzewski, G. A. Voth,; P. Salvador, J. J. D., S. Dapprich, A. D. Daniels,; O. Farkas, J. B. F., J. V. Ortiz, J. Cioslowski,; and D. J. Fox *Gaussian, Inc*, Wallingford CT, 2009.

84. Dyall, K. G., *J. Chem. Inf. Comput. Sci* **2001**, *41*, 30-37.

85. Weigend, F.; Ahlrichs, R., *Phys. Chem. Chem. Phys* **2005**, *7* (18), 3297-3305.

86. Balaraman, E.; Gunanathan, C.; Zhang, J.; Shimon, L. J. W.; Milstein, D., *N.Chem* **2011**, *3* (8), 609-614.

87. Skodje, R. T., Truhlar, D.G., *J. Phys. Chem* **1981**, *85*, 624-628.